Operating Sittaung's Reservoirs

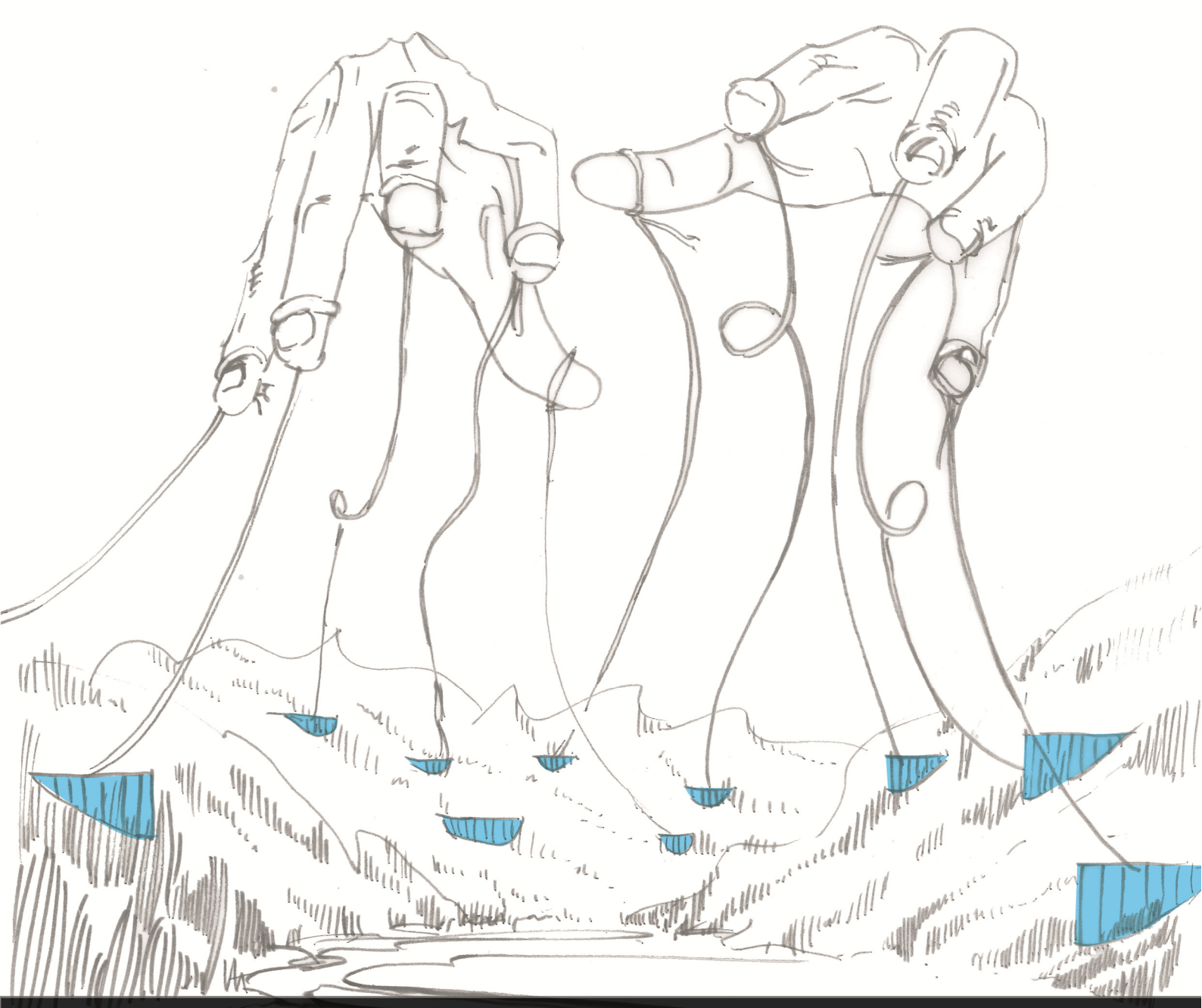

A two-stage model predictive control method for managing a multi-reservoir system for hydropower, irrigation and flood mitigation.

Dorien Lugt

TU Delft

On the cover

The illustration on the cover was made by Aafke Fraaije.

Operating Sittaung's reservoirs

A two-stage model predictive control method for managing a multi-reservoir system for hydropower, irrigation and flood mitigation

by

Dorien Lugt

in partial fulfillment of the requirements for the double degree of

Master of Science

in Applied Mathematics

and

Master of Science

in Civil Engineering

at the Delft University of Technology.

Student number:	4044541	
Thesis committee:	Dr. ir. M. M. Rutten,	TU Delft, CEG, Water Management
	Dr. E. Abraham,	TU Delft, CEG, Water Management
	Prof. dr. ir. A. W. Heemink,	TU Delft, EEMCS, Applied Mathematics
	Dr. J. W. van der Woude,	TU Delft, EEMCS, Applied Mathematics

An electronic version of this thesis is available at `http://repository.tudelft.nl/`.

Abstract

There is an increasing amount of attention for the application of model predictive control (MPC) for the optimal control of multi-purpose multi-reservoir systems (Tian et al. (2015), Raso (2013)). A major advantage of MPC is that multi-variate system dynamics and constraints of the control problem can be explicitly incorporated in the method. Challenges for application to reservoir systems include nonlinearities in the system dynamics and objectives and the large-scale optimization problem that arise when dealing with large systems (Lin and Rutten, 2016).

In this research a two-stage MPC method is presented for the optimal operation of a system of 21 reservoirs for hydropower, irrigation and flood management. The two-stage approach divides the problem into subproblems using the structure of the dynamical system (parallel connection of the reservoirs to the river) and periodicity of the external disturbances to the system (wet season and dry season). This approach reduces computational time for solution of the problem by using a decentralized approach (Christofides et al., 2013) for periods without flood risk, allowing parallel optimization of the reservoirs. In periods with flood risk, a coordinated MPC approach (Rawlings and Stewart, 2007) reduces the size of the problem while optimizing for the system-wide objective to mitigate flood. Spillway dynamics were defined by a complementarity constraint and included in the objective function using the penalty method (Pecci et al., 2017). Results showed appropriate behaviour of the flows through the spillways. The main challenges for solving the nonlinear optimization problem were the scaling of the problem, the normalization of terms in the objective function, determination of appropriate penalties for the spillway constraint and the increasing size of the problem for longer optimization horizons.

The method was applied to a system in the Sittaung river basin, which suffers from frequent floodings (Rest, 2015). Results showed that trade-offs between irrigation, hydropower and flood mitigation for this basin are limited. The main limitation for flood mitigation by the reservoir system are the conduit capacities and optimization horizon of the MPC system. Results for the case study were promising and indicate clear directions for future research and necessary steps to be taken for practical implementation of a MPC system in the Sittaung river basin.

Preface

This thesis report was written as part of the double degree program of the MSc Applied Mathematics and MSc Civil Engineering - Water Management. The workload of this master thesis is 60EC, divided over the subjects as follows 20EC for Applied Mathematics, 18EC for Water Management and 22 EC for both master programs. The total workload for this thesis is larger than that of either MSc program individually. This master research is an integrated project in which both disciplines are represented. While the report is written for audiences of both disciplines, some parts may be of specific interest to readers from one of either disciplines.

Chapter 4, Appendix B, Appendix A, Appendix C and Appendix D may be of specific interest for readers with an interest in applied mathematics. Chapter 2, Appendix E, Appendix F, Appendix G and Appendix H are mainly written for readers interested in the water management aspects of this research. The remaining chapters and appendices integrate the two parts and are hopefully of interest to readers of both disciplines.

I would like to thank Martine Rutten, Edo Abraham, Arnold Heemink and Jacob van der Woude for their supervision of this thesis research. It has been a pleasure to work with you. I would also like to thank Nay Myo Lin, for sharing his knowledge about the Sittaung's reservoirs and for always being available for questions. By the end of this research, Teije van der Horst, Selina Klemm, Mariel Piët, Ellen Minkman, Petra Izeboud and Davíd Brakenhoff were so kind to provide feedback on my draft report. Petra, you did much more than reading my thesis. I really enjoyed our weekly conversations and they were immensely helpful. Juul, thank you for making your PC available to run my experiments, definitely much faster than my old laptop. Sorry for the constant zooming noise in your living room. Aafke, thank you for the illustration on my front page, happy you are part of this important moment. Finally, there is Davíd again. There is so much more to thank you for than proofreading my report, but I am sure you know that.

Contents

1 Introduction

A reservoir is an artificial lake behind a dam that can be used for multiple purposes, e.g. irrigation, hydropower generation and flood mitigation. Reservoir operators often face challenging questions. Should we save water for later or release it now to generate electricity? Should we fill up the reservoir for the dry season or should we leave room to buffer an unexpected flood? Do we want to prevent floods at all costs or is reliable power production more important? The search for the optimal operation of such a system is an optimal control problem (Mizyed et al., 1992). When the system consists of multiple reservoirs, finding the optimal control becomes even more complicated (Labadie, 2004).

In this research, a method for optimal control of a system with 21 reservoirs in the Sittaung river basin in Myanmar is considered. The system is operated for hydropower, irrigation and flood mitigation. The reservoirs in the Sittaung river basin are currently operated in a decentralized way, based on fixed operation rules and expert judgement of the reservoir operators. Floods occur on a yearly basis in the Sittaung river basin, causing both human and socio-economic losses (Rest, 2015). The first aim of this research is

to investigate whether operation of the reservoirs in the Sittaung basin can be improved such that floods are prevented or reduced while taking hydropower generation and irrigation supply into consideration.

A model predictive control (MPC) method is implemented to optimize the multi-reservoir system in the Sittaung basin. Model predictive control is a form of optimal control in which the system's dynamics are explicitly included in the formulation of the optimization problem by means of a simulation model. For large systems, these models have many variables, resulting in large-scale optimization problems. When the formulated objectives or constraints of the system are dependent on the system's variables in a nonlinear way, solving the optimization problem can become challenging. The inclusion of hydropower generation as an objective or including a reservoir spillway in the simulation model typically lead to a nonlinear optimization problem.

Numerous researchers have investigated the application of model predictive control for multi-reservoir operation for hydropower (Setz et al. (2008) Doan et al. (2013)), irrigation (Negenborn et al. (2009)), flood management (Breckpot et al. (2010), Niewiadomska-Szynkiewicz et al. (1996), Tian et al. (2015)) or combinations of these and more objectives (Ficchi et al. (2013) Schwanenberg et al. (2015) Anand et al. (2013) Lin and Rutten (2016)). These researchers mention the large dimensionality of the system as a problem for the optimization. The second aim of this study is

to develop an optimal control method for the operation of a large-scale multi-purpose multi-reservoir system.

One method to solve large-scale problems with MPC methods is by dividing the problem into smaller sub-problems ((Maestre et al., 2011), (Christofides et al., 2013), (Rawlings and Stewart, 2007), (Scattolini, 2009)). These sub-problems can be defined based on the system's structure, objectives or other factors. In this thesis a two-stage MPC method is developed. The two stages follow from the problem characteristics of the reservoir system in the Sittaung basin in Myanmar. The method considers optimal operation for hydropower generation and irrigation for all reservoirs separately in periods without flood risk. This is stage 1 of the method and represents a decentralized approach. In periods with flood risk, the MPC method includes the entire reservoir system to optimize their operation for flood mitigation. This is stage 2, which uses a coordinated approach. The two aims of this research lead to the following research questions and sub-questions.

To what extent can optimal operation of the reservoir system in the Sittaung basin reduce flooding?

What are the trade-offs between hydropower generation, irrigation water supply and flood mitigation in the Sittaung river basin?

When a problem with multiple objectives is investigated, an important question to ask is to what extent the different objectives contradict each other. If we want to reduce flooding in the Sittaung river basin, will this always come at the cost of irrigation and hydropower generation? It is important to know if we can meet irrigation demands and increase hydropower generation, or if we have to choose between different objectives.

What are the limiting factors for flood mitigation in the reservoir system?

In order to determine to what extent the reservoir system can reduce flooding, it is important to determine the factors that limit flood mitigation.

How can model predictive control be applied for optimal operation of a multi-purpose reservoir system of 21 reservoirs?

How can coordinated or decentralized MPC be used to solve a large-scale optimization problem?

The two-stage approach presented in this research is a combination of decentralized and coordinated MPC, which is used to solve a large-scale optimization problem. It is important to determine if this approach results in solutions that are optimal for the system as a whole.

How can the nonlinear dynamics of flow through reservoir spillways be included in the simulation for model predictive control?

Flow through the spillways of reservoirs is a nonlinear process. If the reservoirs are not full, there are no flows through the spillways. If storage in the reservoirs exceeds maximum storage capacity, water will flow through the spillways. Including nonlinear system dynamics in simulation models for model predictive control complicates the solution of the problem. It is important to study how these dynamics can be included in the simulation model, because spillway behaviour is significant for the system's performance in flood mitigation.

What are the challenges of solving a nonlinear optimization problem for optimal control of a multi-purpose multi-reservoir system?

When implementing a model predictive control system, the control problem is transcribed to an optimization problem. If the model predictive control problem includes nonlinear objectives or nonlinear constraints, this results in a nonlinear optimization problem. It is important to study the challenges that arise when solving this problem, because the model predictive control system uses the solution of the nonlinear optimization problem to determine the optimal operation of the system.

Thesis outline This thesis presents the research that was done to answer these questions. In chapter 2 the reservoir system in the Sittaung river basin is presented, which is the case study to which the two-stage MPC method is applied. Chapter 3 presents the simulation model used within the model predictive control system. Chapter 4 describes the structure of the MPC system, the two-stage approach, the transcription to a nonlinear optimization problem (NLP) and the interior-point method used to solve the NLP. The results are presented in chapter 5. Chapter 6 discusses the results and chapter 7 states the conclusions and recommendations for future research.

2

The Sittaung river basin

The case study for this research is the Sittaung river basin located in the south of Myanmar as shown by figure 2.1. The area of the basin is 33000 km^2 (United Nations - Sittaung river valley survey mission, 1964), which is approximately the size of Belgium. The region has a monsoonal and tropical climate, with an average temperature of 28° Celsius and little variation in temperature throughout the year (United Nations - Sittaung river valley survey mission, 1964). Almost 90% of the annual precipitation falls during the wet season, which is between May and October. Annual precipitation in the north of the basin is around 890 mm, which is much lower than in the south where it is betweeh 3800 and 5000 mm (United Nations - Sittaung river valley survey mission, 1964). The wettest months are July, August and September. The meandering length of the Sittaung river is about 640 km long (Kyi, 2016) and its mean annual runoff is 50 M m^3 (Rest, 2015). The river starts in the Shan plateau and flows towards the Gulf of Martaban of the Andaman Sea (figure 2.2).

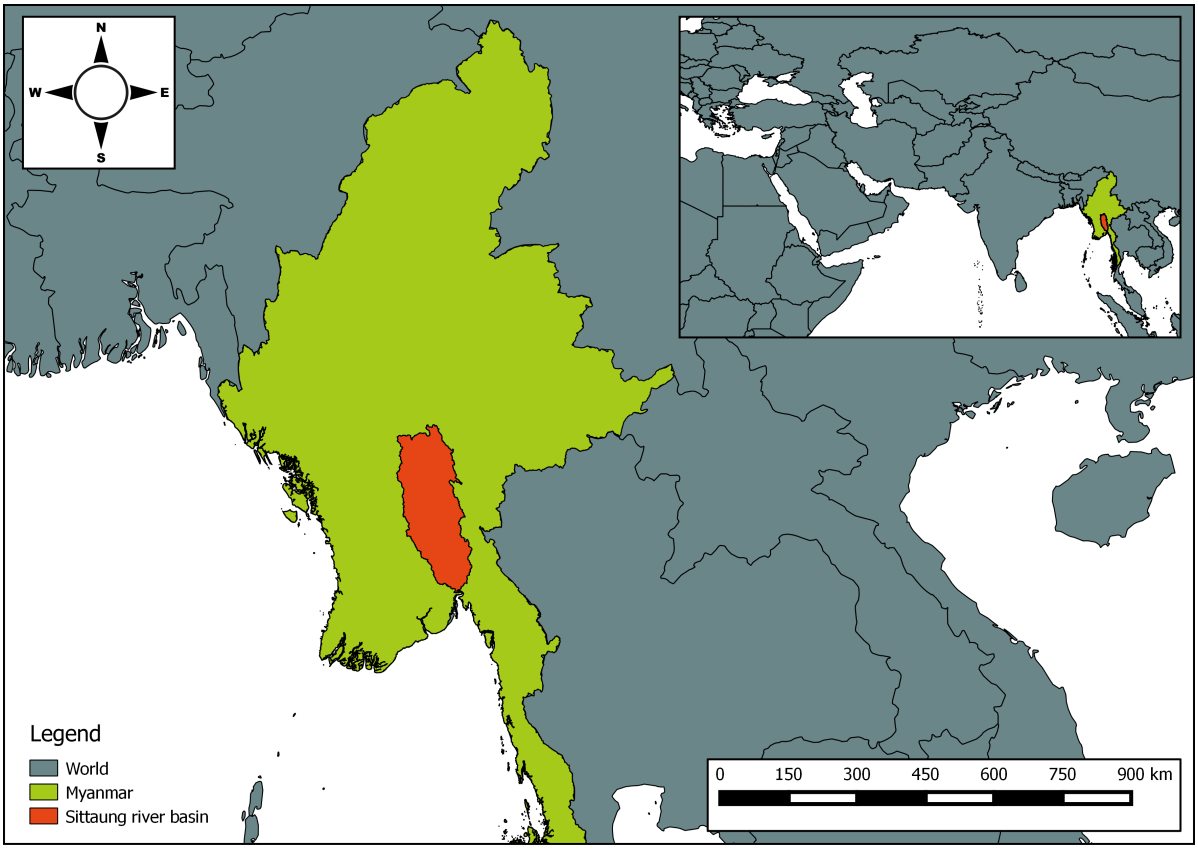

Figure 2.1: Location of Myanmar in the world and the location of the Sittaung river basin in Myanmar.

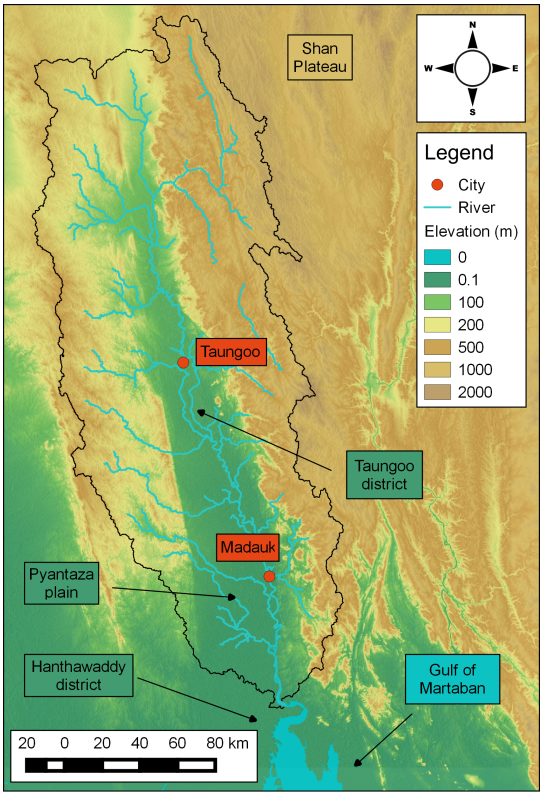

Figure 2.2: The figure shows the elevation map of the Sittaung river basin and surrounding areas, the 7.5-arc-second product of the Global Multi-resolution Terrain Elevation Data 2010 (GMTED2010). The locations of the cities Taungoo and Madauk, the Hanthawaddy district, Pyantaza plain, Taungoo district, Shan plateau and the Gulf of Martaban are indicated.

In 1964 the United Nations published a report called "Sittang Valley Water Resources Development", which included an analysis of the floods in the region ((United Nations - Sittaung river valley survey mission, 1964)). In the wet season, floods occur frequently in the south part of the basin. The main regions affected by floods are the Pyuntaza Plain, the pre-deltaic zone of the Sittaung basin, the coastal part of the Hanthawaddy district and the lowlands of Taungoo district, indicated in figure 2.2. The floods in the first three areas are caused by tidal effects in the lower part of the delta, which are not considered in this research. The focus in this research is on the lowlands of the Taungoo district. The report of the United Nations recommended the development of reservoirs in the Sittaung basin to reduce floods in the lowlands of the Taungoo district. Most of the reservoirs that currently exist in the basin were constructed following these recommendations.

Figure 2.3 shows the reservoir catchment areas of the 21 reservoirs included in this study. Each of those reservoirs serves one or multiple purposes, being hydro-power generation, irrigation storage and flood control. All reservoirs are located on a different tributary of the Sittaung river, except for the Upper Paunglaung and the Lower Paunglaung reservoir. These reservoirs form a cascade, but the Upper Paunglaung reservoir is neglected in this model. Table **??** in Appendix **??** gives the storage and conduit capacity of each reservoir, the waterspread area, the irrigable area and the area of the reservoir catchment for each reservoir. The conduits of the reservoir are the controlled outlet of the reservoir. The waterspread area of a reservoir is the area of the water surface of the reservoir. The irrigable area is the maximum area that could potentially be irrigated for a reference year given the storage and conduit capacity. For some reservoirs included in this study, one or more of these characteristics of the reservoirs were not available in the data. Assumptions made for these characteristics are described in Appendix F.

Even after the construction of the reservoirs according the recommendations of United Nations - Sittaung river valley survey mission (1964), floods are still occurring several times a year Rest (2015). The unevenly distributed precipitation throughout the year and basin necessitate irrigation in the dry season and in the

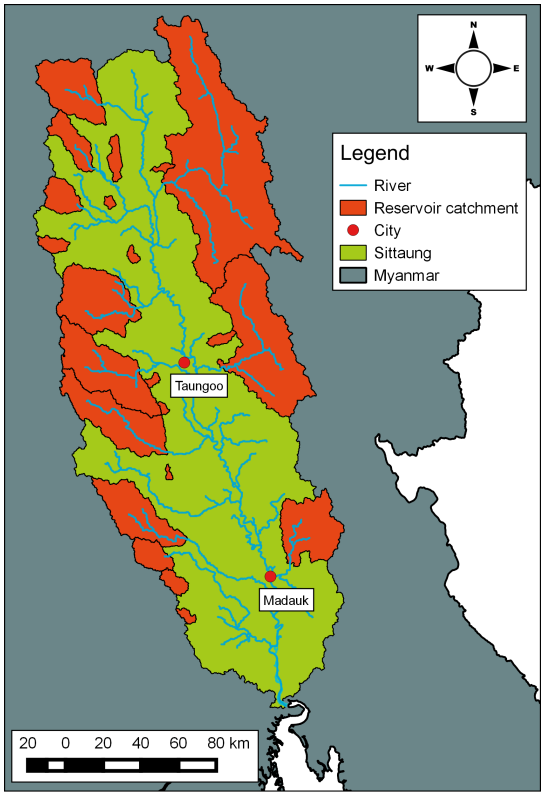

Figure 2.3: Locations of the reservoirs and their catchments in the Sittaung river basin.

north throughout the year (Hasman, 2014). Energy consumption in Myanmar has grown 402% between 1990 and 2013 and demands are expected to grow with 280% - 475% until 2030(Dobermann, 2016). Most of the energy in Myanmar comes from hydropower plants. The hydropower stations in the Sittaung river basin generate about 12% of the countries total electricity (Kyi, 2015). In this study, operation of the reservoir system for flood mitigation, hydropower generation and irrigation supply is considered. Not all reservoirs in the basin are operated for all of the three purposes. In this study, the aim was to investigate the potential of the reservoir system for the basin, therefore it was assumed that all reservoirs can be used for all three purposes. The current operation of the reservoir system is based on fixed operation rules and expert judgement of the reservoir operation. Operation of the reservoirs is currently uncoordinated.

2.1. The hydrological and meteorological data available for the basin

Data available for this study were groundstation measurements and remote sensing data. At the start of the research a data quality analysis was performed which is presented in Appendix E, also for data that were not further used in the research. The considered data are listed here.

Ground measurements At nine reservoir dams, daily measurements of precipitation, water levels in and outflows to the reservoir are available. Periods for which data are available differ per reservoir, falling between 2008 and 2015. Table 2.1 shows the period of available ground measurements for the reservoirs, the catchment area in km^2, the capacity of the reservoir in m^3 and the percentage of missing discharge data. Figure 2.4 shows the locations of these reservoirs and the corresponding catchments.

Water level measurement Daily mean water depths in the Sittaung river at the station Taungoo and Madauk, measured by the Department of Meteorology and Hydrology of Myanmar, were available between January 1st, 2013 and December 31st, 2015.

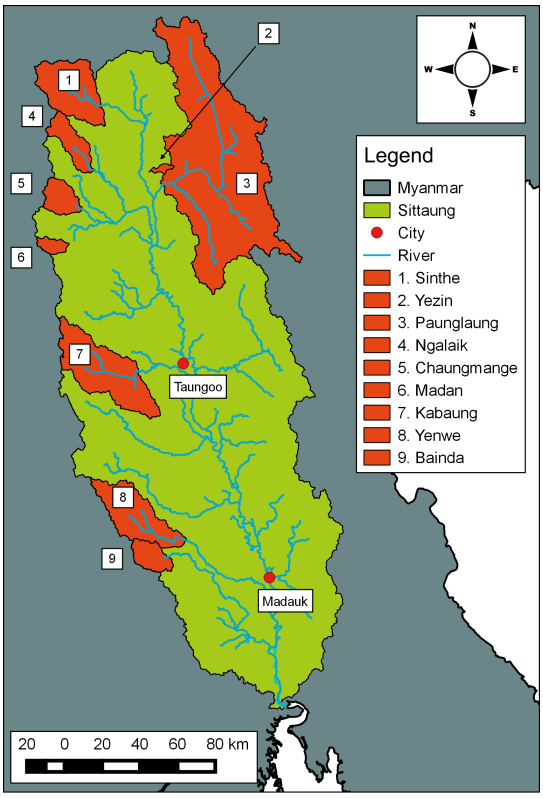

Figure 2.4: Locations of the reservoir catchments in the Sittaung river basin for which daily measurements of water levels, outflows and precipitation at the dam location were available for this research. Data have been provided by the Ministry of Agriculture and Irrigation.

Table 2.1: Details of reservoir dams in the Sittaung river basin for which daily measurements of water levels, outflows and precipitation at the dam location were available for this research. Data have been provided by the Ministry of Agriculture and Irrigation.

No.	**Reservoir**	**Capacity (Million m^3)**	**Catchment area (km^2)**	**Start data**	**End data**	**Missing discharge data (%)**
1	Chaunmange Dam	113	265	1/1/'09	28/2/'15	15 %
2	Madan Dam	45	100	1/6/'09	28/2/'15	76 %
3	Ngalaik Dam	93	328	1/1/'09	31/3/'15	51 %
4	Yezin Dam	90	33	1/1/'09	19/3/'15	41 %
5	Sinthe Dam	176	809	1/1/'09	19/3/'15	27 %
6	Paunglaung Dam	678	4791	1/1/'10	28/2/'15	0 %
7	Yenwe Dam	1149	842	1/1/'11	28/2/'15	0 %
8	Bainda Dam	461	246	1/1/'10	28/2/'15	19 %
9	Kabaung Dam	1084	1178	1/1/'08	28/2/'15	15 %

Cross-section measurements Rest (2015) presents cross-section measurements at 28 locations in the Sittaung river taken between February and MArch 2015. Cross-section 8, near Taungoo city, was used in this study.

GMTED2010 Global Multi-resolution Terrain Elevation Data 2010 (GMTED2010) was used to derive catchment and subcatchment areas. The GMTED2010 dataset is a collaboration of U.S. Geological Survey (USGS) and the National Geospatial-Intelligence Agency (NGA). For this study the mean elevation product with 7.5-arc-second spatial resolution was retrieved from `https://lta.cr.usgs.gov/GMTED2010` on September 19, 2016.

CLIMWAT 2.0 The climatic database CLIMWAT 2.0 for CROPWAT is a joint publication of the Water Decelopment and Management Unit and the Climate Change and Bioenergy Unit of FAO, Food and Agriculture Organization of the United Nations. The "reference evapotranspiration" parameter or potential evaporation used in this research is a long-term monthly average calculated with the Penman-Monteith method in mm/-day. For this research the average over all stations within the region with latitudes 17.5-20.75 ° and longitudes 95.5-97 ° was used, being the stations named Yamethin, Tharrawaddy, Bago, Toungee, Pyinmana, Loikaw. Data are retrieved on September 13, 2016.

TRMM As ground measurements for precipitation are only available for nine locations in the basin, satellite data are used to capture spatial variations of precipitation within the basin. The Tropical Rainfall Measuring Mission (TRMM) is a joint mission of NASA and the Japan Aerospace Exploration Agency for precipitation measurement. For this research the daily precipitation totals of the 3B42/TMPA Research Version were used. The TMPA dataset is derived using the Version 7 TRMM Multi-Satellite Precipitation Analysis. From this dataset the variable 'precipitation' for the period 1/1/'08 to 31/3/'15 for the region of the Sittaung basin was used. The dataset was downloaded from `https://pmm.nasa.gov/data-access/downloads/trmm` on February 16, 2017.

Global (30m) HAND For topography classification the Height Above Nearest Drainage (HAND) was used. The HAND is a normalized Digital Elevation Model (DEM) using the nearest drainage, derived from the SRTM (30m), having one arc-second resolution. Global (30m) HAND was created by **?** and retrieved from `https://code.earthengine.google.com/9a86d92fa2ecc087047f8e84b3b83295` on January 3, 2017.

3

The model of the system dynamics

Model predictive control (MPC) is a control strategy for a system using a model to simulate the system's response to control actions in order to find the optimal operation strategy. In this chapter the model of the system is discussed.

The model of the system dynamics applied in this research is linear, time invariant and discrete in time. MPC methods for nonlinear models exist (Van den Boom and Backx, 2005), but their usage makes the MPC system complexer. The model is discrete in time because the MPC is developed for discrete time control. On a daily basis, control actions in the system and releases from the reservoir are performed or considered by the controller. The assumption that the linear, time-invariant and discrete-time model of the system dynamics is a sufficient approximation of the real system dynamics is discussed for each of the model components presented in this chapter.

The model only describes the parts of the system which are influenced by or relevant to control actions. These parts will be referred to as the internal system in this thesis. For example, the storages in the reservoirs are part of the internal system. They are affected by operational decisions concerning the reservoir outflows and are relevant to the water availability for hydropower and irrigation. Part of the catchment outflow cannot be controlled by reservoir operation, because it flows directly into the river without passing through a reservoir. Hence, it is not part of the internal system. However, these river inflows do influence the water levels of the river, which are relevant to flood mitigation and therefore form part of the internal system. This makes the uncontrolled inflows into the river relevant to the control problem, even though they are not affected by control actions. They are defined as external disturbances of the system. External disturbances are defined as factors affecting the internal system dynamics, which can not be affected by control actions. Predictions of future external disturbances are used as input for the internal system model. In some applications a prediction model for the external disturbances is used. This does not have to be linear because it is not part of the controller. In section 3.7 the prediction of external disturbances is discussed.

The system of reservoirs and the Sittaung river is a multivariate system with multiple variables to control (outflows through the conduits) and multiple variables to be controlled (storage in the reservoirs, water level in the river). It is a so-called multi-input multi-output system. In this work a state-space description of the system dynamics was used. The advantage of state-space models is that they are easier to implement for multivariate systems (Camacho et al. (2007) Van Overloop (2006)). Other options for describing the system behaviour are impulse/step response models and transfer function models. These can easily be converted into state-space models (Van den Boom and Backx, 2005).

The concept of a state-space represenation is introduced in section 3.1. The model of the system consists of two types of model components, the reservoirs and the river sections. In sections 3.2 to 3.3 the model components modelling the reservoirs and the river sections are presented. Section 3.4 describes how these components are coupled to form the model of the entire system. The hydropower generated by a reservoir is a function of the water levels and the outflow through the conduit. Section 3.5 describes how the generated hydropower is estimated from the simulated storage in the reservoir and the choice of outflows through the conduit by the controller. The irrigation offtake is determined by the controller based on the irrigation

demands. In section 3.6 an estimation of the irrigation demands used as input in the model is given.

3.1. The state space representation for the system dynamics model

In the state-space representation a distinction is made between variables of state x^k, input u^k and output y^k and external disturbances w^k, where k represents the discrete timestep. Van den Boom and Backx (2005) present the following discrete time state-space representation for linear time-invariant systems:

$$x^{k+1} = Ax^k + Bu^k + Dw^k \tag{3.1}$$

$$y^k = Fx^k + Gu^k \tag{3.2}$$

State variables x are the system variables necessary to describe the state of the system at any given timestep k. Decisions made by the operator, e.g. releasing water through the conduits, are represented by inputs u. The state variables are defined such that the model can fully determine the state of the internal system for the next timestep based on the state, inputs and external disturbances of the current timestep. The variables of interest to the objectives may be different from the state variables. For example, a state variable is the storage in a river segment, whereas the variable of interest is the water level in that river segment. The outputs y represent all the states of the system model that are relevant to the control objectives. Equation 4.2 shows how the outputs are modelled as a function of the state and input variables.

3.2. The model component for the reservoirs dynamics

As discussed in chapter 2, 22 reservoirs in the system will be considered. Except for the Upper and Lower Paunglaung the outflow from the reservoirs flows to the Sittaung river without flowing into another reservoir first. The Upper and Lower Paunglaung are two reservoirs in cascade, meaning that the Upper Paunglaung is located upstream of the Lower Paunglaung reservoir and its outflow flows into the Lower Paunglaung reservoir. These two reservoirs are included in the model as one reservoir. This means that all reservoirs in the system model are connected in parallel to the main river and their operations do not interfere. The outflows of all reservoirs do come together in the Sittaung river. Therefore, the water level in the river is influenced by the operation of all reservoirs combined.

Figure 3.1 shows a schematic overview of a reservoir in the Sittaung basin. The reservoir storage consists of an active storage and a inactive (dead) storage. The dead storage is the storage in the reservoir that cannot be drained through the conduits or spillways. It is used to let sediments settle and create an area for fish during periods with low water levels. When reservoir storage is mentioned in this thesis, the active storage of the reservoir is meant. This is the storage of the reservoir that can be released through the conduit and used for irrigation supply or hydropower generation. The variable S_{res} [L^3] indicates the storage in the reservoir and is a state variable of the system. The reference level for the water levels in the reservoir is the level of the conduits, i.e. the level that represents the divide between active and dead storage. The storage capacity is the maximum (active) storage in the reservoir before it overflows. It is the volume between the reference level and the spillway crest level. The storage capacity is indicated with $\overline{S_{\text{res}}}$ [L^3].

The inflow to the reservoir The inflow to the reservoir $Q_{\text{in,res}}$ [$L^3\ T^{-1}$] cannot be controlled by the operation of the reservoir. It is an external disturbance to the system. Section 3.7 discusses the prediction of external disturbances.

The outflow through the conduits of the reservoir The reservoir dam has two types of outlets, the conduits and the spillways. The flow through the conduits can be controlled by (partially) opening or closing the conduits with a control gate. The kinetic energy of the water flowing through the conduits is converted into electricity by turbines and the generator. The operator of a reservoir can change the gate settings in order to change the outflow through the conduits. The flow through the conduit is a nonlinear function of the water level in the reservoir, the gate height and conduit characteristics. In this model however, the flow through the

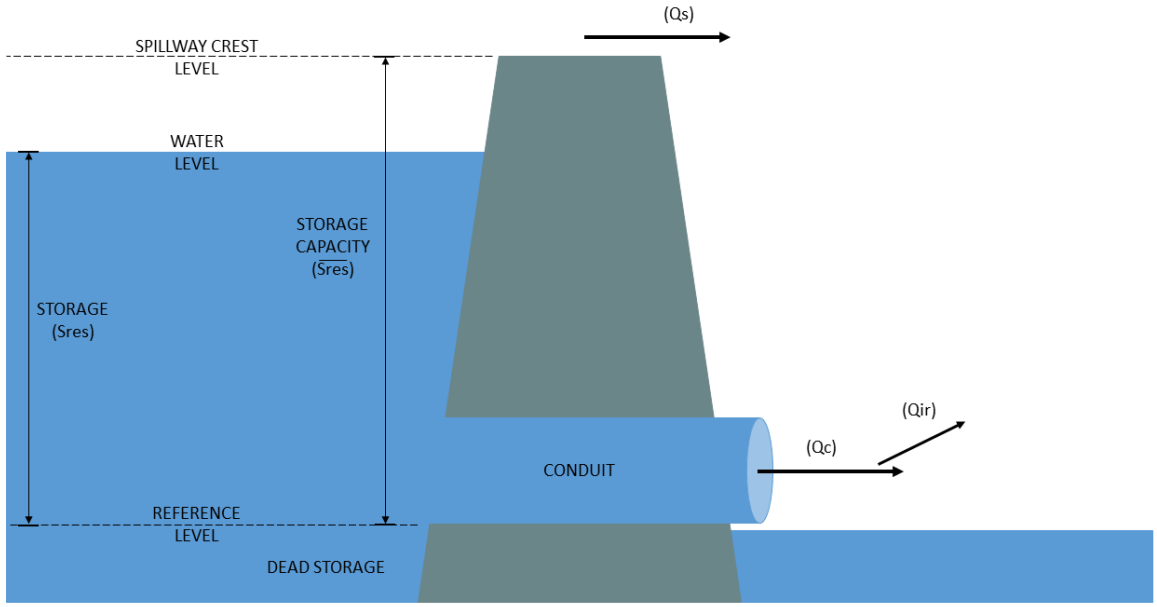

Figure 3.1: Schematic representation of a reservoir with overflow spillways.

conduits is included as a control variable rather than the settings of the gate. This simplifies system dynamics. The conversion of the suggested optimal flows through the conduits to settings of the gate can be arranged by a local feedback or feedforward controller. This is beyond the scope of this research. The sum of flows through all conduits of the reservoir are included as one variable Qc [L^3 T^{-1}]. The conduit capacity is indicated with $\overline{Q_c}$ [L^3 T^{-1}]. The flow through the conduit is a control variable, which can be chosen by the operator or the controller.

The outflow through the spillway of the reservoir The spillways of the reservoirs in the Sittaung basin cannot be controlled. They function like overflow weirs, meaning that water flows through the spillways when the water level in the reservoir exceeds the crest level of the spillway. The flow through the spillway is a nonlinear function of the water level in the reservoir, the crest level and width of the spillway. The crest level of the spillway determines the storage capacity of the reservoir. Even though the flow through the spillway varies in time as a function of the water level, integrated over one day it is assumed to be equal to the volume exceeding the storage capacity of the reservoir on that day. Thus, on days when the storage in the reservoir is below the maximum storage capacity, the flow through the spillway is zero. Flow through the spillway does not generate hydropower, but does end up in the river section downstream of the reservoir. The flow through the spillway is indicated with Qs [L^3 T^{-1}] and is a state variable of the system as it cannot be controlled by the operator. It is defined as

$$Q_s^k = \begin{cases} 0 & \alpha < 0 \\ \frac{\alpha^k}{\Delta t} & \alpha^k > 0 \end{cases}, \tag{3.3}$$

with

$$\alpha^k = S_{res}^k + \left(-Q_c^k + Q_{in,res}^k\right)\Delta t - \overline{S_{res}}. \tag{3.4}$$

The storage in the reservoir The storage in the reservoir at timestep k+1 is given by the water balance

$$S_{\text{res}}^{k+1} = S_{\text{res}}^{k} + \left(-Q_{\text{c}}^{k} - Qs^{k} + Q_{\text{in,res}}^{k}\right)\Delta t. \tag{3.5}$$

The offtake for irrigation The offtake for irrigation Q_{ir} [$\text{L}^3\ \text{T}^{-1}$] occurs downstream of the conduit. The offtake for irrigation is chosen by the operator and it is therefore a control variable to the system. It is limited by the demand for irrigation $\overline{Q_{\text{ir}}}$ [$\text{L}^3\ \text{T}^{-1}$].

$$Q_{\text{out,res}}^{k} = Q_{\text{c}}^{k} + Q_{\text{s}}^{k} - Q_{\text{ir}}^{k}. \tag{3.6}$$

If the irrigation offtake would not be limited by the demand, the controller could prevent floods by using all reservoir outflow for irrigation. This is not a realistic scenario. The demands for irrigation are estimated in section 3.6.

The water level in the reservoir The output variables for the reservoir are the outflow through the conduit Q_c, irrigation offtake Q_{ir}, the flow through the spillway Q_s and water level in the reservoir. The variables Q_c and Q_{ir} are control variables and Q_s is a state variable. The water level in the reservoir is not a state variable, but is related to the storage in the reservoir, which is a state variable S_{res}. The water level in the reservoir is calculated using a linear relation to the storage. It is calculated by dividing the storage through the waterspread area A_{res} (m^2) of the reservoir. The linear relation between storage and water level is a simplification, as the reservoirs in the Sittaung basin are not linear. Section 5.1.4 of chapter 5 discusses the implications of this assumption for the calculated hydropower production. Table **??** in Appendix F gives the waterspread area for each reservoir in the model.

3.3. The model component for the river sections dynamics

The routing method used to describe the propagation of a flood wave through the Sittaung river is the Muskingum routing method (Gill, 1978). The river is divided into segments, and the routing parameters vary per segment. The Muskingum method assumes the outflow from a river segment is a function of storage and inflow to the segment. It is based on the continuity equation along with an assumed relationship between the storage and the in- and outflows from a reach. Other methods exist for flood routing of which include the Saint-Venant equations. The Saint-Venant equations are based on the continuity and momentum equations, and describe the propagation of a flood wave more realistically. However, the Saint-Venant equations require more information about the river characteristics for the choice of parameter values and data for the calibration of these parameters. Another disadvantage is that the numerical implementation of the Saint-Venant equations results in many more state variables than the Muskingum routing method. This increases the size of the optimization problem, which was found to be a limiting factor for the solution of the control problem in this research. The Muskingum method is used in many flood forecasting systems an provides reasonable estimates of the routing time and of maximum discharges, especially when the method is applied for multiple segments with parameters estimated per segment (Koussis, 2009). Therefore, the Muskingum routing method is used in this research. The Muskingum equation is given by equation 3.7.

$$S_{\text{riv}} = K\left(xQ_{\text{in,riv}} - (1-x)Q_{\text{out,riv}}\right), \tag{3.7}$$

where S_{riv} [L^3] is the storage in the segment, $Q_{\text{in,riv}}$ [$\text{L}^3\ \text{T}^{-1}$] the rate of inflow to the segment at the upstream boundary and $Q_{\text{out,riv}}$ [$\text{L}^3\ \text{T}^{-1}$] the rate of outflow from the segment at the downstream boundary. All three variables are state variables of the system. The Muskingum equation has two coeffcients, x and K, which are usually calibrated on historical flood data (Gill, 1978). The parameter x is the weighting factor for inflow versus outflow and varies between 0 and 0.5. It represents the attenuation of the flood peak while travelling through the reach. The value $x = 0$ causes immediate attenuation of the flood wave, as would occur in a reservoir. If $x = 0.5$ there is no attentuation of the flood peak over the reach. For a natural system it is known that the parameter is between 0 and 0.3 (Song et al., 2011).The parameter x was set to value 0.3. The constant

K [T] is the the storage-time coefficient, with a value usually approximated as the flow travel time through the reach. In the Sittaung river, measurements of water levels are only available once a day at eleven locations in the river as discussed in Appendix E. The travel time of a flood wave through the Sittaung river is typically only a few days (Nay Myo Lin, 2016) and can not be estimated from the measurements. The travel speed of a flood wave is approximated at 100 km per day, 1.25 m s^{-1}, based on expert judgement. The value of parameter K is set to the length of the river segment [m] divided by 1.25 m s^{-1}, which is the approximate travel time of a flood wave through the river segment. Table G.1 in Appendix G gives the length of each river segment [km] and the value for K per river segment.

The storage in the river segment The continuity equation for the storage in the river segment is given by equation 3.8.

$$Q_{\text{in,riv}} - Q_{\text{out,riv}} = \frac{dS_{\text{riv}}}{dt} \tag{3.8}$$

Discretization of this equation results in an expression for the storage in the river segment by equation 3.9,

$$S_{\text{riv}}^{k+1} = S_{\text{riv}}^{k} + \frac{Q_{\text{in,riv}}^{k+1} + Q_{\text{in,riv}}^{k}}{2}\Delta t - \frac{Q_{\text{out,riv}}^{k+1} + Q_{\text{out,riv}}^{k}}{2}\Delta t. \tag{3.9}$$

The outflow from the river segment Combining equation 3.9 with equation 3.7 results in an expression for the outflow from the river segment in terms of the inflow,

$$Q_{\text{out,riv}}^{k+1} = c_1 Q_{\text{in,riv}}^{k+1} + c_2 Q_{\text{in,riv}}^{k} + c_3 Q_{\text{out,riv}}^{k}. \tag{3.10}$$

The parameters in this equation follow from equation 3.7 and equation 3.9. The values of c_1, c_2 and c_3 are different for each river segment because K is different for each river segment. The values are given in table G.1 of Appendix G.1.

$$c_1 = \frac{\Delta t + 2Kx}{\Delta t + 2K - 2Kx} \tag{3.11}$$

$$c_2 = \frac{\Delta t + 2Kx}{\Delta t + 2K - 2Kx} \tag{3.12}$$

$$c_3 = \frac{-\Delta t + 2K - 2Kx}{\Delta t + 2K - 2Kx} \tag{3.13}$$

The water levels in the river segments The output variable are the water levels in the river segment in which floods are considered, near Taungoo city. A linear relation is assumed between the water level and the storage in the river segment near Taungoo, which means that the cross-section is assumed to be rectangular. Figure 3.2 shows a measurement of the cross-section near Taungoo city (Rest, 2015). The figure shows that assuming a rectangular cross-section is reasonable. The width of the segment in the river is 200 m. The length of the segment is 6.9 km.

3.4. The coupling of the model components

The model components for reservoirs and the river segments are coupled to form a model for the system dynamics of the entire reservoir system. Seventeen subcatchments are derived that flow directly into the river segments. Each subcatchment flows into a river reach at the upstream boundary of that reach. This means that there are also 17 river segments. In some subcatchments, one or more reservoirs are located. The

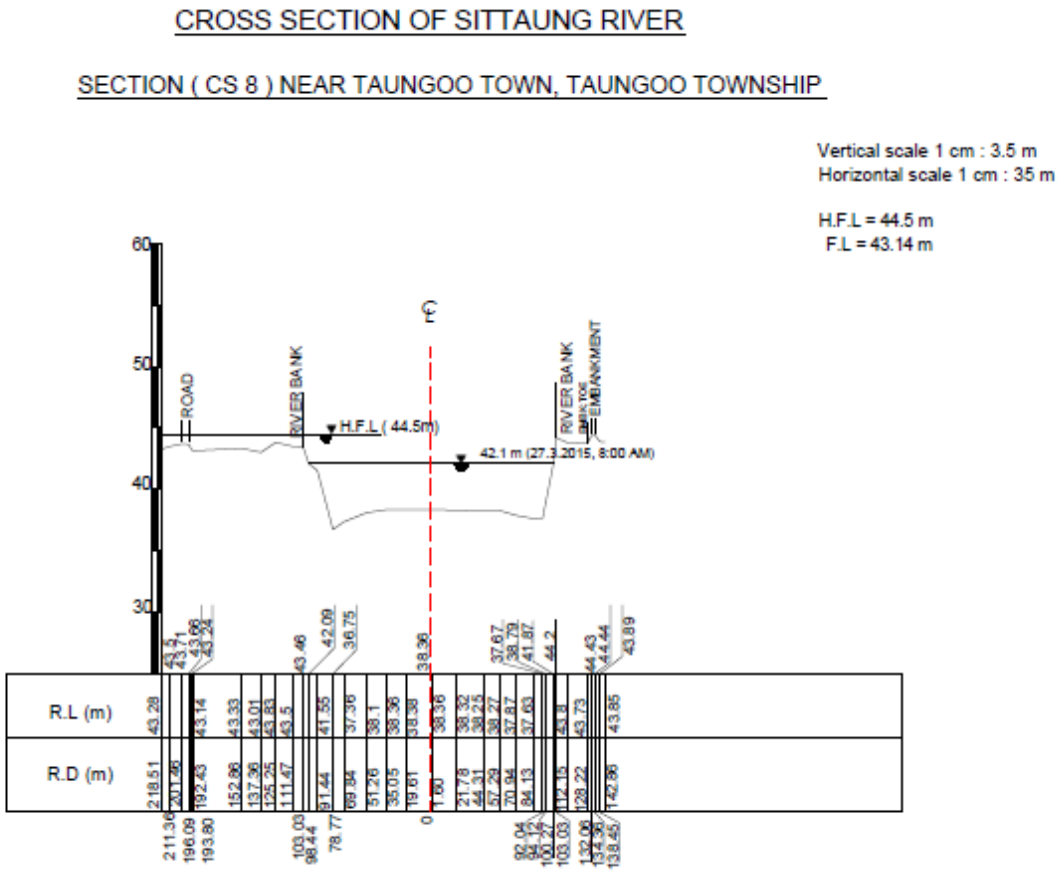

Figure 3.2: Cross section measurement of the Sittaung river near Taungoo town (Rest, 2015)

outflow from the reservoir(s) in a subcatchment is also added as inflow to the river segment connected to that subcatchment. Figure 3.3a shows the 17 subcatchments and figure 3.3b shows the 21 reservoirs located in these subcatchments.

The reservoir components and river segment components are coupled to form one system model. The way these components are coupled is formulated by defining $Q_{\text{in,riv}}$, which represents the inflow to the river segments. The set $\mathbb{S}_i$ is defined in equation 3.14.

$$\mathbb{S}_i := \{j | \text{Reservoir j is located in subcatchment i}\} \tag{3.14}$$

Table F.1 in Appendix F shows which reservoirs are located in which subcatchment. The inflow for section i of the river is determined by taking the sum of the outflow from the connected subcatchment, the outflows from the reservoirs located in that subcatchment and the outflow from the upstream river section.

$$\left(Q_{\text{in,riv}}\right)_i = \left(Q_{\text{out,riv}}\right)_{i-1} + \sum_{j \in \mathbb{S}_i} \left(Q_{\text{out,res}}\right)_j + \left(Q_{\text{out,catchm}}\right)_i, \tag{3.15}$$

where $Q_{\text{out,res}}$ is defined in equation 3.6. The variable $\left(Q_{\text{out,catchm}}\right)_i$ [$\text{L}^3\ \text{T}^{-1}$] is defined as the uncontrolled outflow from subcatchment i and is an external disturbance to the system.

All the equations for the system dynamics, are linear except for equation 3.3. The system of state equations can be written in the form of equation 4.1 without the spillway equation. Chapter 4 discusses how the equa-

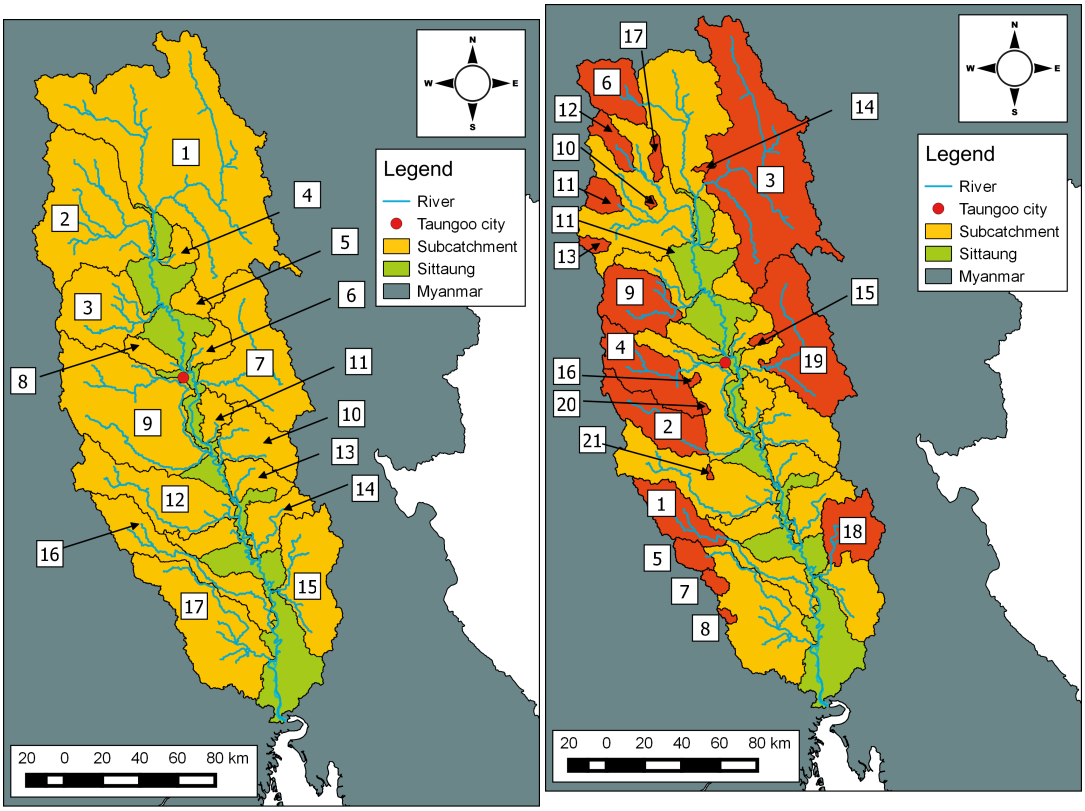

(a) The 17 subcathments defined for the model.

(b) The subcatchments with the 21 reservoirs included in the model.

tions for the system dynamics are included in the definition of the optimization problem. The nonlinearity of the spillway will be also be further discussed. The variables of the model of the system dynamics, their units, range and type of variable are presented in table 3.1.

3.5. The estimation of hydropower generation

The power produced by a hydropower dam is a function of the flow through the conduit $Q_{c,s}$ (in $m^3 s^{-1}$) and the height difference h (m) over which the water flows. The power P (Watt) or (kg m^2 s^{-3}) is given by the equation

$$P = \eta \rho Q_{c,s} g h, \tag{3.16}$$

with ρ the density of the water, 1000 kg m^{-3}, and g the gravitational acceleration with the conventional standard value of 9.81 m s^{-2} (Olofintoye et al., 2016). The efficiency of conversion from hydraulic energy to mechanical energy η (-) is plant specific. Kyi (2015) found an estimated average efficiency of 40 % for the reservoirs in the Sittaung basin Kyi (2015). To calculate the energy E produced in kWh during a period Δt (hrs),

$$E = P \cdot \Delta t \cdot 10^{-3}. \tag{3.17}$$

In the optimization, timesteps of one day are used, so $\Delta t = 24$ hrs. Combining all constant factors in one new constant, this results in

$$E = 24 \cdot 10^{-3} \cdot 9.81 \cdot 1000 \cdot 0.4 \cdot Q_{c,s} \cdot h = 24 \cdot 9.81 \cdot 0.4 \cdot Q_{c,s} \cdot h. \tag{3.18}$$

Table 3.1: The variables of the model for the system dynamics with their units and range. The type of variable is indicated with x for state variable, u for control variable and w for external disturbances. If a variable is a combination of other variables the type is indicated as a combination of types.

Symbol	Units	Range	Type	Variable
Sres	$[L^3]$	$[0, \overline{S_{res}}]$	x	Storage in the reservoir
Qs	$[L^3\ T^{-1}]$	$[0, \infty]$	x	Flow through the spillway
Qc	$[L^3\ T^{-1}]$	$[0, \overline{Q_c}]$	u	Flow through the conduit
Qir	$[L^3\ T^{-1}]$	$[0, \overline{Q_{ir}}]$	u	Irrigation offtake
Qin,res	$[L^3\ T^{-1}]$	$[0, \infty]$	w	Inflow to the reservoir
Qout,res	$[L^3\ T^{-1}]$	$[0, \infty]$	x,u	Outflow from the reservoir
Sriv	$[L^3]$	$[0, \infty]$	x	Storage in the river section
Qin,riv	$[L^3\ T^{-1}]$	$[0, \infty]$	x,u,w	Inflow to the river section
Qout,riv	$[L^3\ T^{-1}]$	$[0, \infty]$	x	Outflow from the river section
Qout,catchm	$[L^3\ T^{-1}]$	$[0, \infty]$	w	Outflow from the subcatchment to its river section

Since the variable used for flow through the conduit in the model is not $Q_{c,s}$ (m^3s^{-1}) but Q_c in (m^3days^{-1}), this becomes

$$E = 24 \cdot 9.81 \cdot 0.4 \frac{1}{24 \cdot 3600} \cdot Q_c \cdot h = \frac{9.81 \cdot 0.4}{3600} \cdot Q_c \cdot h. \tag{3.19}$$

The height difference for a reservoir (the hydraulic head) is assumed to be the difference between the conduit level (reference level) and the water level in the reservoir (figure 3.1). It is assumed that the tailwater level, the water level immediately downstream of the reservoir, is below the level of the conduit and therefore does not influence the hydraulic head in the reservoir. For reservoir dams in rivers with steep bedslope this assumption is generally valid, like the Sittaung basin. The assumption of linear reservoirs changes equation 3.19 to equation 3.20.

$$E = \frac{9.81 \cdot 0.4}{3600} \cdot Q_c \cdot \frac{S_{res}}{A_{res}} \tag{3.20}$$

3.6. The estimation of irrigation demand

No data were available for the exact irrigation demands for most reservoirs in the Sittaung basin. The demands were estimated based on the irrigable area reported for the reservoirs. The definition of irrigable area is the total area equipped for irrigation, and represents the maximum area that could be irrigated by the reservoir. It was assumed that the total irrigable area is used for rice production, as rice is the most important agricultural commodity in Myanmar. There are two growing cycles for rice in Myanmar. The irrigation demand of rice crops was estimated using information from the Food and Agricultural Organization (FAO). Appendix H shows the estimation of irrigation demands in detail. For three of the reservoirs, actual irrigation offtakes were available and these are compared to the estimation. For all three reservoirs the demands were overestimated. In chapter 6 the effect of this overestimation on the results will be discussed.

Note that the actual irrigated area for a reservoir catchment may differ from the irrigable area and that rice is not the only crop produced in the basin. Also, it is assumed that the total water demand of the crop is provided through irrigation, regardless of the amount of precipitation. The effect of these assumptions is discussed in chapter 6.

3.7. The model of the external disturbances

The model of the system dynamics requires a prediction of future external disturbances to predict the system's responses to control actions. The external disturbances to the system described here are the outflows

from the reservoir catchments to the reservoirs and the outflows from the subcatchments to the river. These outflows can be predicted from meteorological measurements or predictions using a hydrological model. In this research, a synthetic timeseries of catchment outflows was generated. An attempt to develop a hydrological model for the subcatchment did not produce satisfying results, due to the limited availability of (reliable) data in the basin.

The synthetic timeseries for outflows from the reservoir catchments and subcatchment was derived from the inflow data series to the Paunglaung reservoir between January 1, 2010 and February 28, 2015. These inflows are scaled by the catchment area relative to the area of the Paunglaung reservoir catchment. This series was chosen as it is the longest series of observations, it has no missing data points and the least data points identified as implausible in the data quality assessment (Appendix E).

In the system a distinction is made between the optimization horizon, the number of timesteps for which the control is optimized, and the prediction horizon, the number of timesteps for which predictions are assumed to be available. The prediction horizon is assumed to be 3 days, as no reliable predictions can be expected further ahead if a prediction model would be used. For the remaining period an estimation of the seasonality of inflows is provided to the model. Because no prediction model is used in this study, the synthetic outflow series is used for the 'predicted' outflows. The seasonality is generated from this four-year synthetic outflow series. Outflows on each day are averaged for all available years in the series, from 2010 to 2014. Then, the 15-day moving average of this timeseries is taken. Figure 3.4 shows the inflow timeseries of the Paunglaung reservoir (grey area) which is used for the predicted outflow and the seasonality (red line).

When the model predictive control system is implemented for actual operation, the model receives the past external disturbances measured in the real system. In the experimental implementation of the model predictive control system, the same external disturbances were used as 'measured past external disturbances' as were predicted for these days. This means that in the experimental set-up, the predictions are perfect with no uncertainty. There are several ways to deal with prediction uncertainties of external disturbances in model predictive control, but the consideration of these is beyond the scope of this research.

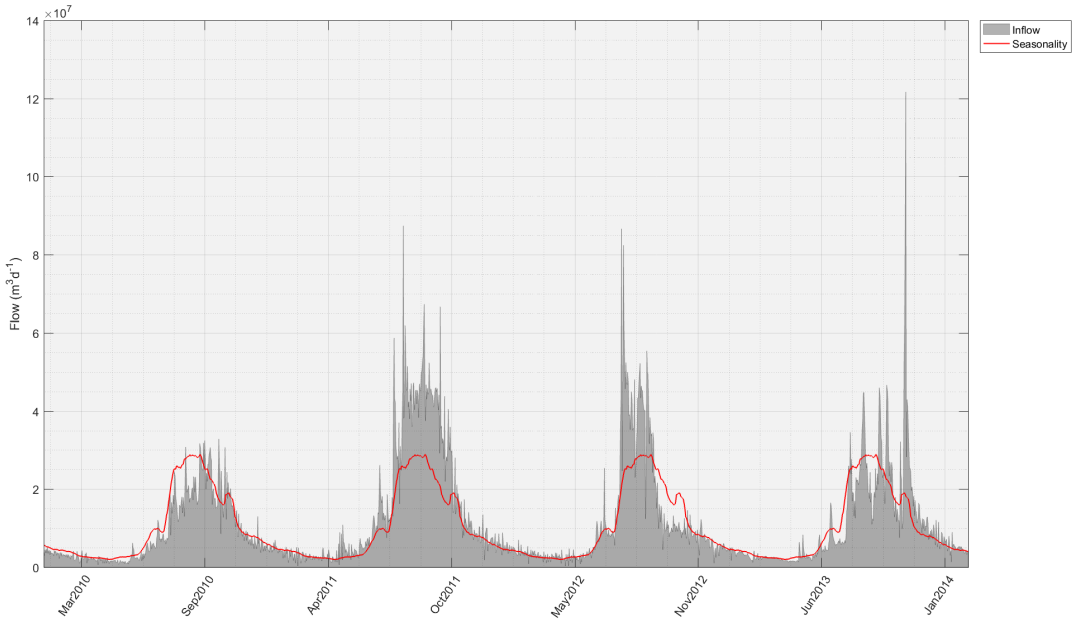

Figure 3.4: Inflows to the Paunglaung reservoir between January 1, 2010 and February 8, 2014 (grey). The red line is the seasonality derived by taking the average inflow for each day over the years in the dataset and then taking the 15-day moving average of that timeseries.

4

The two-stage model predictive control system

This chapter presents the two-stage MPC approach developed for the reservoir system in the Sittaung basin. Section 4.1 introduces the general structure of the MPC system. In section 4.3, a two-stage MPC method combining decentralized MPC (stage 1) and coordinated MPC (stage 2) is presented. In section 4.4 the optimization problem is formulated for both stages. The optimization problems are non-linear. They are solved with an interior-point method. Finally, section 4.5 discusses the interior-point method used in this research.

4.1. The general structure of the MPC system

Model predictive control (MPC) is a control strategy for a system using a model to simulate the system's response to control actions for finding optimal operation. Various applications of MPC include robotics, chemical industry, the oil industry and aviation. The development of MPC techniques was motivated by multivariate constrained control problems, which were difficult to solve with the available methods at the time. In the simulation model of the system dynamics, the large-scale multivariate system dynamics is included explicitly in the controller. Also, an advantage of MPC as opposed to classical control methods is that constraints can be explicitly included (Camacho et al., 2007). The core principle of MPC methods is the receding horizon principle (García et al., 1989). The system simulated system response is calculated for a finite optimization horizon for which optimal control is calculated. The optimal control is implemented for the first timestep only. At the next timestep, the optimization horizon is shifted one timestep ahead and the optimal control is recalculated. This principle allows for an on-line (real-time) optimization approach, incorporating up to date information about the system and the most recent predictions at each time step. Van den Boom and Backx (2005) remark that MPC is more akin to a methodology than a single technique. They identify five things present in all MPC methods: a prediction model for the internal system dynamics and for the external disturbances, an objective function, constraints, optimization and the receding horizon principle. Each of these items is discussed with respect to the operation of the reservoir system in the Sittaung basin. Control actions are, in this case, the operation of the conduits and irrigation offtakes. The daily timesteps for the MPC system and control actions correspond to the daily operating schedule implemented by the reservoir operators. The objective function, constraints, internal system and external disturbances are discussed more broadly as the choice of these items is different for stage 1 and 2 (the two-stage approach is further described in section 4.3. The exact definitions are presented in section 4.4.

The objectives and constraints in the optimal control problem formulation The objective function is a performance index based on the objectives of the control problem. In the Sittaung basin the objectives are flood mitigation, maximizing hydropower generation, and sufficient water for irrigation. These objectives are combined in the objective function as a weighted sum. The weights indicate the relative importance of the

objective.

The constraints define the limitations of the system, for example the capacities of the conduits or reservoirs. Constraints can also be used to enforce specific system behaviour, for example ensuring that irrigation off-takes are never larger than the irrigation demand.

The internal system and external disturbances The internal system is the part of the system affected by control actions and relevant for the control objectives. For example, the storages in the reservoirs are part of the internal system. They are affected by operational decisions for the reservoir conduits and relevant to the water available for hydropower and irrigation. Part of the catchment outflow flowing directly into the river, and therefore not passing through a reservoir, cannot be controlled by reservoir operation. Hence, they are not part of the internal system. These inflows influence the water levels in the river, which is part of the internal system dynamics. This makes the inflows relevant to the control problem. They are defined as external disturbances of the system. External disturbances are factors affecting the internal system dynamics, but that can not be affected by control actions.

The internal system is modelled using a state-space model. In a state-space representation a distinction is made between state variables x^k, input u^k and output y^k variables and external disturbances w^k, with k the discrete timestep. Van den Boom and Backx (2005) presents the following discrete time state-space representation for linear time-invariant systems:

$$x^{k+1} = Ax^k + Bu^k + Dw^k \tag{4.1}$$

$$y^k = Fx^k + Gu^k \tag{4.2}$$

State variables x are the system variables necessary to describe the state of the system at any given timestep k. Inputs u represent the control actions, which are decisions made by the operator, such as the releases through the conduits of the reservoirs. Outputs y are all states of the system model that are measured in the real system, such as the water level in the river. Equation 4.1 shows that the model can fully determine the state of the internal system for the next timestep based on the state, inputs and external disturbances on the current timestep. Equation 4.2 gives a model for the outputs as a function of the state and input variables.

Note that, the discrete state-space model is an approximation of the continuous system dynamics. The reason for considering the discrete time state-space model is, that the state equations are included in discrete form in the nonlinear optimization problem presented later in this chapter. Section 4.2 discusses the transcription of the optimal control problem to the nonlinear optimization problem.

Figure 4.1 is based on figure 1.2 in Camacho et al. (2007) and demonstrates the basic structure of MPC at discrete timestep k for an optimization horizon of T_{opt} timesteps. The model of the internal system predicts the system's response to future inputs (control actions) and predicted future external disturbances at timesteps $k \ldots (k + T_{\text{opt}} - 1)$, using information about the inputs, outputs and external disturbances of the real system at timestep $k-1$. In the case of the Sittaung basin, the model of the internal system would model the storage in the reservoir (predicted output) in response to the decision to close the conduit today (future input). For this, the model needs information about yesterday's outflows from the conduit (past input), reservoir storage (past output) and reservoir inflow (past external disturbance). Also, it needs a prediction of tomorrow's inflow to the reservoir (predicted external disturbance). The predicted outputs of the system are used by the optimizer.

The optimizer The optimizer uses the predicted outputs to optimize future inputs at all timesteps in the optimization window, $k \ldots (k + T_{\text{opt}} - 1)$, while considering the cost function and constraints. For example, the optimizer uses the predicted storages in the reservoir for different conduit releases, to decide which conduit releases would maximize hydropower generation over the total optimization horizon. In doing so, the optimizer takes the maximum conduit capacity into account.

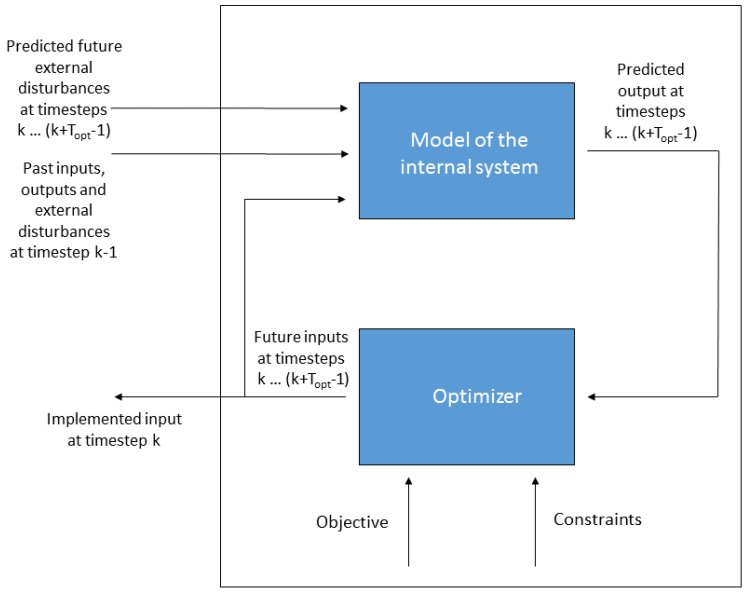

Figure 4.1: Structure of the MPC method performed on timestep k.

The receeding horizon principle At timestep k, the optimization determines optimal releases through the conduit for each timestep in the optimization horizon. However, the control actions are implemented for timestep k only. At timestep $k+1$, this procedures is repeated for the window of timesteps $(k+1)...(k+T_{\text{opt}})$, with the actual flow through the conduit, storage and inflow to the reservoir at timestep k available to the MPC system. When solving the optimization problem at timestep $k+1$ for the time window $(k+1)...(k+T_{\text{opt}})$, the optimal solution for timesteps $(k+1)...(k+T_{\text{opt}}-1)$ calculated at timestep k is provided as an initial solution to the optimization algorithm. This is called warm-starting and often reduces computation time significantly. The effect of warm-starting is considered in chapter 5.

4.2. The transcription method for the control problem to an optimization problem

The MPC system solves an optimal control problem. An optimal control problem can be stated in general form

$$\begin{aligned}
\underset{u(t)}{\text{minimize}} \quad & \int_{t_0}^{t_f} \mathscr{L}(u(t), x(t), w(t), t)\, dt \\
\text{subject to} \quad & \frac{dx(t)}{dt} = Ax(t) + Bu(t) + Dw(t), \qquad t \in [t_0, t_f], \\
& c(x(t), u(t), w(t), t) \leq 0, \qquad t \in [t_0, t_f], \\
& x(t_0) = x_0.
\end{aligned}$$

Here, $x(t) \in \mathbb{R}^{n_x}$, $u(t) \in \mathbb{R}^{n_u}$ and $w(t) \in \mathbb{R}^{n_w}$ are vectors of control and state variables and external disturbances at time t, with n_x the number of state variables, n_u the number of control variables and n_w the number of external disturbances. $\mathscr{L} : \mathbb{R}^{n_x} \times \mathbb{R}^{n_u} \times \mathbb{R}^{n_w} \times [t_0, t_f] \to \mathbb{R}$ is the objective function. $c(x(t), u(t), w(t), t) : \mathbb{R}^{n_x} \times \mathbb{R}^{n_u} \times \mathbb{R}^{n_w} \times [t_0, t_f] \to \mathbb{R}^{n_c}$ is a vector function for the path constraints, with n_c the number of path constraints. A, B, D are constant real matrices and x_0 a real vector of appropriate sizes. The objective function presented here is in Lagrange form, optimizing the performance over the trajectory from t_0 to t_f. Other options are a Mayer form or Bolza form, which will not be considered here (Betts, 2010). The problem is subject to the state equations, path constraints and initial conditions. The state equations are given for a linear

time-invariant system (the system considered in this research). The control problem is a continuous-time problem, making it an infinite-dimensional problem. The MPC method used to solve this problem requires it to be transcribed into a finite-dimensional approximation of the problem, characterised by a finite set of variables and constraints (Betts, 2010). The finite-dimensional approximation of the problem is a mathematical programming problem. In order to do this, the problem is considered on discrete timesteps for a finite optimization horizon. The objective function, state equations and constraints are all discretized. The control variables and input variables at each discrete timestep in the optimization horizon are treated as optimization variables in the optimization problem. Note that the size of the NLP depends on the number of state and input variables of the control problem and the defined optimization horizon.

The discretization of the control problem is an approximation of the control problem. The reservoir system in the Sittaung basin is currently operated on a daily basis, the operators of the reservoirs change the settings of the conduits of the reservoirs once a day. Also, most of the data available to calibrate the model of the system dynamics and validate the control system are only available on a daily basis. For this reason, the discrete timesteps were chosen to be one day. The discretization of the system dynamics, constraints and objective function is expected to be sufficiently accurate for the application in this research. Before describing the optimization problem in section 4.4, the two-stage MPC method implemented in this research is described in section 4.3.

4.3. The two-stage MPC method

One of the aims of this research is to investigate whether better coordination of the operation of the reservoirs in the basin would improve flood control. The internal system for the MPC must then be defined as the complete system of 21 reservoirs and the river dynamics, with one control problem optimizing all reservoirs simultaneously. For the model set-up as described in chapter 3 including all 21 reservoirs and the 17 river sections, this would result in $21 \cdot 4 + 17 \cdot 3 = 303$ state and control variables per timestep. For an optimization horizon of one year, 365 days, this results in an NLP with 110 595 optimization variables. Even though methods for solving problems of this size are available, for nonlinear constrained optimization problems this can be computationally expensive (Betts (2010) , Gould et al. (2005)).

In this research, a two-stage MPC method is suggested. This two-stage method is a way to reduce the optimization problem for the Sittaung basin to smaller sub-problems when possible. Many researchers have investigated ways to apply MPC on large-scale problems by solving smaller sub-problems. Christofides et al. (2013) distinguish between centralized and decentralized MPC. In centralized MPC all control variables are optimized with respect to one objective function in one optimization problem. Centralized model predictive control results in a system wide optimal solution, but the large number of state and control variables may result in large computation times, especially for nonlinear constrained optimization problems. In decentralized control, various subproblems are optimized separately without taking interaction or system-wide objectives into account. This decreases the size of the optimization problem, but system wide optimality is not always achieved. Rawlings and Stewart (2007) discuss communication-based control and cooperative control in addition to centralized and decentralized control. In communication-based control each subsystem is optimized using a model of the subsystem and an interaction model. Information about control actions and states of other subsystems at previous timesteps is available to the subsystem, but the objective function for each subsystem is local. Cooperative control also uses an interaction model as well as information about control actions and states of other subsystems. Communication-based control differs in that it uses a copy of the system-wide objective function for the optimization of each subsystem, instead of the local objective function. Maestre et al. (2011) also present a distributed model predictive control method in which the subsystems exchange information and aim for system-wide optimality.

The application of these types of MPC methods on water systems has been investigated by Anand et al. (2013), Breckpot et al. (2010),Doan et al. (2013) , Negenborn et al. (2009) and Niewiadomska-Szynkiewicz et al. (1996). Negenborn et al. (2009) present an overview of distributed model predictive control methods for irrigation canals. Anand et al. (2013) apply coordinating multiple model predictive controllers to the management of a two multi-purpose reservoir system with the objectives of hydropower generation, flood protection for the upstream reservoir, and irrigation supply and flood protection for the downstream reservoir. Niewiadomska-Szynkiewicz et al. (1996) consider a hierarchical real-time control method for flood operation of a system of three reservoirs in the southern part of Poland. Each of the reservoirs had hydropower generation and

water supply as a local objective as well as flood protection as a system-wide objective. Breckpot et al. (2010) studies a three-reservoir system for flood control in a river and Doan et al. (2013) studies a three-reservoir cascade system for hydropower generation. No literature was found on the application of MPC methods for multi-purpose reservoir system of 21 reservoirs size or larger.

The method presented in this research makes use of a decentralized MPC method (stage 1) and a coordinated MPC method (stage 2). The reservoirs in the basin are each defined as a subsystem of the total system of reservoirs and the Sittaung river. The decentralized MPC of stage 1 is used in periods without flood risk. Each of the subsystems is optimized separately for hydropower generation and irrigation supply. In periods of flood risk, the method switches to the coordinated MPC of stage 2. For stage 2, each of the subsystem is optimized for the system-wide objective of flood mitigation and hydropower generation. The switching from stage 1 to 2 and from stage 2 to 1 occurs based on the water levels in the river. Figure 4.2 gives a schematic overview of this procedure. The respective optimization problems for stage 1 and stage 2 are formulated in section 4.4.

Stages 1 and 2 each have their respective optimization horizons, T_{opt1} and T_{opt2}. At timestep k, the stage 1 optimization problem is solved individually for each of the reservoirs for hydropower generation and irrigation water supply. Then, the model for the total reservoir system and river dynamics simulates the water levels in the river for the stage 1 optimal operation of all reservoirs for timesteps $k...(k+T_{\text{opt2}}-1)$. If no flood is expected at the defined flood location based on this simulation, the optimal operation of stage 1 is implemented for timestep k and the process starts again for timestep $k+1$. If a flood is expected at the flood location at one or more timesteps between $k...(k+T_{\text{opt2}}-1)$, the system switches to stage 2 for the reservoirs upstream of the flood location. Note that the reservoirs downstream of the flood location are always optimized in stage 1, as their operation does not have impact on floods.

In stage 2, the control actions for one subsystem (reservoir) are optimized for the system-wide objectives of stage 2, flood mitigation and hydropower generation. Stage 2 loops over all reservoirs upstream of the flood location, optimizing the operation of one reservoir at a time. The optimal operation of the optimized subsystem is fixed before moving to the next subsystem. This means that when optimizing subsystem j, the operation of subsystems $1...(j-1)$ is fixed at the stage 2 optimization of the current timestep. The operation of the reservoirs that have not been optimized for stage 2 at this timestep, is fixed at the initial solution provided to stage 2. This is either the stage 1 optimal operation of the current timestep if the MPC system switched to stage 2 at this timestep, or the stage 2 optimal operation of the previous timestep if the MPC system was already in stage 2 in the preceding timestep.

After the optimization for all subsystems upstream of the flood location is performed, the optimal solution is implemented for timestep k. The maximum water level at the flood location in the simulation for all timesteps $k...(k+T_{\text{opt2}}-1)$ is considered. If this water level is lower than a specified flood level minus an offset, the MPC system will switch back to stage 1. If the maximum water level is higher than the specified flood level minus offset, the MPC system will continue in stage 2. In this research, the criterion for switching back has not been studied, this should be investigated in future work.

4.4. The formulation of the optimization problem

The control problem is formulated as a non-convex non-linear programming problem for both stages. In this section the objective function and constraints are given. The gradient of the objective, Jacobian of the constraints and Hessian of the Lagrangian are given in Appendix C for stage 1 and in Appendix D for stage 2. Table 4.1 gives the optimization variables for both stages of MPC.

4.4.1. The formulation of the optimization problem for stage 1

In stage 1 the MPC system optimal control for only one reservoir only is determined, optimizing for hydropower generation and irrigation supply. The internal system in this case describes a single reservoir, modelled with one linear equality constraint and two linear inequality constraints.

The optimization variables and variable bounds for stage 1 The variables of the reservoir are the storage in the reservoir S_{res} (m^3), the flow through the conduit Q_{c} ($\text{m}^3\ \text{d}^{-1}$), the flow through the spillway Q_{s} ($\text{m}^3\ \text{d}^{-1}$)

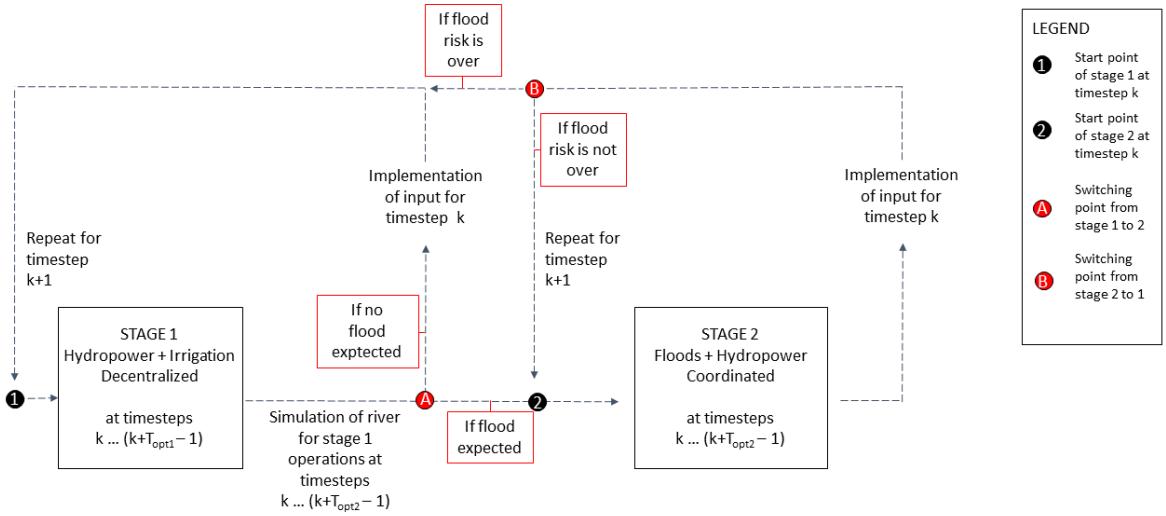

Figure 4.2: Schematic representation of the two-stage MPC method.

and the irrigation offtake Q_{ir} ($\text{m}^3\ \text{d}^{-1}$). Hence, for stage 1 there are only four variables at each timestep k, where each timestep is one day.

The storage in the reservoir is limited by the storage capacity $\overline{S_{\text{res}}}$ (m^3) for that reservoir and the conduit release is limited by the capacity of the conduit $\overline{Q_{\text{c}}}$ ($\text{m}^3\ \text{d}^{-1}$). The irrigation offtake is limited by the demand $\overline{Q_{\text{ir}}}$ ($\text{m}^3\ \text{d}^{-1}$), ensuring that no more water is used for irrigation beyond what is required. This is necessary because the water taken for irrigation does not flow into the river. If the irrigation offtake were not limited from above, the stage 2 optimization could prevent water passing through the conduit from flowing into the river in order to prevent floods. Note that the reservoir capacity $\overline{S_{\text{res}}}$ and conduit capacity $\overline{Q_{\text{c}}}$ are different per reservoir and that the irrigation demands $\overline{Q_{\text{ir}}}$ are different per reservoir and per month. This is indicated by subscript $(\cdot)_j$ and superscript $(\cdot)^k$ where necessary, but these were omitted in table 4.1 to keep the table legible.

The optimization variables are combined in the vector x. To make notation in stage 2 easier, a distinction is made between reservoir variables x_{res} and river and flood variables x_{riv} and x_{fl}. For stage 1, only reservoir variables are included in the optimization, so when

$$x_{\text{res}}^k := \begin{bmatrix} S_{\text{res}}^k & Q_{\text{s}}^k & Q_{\text{c}}^k & Q_{\text{ir}}^k \end{bmatrix}, \tag{4.3}$$

the optimization variables are defined as

$$x^T := x_{\text{res}}^T = \begin{bmatrix} x_{\text{res}}^1 & \dots & x_{\text{res}}^{T_{\text{opt}}} \end{bmatrix} \tag{4.4}$$

$$= \begin{bmatrix} S_{\text{res}}^1 & Q_{\text{s}}^1 & Q_{\text{c}}^1 & Q_{\text{ir}}^1 & \dots & S_{\text{res}}^{T_{\text{opt}}} & Q_{\text{s}}^{T_{\text{opt}}} & Q_{\text{c}}^{T_{\text{opt}}} & Q_{\text{ir}}^{T_{\text{opt}}}, \end{bmatrix} \tag{4.5}$$

with

The objective function for stage 1 In stage 1 two terms are included in the objective function, the hydropower generation $f_{\text{hp}}(x)$ and irrigation supply $f_{\text{ir}}(x)$, both of which will be maximized. Both terms are

Table 4.1: Variables in optimization problem for each timestep of the optimization horizon with their symbol, units, bounds and meaning. The columns 'Stage 1' and 'Stage 2' specify if the variable was included in the optimization problem and if so, for how many components.

	Variable	Symbol	Unit	Bounds	Stage 1	Stage 2
Reservoir	Storage of the reservoir	S_{res}	m^3	$[0, \overline{S_{\text{res}}}]$	1	1
	Spillway release	Q_{s}	m^3d^{-1}	$[0, \infty]$	1	1
	Conduit release	Q_{c}	m^3d^{-1}	$[0, \overline{Q_{\text{c}}}]$	1	1
	Irrigation offtake	Q_{ir}	m^3d^{-1}	$[0, \overline{Q_{\text{ir}}}]$	1	1
River section	Storage of river section	S_{riv}	m^3d^{-1}	$[0, \infty]$	-	17
	Inflow to river section	$Q_{\text{in,riv}}$	m^3d^{-1}	$[0, \infty]$	-	17
	Outflow from river section	$Q_{\text{out,riv}}$	m^3	$[0, \infty]$	-	17
Flood constraint	Slack variable	d	m^3	$[0, \infty]$	-	1
Total per timestep					4	56

normalized by division through their maximum values $\overline{f_{\text{hp}}}$ and $\overline{f_{\text{ir}}}$. The weights β_1 and β_2 are varied to change the relative importance of hydropower and irrigation. β is the scaling factor for the objective function, which will be discussed in subsection 4.5.2.

$$f(x) := \hat{\beta}\left(\beta_1 f_{\text{hp}}(x) + \beta_2 f_{\text{ir}}(x)\right) \tag{4.6}$$

As discussed in section 3.5 of chapter 3, hydropower generation is calculated as the flow through the conduit times the storage in the reservoir multiplied by a positive constant factor. The constant is left out of the objective function because it disappears in the normalization otherwise. The term $f_{\text{hp}}(x)$ is defined as

$$f_{\text{hp}}(x) := \frac{1}{\overline{f_{\text{hp}}}} \sum_{k=1}^{T_{\text{opt}}} \left(S_{\text{res}}^k Q_{\text{c}}^k\right) \tag{4.7}$$

$$\overline{f_{\text{hp}}} = T_{\text{opt}} \overline{S_{\text{res}} Q_{\text{c}}} \tag{4.8}$$

Note that the hydropower term makes the objective function non-convex. The term for irrigation supply is defined as

$$f_{\text{ir}}(x) := \frac{1}{\overline{f_{\text{ir}}}} \sum_{k=1}^{T_{\text{opt}}} \left(Q_{\text{ir}}^k\right). \tag{4.9}$$

The maximum irrigation supply is the demand, which is time dependent and therefore indicated with a superscript k. In order to normalize the irrigation term, the factor is defined as the yearly average of the irrigation demand per day times the optimization horizon (equation 4.10). Note that the irrigation term can exceed one if the optimization horizon is not equal to one year and the period considered has above-average irrigation demands. The reason why the term is not normalized with the demand itself, which is the exact maximum for this term, is that in periods of higher demand the irrigation term would be scaled with a larger factor. This is undesirable because less weight is given to irrigation in periods of high demand. Scaling with the yearly average demand applies the same factor for each considered period. Multiplication with T_{opt} for

both scaling factors, $\overline{f_{\text{hp}}}$ and $\overline{f_{\text{ir}}}$, is done so that the objective function does not become significantly smaller for small optimization horizons than for large optimization horizons. This relates to the issue of scaling of the objective function, which is discussed in subsection 4.5.2.

$$\overline{f_{\text{ir}}} := \frac{T_{\text{opt}}}{365} \sum_{k=1}^{365} \left(\overline{Q_{\text{ir}}}^{k} \right) \tag{4.10}$$

The constraints for stage 1 The dynamics of the reservoir, as given by equation 3.5 in chapter 3, are included in the optimization problem through the linear equality constraint $c^k_{\text{eq1}}(x$ defined in equation 4.11. Note that $Q^{k-1}_{\text{in,res}}$ is the inflow to the reservoir (m^3d^{-1}) at time $k-1$. This is fixed and not an optimization variable. It is an external disturbance to the control problem as discussed in section 3.7.

$$c^k_{\text{eq1}}(x) := -S^k_{\text{res}} + S^{k-1}_{\text{res}} + \left(-Q^{k-1}_{\text{c}} - Q^{k-1}_{\text{s}} \right) \Delta t + Q^{k-1}_{\text{in,res}} \Delta t = 0 \tag{4.11}$$

The flow through the conduit during a single timestep can never be larger than the storage in the reservoir at the beginning of that timestep, as stated by linear inequality constraint $c^k_{\text{ineq1}}(x)$ defined in equation 4.12. Also, the offtake for irrigation happens downstream from the conduit and can therefore never be larger than the conduit release, as stated by linear inequality constraint $c^k_{\text{ineq2}}(x)$ defined in equation 4.13.

$$c^k_{\text{ineq1}}(x) := Q^k_{\text{c}} - S^k_{\text{res}} \leq 0 \tag{4.12}$$

$$c^k_{\text{ineq2}}(x) := Q^k_{\text{ir}} - Q^k_{\text{c}} \leq 0 \tag{4.13}$$

Note that the constraints are all linear, so that the equality and inequality constraints can be written in the form

$$A_e x - b_e = 0 \quad \text{and} \quad A_i x - b_i \geq 0, \tag{4.14}$$

with constant matrices $A_e \in \mathbb{R}^{(m \times n)}$ and $A_i \in \mathbb{R}^{(p \times n)}$ and constant vectors $b_e \in \mathbb{R}^m$ and $b_i \in \mathbb{R}^p$ for n the number of optimization variables, m the number of equality constraints and p the number of inequality constraints. For stage 1, $n = 4 \cdot T_{\text{opt}}$, $m = T_{\text{opt}}$ and $p = 2 \cdot T_{\text{opt}}$.

The first- and second-order derivatives of the objective function and constraints The gradient of the objective, the Jacobian of the constraints and the Hessian of the Lagrangian, are given in appendix C. These derivative matrices are fed to the optimization algorithm and will be used in further analysis of the optimization problem in section 4.5.

4.4.2. The formulation of the optimization problem for stage 2

In stage 2, the internal model of the complete system is included in the optimization. The method by which floods are penalized and spillway behaviour is included is discussed. The resulting NLP is discussed in relation to the variables, variable bounds, the constraint and objective function. The gradient of the objective, the Jacobian of the constraints and the Hessian of the Lagrangian for stage 2 are given in appendix D.

Penalizing floods in the objective function The aim of stage 2 of the MPC system is to prevent or reduce floods. However, it is not always possible to prevent floods in river section 7, the section near Taungoo city, by adjusting the reservoir operation. If the water level is required to stay below flood level in an inequality constraint, this could result in an optimization problem without feasible solutions. For this reason, an additional variable is introduced x^k_{fl}, to define the inequality constraint $c^k_{\text{ineq3}}(x)$,

$$c^k_{\text{ineq3}}(x) := \left(S^k_{\text{riv}}\right)_7 - x^k_{\text{fl}} - A_{\text{riv}} L_{\text{flood}} \leq 0. \tag{4.15}$$

where A_{riv} is the conversion factor [m^2] from water level to storage for river section 7 (table G.1 appendix G). The parameter L_{flood} is the defined flood level in meters. The variable x^k_{fl} is defined to be positive. It is the volume with which the storage in section 7 exceeds the maximum storage based on the flood level. The sum of x^k_{fl} at all timesteps in the optimization horizon is minimized in the objective function by including the term

$$f_{\text{fl}}(x) := \frac{1}{\overline{f_{\text{fl}}}} \sum_{k=1}^{T_{\text{opt}}} x^k_{\text{fl}}. \tag{4.16}$$

This flood term in the objective function is penalizing the exceedence of the flood level instead of limiting the water level directly. It is not clear how the flood term in the objective function should be normalized, because no strict maximum can be defined. The flood term was normalized by dividing it by the average exceedence of a flood level in stage 1 for the year considered in stage 2 times the optimization horizon,

$$\overline{f_{\text{fl}}} := \frac{T_{\text{opt}}}{365} \sum_{k=1}^{365} \overline{x_{\text{fl}}}^k, \tag{4.17}$$

where $\overline{x_{\text{fl}}}^k$ is the total discharge above flood level in stage 1, i.e.

$$\overline{x_{\text{fl}}}^k := \left(\left(S^k_{\text{riv}}\right)_7 - A_{\text{riv}} L_{\text{flood}}\right)^+. \tag{4.18}$$

In order to use the same normalization factor when different flood levels are considered, a typical flood level will be chosen in chapter 5 based on the results of stage 1. It is possible that the sum of flood variables for the optimization horizon is larger than the normalization factor. However, it scales the flood term in the objective to a smaller value which simplifies the selection of the right weights for the other objectives.

The inclusion of the spillway dynamics in the optimization problem The non-linear and non-smooth equation (eq. 3.3, chapter 3) describes the flow through the spillway. This equation states that the spillway only releases water if the storage in the reservoir exceeds the storage capacity. The amount spilled is exactly this exceeding amount. This equation was not required in stage 1, because maximizing hydropower generation and irrigation supply without any other objectives will never result in a policy were more water is spilled than absolutely necessary. Flow through the conduit generates hydropower whereas flow through the spillway does not, so the optimal operation maximizing hydropower generation will always prefer flow through the conduit over flow through the spillway if it decides to release water from the reservoir. Also, the higher the water level in the reservoir, the more hydropower is produced. So the optimization will only decide to release water through the spillway if the storage in the reservoir exceeds its maximum capacity.

In stage 2 however, when flood control is included in the objective, the flow through the spillway needs to be prescribed to ensure only physically meaningfull spilling occurs. If the flow through the spillway is a free variable in the optimization, an optimal solution for preventing floods could be to spill water when the reservoir is not yet full. In reality, this is not possible. The flow through the spillway could be formulated using a complementarity constraint,

$$Q^k_{\text{s}}\left(Q^k_{\text{s}}\Delta t - \alpha^k\right) = 0, \quad Q^k_{\text{s}} \geq 0, \quad \left(Q^k_{\text{s}}\Delta t - \alpha^k\right) \geq 0, \tag{4.19}$$

with α as defined in equation 3.4 in chapter 3,

$$\alpha := S_{\text{res}}^k + \left(-Q_{\text{c}}^k + Q_{\text{in,res}}^k\right)\Delta k - \overline{S_{\text{res}}}. \tag{4.20}$$

The term α can be understood as the volume exceeding the storage capacity at timestep k if the spillway constraint does not become active. A complementarity constraint ensures that two terms are complementary to one another, meaning that for two positve terms their inner product should be zero. Note that the formulation of the complementarity constraint is equivalent to equation 3.3 in chapter 3

$$Q_{\text{s}} = \begin{cases} 0 & \alpha < 0 \\ \frac{\alpha}{\Delta k} & \alpha > 0 \end{cases}. \tag{4.21}$$

When the exceeding amount α^k is negative, i.e. the storage capacity is larger than the current storage, no spilling should occur. If the term $\left(Q_{\text{s}}^k \Delta t - \alpha^k\right)$ in equation 4.19 is strictly positive, the complementarity constraint requires that $Q_s^k = 0$. When α^k is positive, the current storage will exceed the storage capacity if the spillway constraint is not in place. In that case, the spillway should spill exactly the exceeding amount, as expressed by equation 4.21. In that situation, the term Q_{s}^k is strictly positive, so equation 4.19 requires $\left(Q_{\text{s}}^k \Delta t - \alpha^k\right) = 0$.

Complementarity constraints are hard to deal with for solvers of nonlinear programs as they are not smooth Betts (2010). Including a complementarity constraint as a soft constraint, which allows the solver to solve for it approximately instead of exactly, is a typical work-around for this problem. The violation of the complementarity constraint is included in the objective function with the following term

$$f_{\text{sp}}(x) := \frac{1}{\overline{f_{\text{sp}}}} \sum_{k=1}^{T_{\text{opt}}} Q_{\text{s}}^k \left(Q_{\text{s}}^k \Delta t - \alpha^k\right). \tag{4.22}$$

Note $Q_{\text{s}}^k \geq 0$ is required by the variable's lower bound and that

$$\left(Q_{\text{s}}^k \Delta t - \alpha^k\right) = \overline{S_{\text{res}}} - \left(S_{\text{res}}^k + \left(-Q_{\text{sp}}^k - Q_{\text{c}}^k + Q_{\text{in,res}}^k\right)\Delta k\right) \tag{4.23}$$

$$= \overline{S_{\text{res}}} - S_{\text{res}}^{k+1} > 0, \tag{4.24}$$

$$\tag{4.25}$$

as required by the upper bound on S_{res}^k. This means that the term $f_{\text{sp}}(x)$ is always positive for a feasible solution. The term is minimized by penalizing it in the objective. In this way, the complementarity constraint is included as a soft constraint instead of a hard constraint. The stage 2 optimization problem is solved iteratively with a spillway penalty increasing from 0 to larger values, using the solution of each iteration as a starting point for the next iteration Pecci et al. (2017). In subsection 5.2.2 of chapter 5 appropriate choices for a value of the penalty are discussed. The following paragraphs describe the NLP problem formulation for stage 2.

The optimization variables and variable bounds for stage 2 Table 4.1 shows the variables and their bounds, for stage 1 and 2. The variables and variable bounds for the reservoirs in stage 2 are the same as for stage 1. For stage 2, the three variables per river section are included: the storage in the river section S_{riv}, the inflow to the river section $Q_{\text{in,riv}}$ and the outflow from the river section $Q_{\text{out,riv}}$. The variables are all limited from beneath by zero and unlimited from above.

Finally, the flood variable x_{fl} is included in stage 2. This is the amount by which the storage in the river section near Taungoo exceeds the maximum storage based on the defined flood level. This variable allows

floods to be included in the objective function as discussed earlier. The flood variable is bounded from below by zero.

The optimization variables x for stage 2 are

$$x := \begin{bmatrix} x_{\text{res}}^1 & x_{\text{riv}}^1 & x_{\text{fl}}^1 & \dots & x_{\text{res}}^{T_{\text{opt}}} & x_{\text{riv}}^{T_{\text{opt}}} & x_{\text{fl}}^{T_{\text{opt}}} \end{bmatrix}^T, \tag{4.26}$$

with

$$x_{\text{res}}^k := \begin{bmatrix} S_{\text{res}}^k & Q_{\text{s}}^k & Q_{\text{c}}^k & Q_{\text{ir}}^k \end{bmatrix}^T, \tag{4.27}$$

and

$$x_{\text{riv}}^k := \begin{bmatrix} (S_{\text{riv}}^k)_1 & \left(Q_{\text{in,riv}}^k\right)_1 & \left(Q_{\text{out,riv}}^k\right)_1 & \dots & (S_{\text{riv}}^k)_{17} & \left(Q_{\text{in,riv}}^k\right)_{17} & \left(Q_{\text{out,riv}}^k\right)_{17} \end{bmatrix}^T. \tag{4.28}$$

The notation $(.)_i$ is used to indicate the variable for river section i.

The objective function for stage 2 Two terms are added to the objective function, the flood term $f_{\text{fl}}(x)$ for the minimization of floods and the spillway term $f_{\text{sp}}(x)$ for the minimization of violation of the spillway constraint,

$$f(x) := \hat{\beta}\left(\beta_1 f_{\text{hp}}(x) + \beta_2 f_{\text{ir}}(x) - \rho_1 f_{\text{fl}}(x) - \rho_2 f_{\text{sp}}(x)\right). \tag{4.29}$$

The terms $f_{\text{fl}}(x)$ and $f_{\text{sp}}(x)$ are defined by equation 4.16 and equation 4.22. The parameters ρ_1 and ρ_2 are weight factors. Chapter 5 discusses appropriate choices for the weight factors based on the results. Note that for stage 2, not only the term $f_{\text{hp}}(x)$ makes the objective function non-convex, but also the term $f_{\text{sp}}(x)$.

The constraints for stage 2 The linear equality constraint for the reservoir dynamics in stage 2 is the same as $c_{\text{eq1}}(x)$ given by equation 4.11. Additional equality constraints are derived from the governing equations for the river dynamics as presented in chapter 3. Equation 3.9 and equations 3.10-3.13 give the relations for the variables S_{riv} and $Q_{\text{out,riv}}$. Equation 3.15 prescribes $Q_{\text{in,riv}}$. These can be rewritten as linear equality constraints:

$$\left(c_{\text{eq2}}^k\right)_i(x) := \left(S_{\text{riv}}^k\right)_i + \frac{\Delta t}{2}\left(Q_{\text{in,riv}}^k\right)_i - \frac{\Delta t}{2}\left(Q_{\text{out,riv}}^k\right)_i - \left(S_{\text{riv}}^{k+1}\right)_i + \frac{\Delta t}{2}\left(Q_{\text{in,riv}}^{k+1}\right)_i - \frac{\Delta t}{2}\left(Q_{\text{out,riv}}^{k+1}\right)_i = 0, \quad \text{for } i = 1,\dots,17, \tag{4.30}$$

and

$$\left(c_{\text{eq3}}^k\right)_i(x) := c_2\left(Q_{\text{in,riv}}^k\right)_i + c_3\left(Q_{\text{out,riv}}^k\right)_i + c_1\left(Q_{\text{in,riv}}^{k+1}\right)_i - \left(Q_{\text{out,riv}}^{k+1}\right)_i = 0, \quad \text{for } i = 1,\dots,17, \tag{4.31}$$

with c_1, c_2 and c_3 defined as in equation 3.11 - 3.13 in chapter **??**. The constraint becomes

$$\left(c_{\text{eq4}}^k\right)_i(x) := \left(Q_{\text{out,riv}}^k\right)_{i-1} - \left(Q_{\text{in,riv}}^k\right)_i + \sum_{j\in\{\mathbb{S}_i\cap\hat{j}\}}\left(Q_{\text{out,res}}^k\right)_j + \left(Q_{\text{out,catchm}}^k\right)_i + \sum_{j\in\{\mathbb{S}_i\setminus\hat{j}\}}\left(Q_{\text{out,res}}^k\right)_j = 0, \quad \text{for } i = 1,\dots,17, \tag{4.32}$$

with $\mathbb{S}_i$ as defined in equation 3.14 in chapter 3 and $\widehat{j}$ the reservoir for which the operation is adjusted in the optimization.

The linear inequality constraints $c^k_{\text{ineq1}}(x)$ and $c^k_{\text{ineq2}}(x)$ given by equations 4.12 and 4.13 for stage 1 are also included in stage 2. The inequality constraint $c^k_{\text{ineq3}}(x)$ presented in equation 4.15 is the final inequality constraint for stage 2.

Just as in stage 1, all linear, so that the equality and inequality constraints can be written in the form

$$A_e x - b_e = 0 \quad \text{and} \quad A_i x - b_i \geq 0, \tag{4.33}$$

with constant matrices $A_e \in \mathbb{R}^{(m\times n)}$ and $A_i \in \mathbb{R}^{(p\times n)}$ and constant vectors $b_e \in \mathbb{R}^m$ and $b_i \in \mathbb{R}^p$ for n the number of optimization variables, m the number of equality constraints and p the number of inequality constraints. The vectors and matrices re given in D. For stage 1, $n = 56 \cdot T_{\text{opt}}$, $m = 52 \cdot T_{\text{opt}}$ and $p = 3 \cdot T_{\text{opt}}$.

The first- and second-order derivatives of the objective function and constraints The gradient of the objective, Jacobian of the constraints and Hessian of the Lagrangian are given in appendix D. These matrices are provided to the optimization algorithm and will be used in further analysis of the optimization problem in section 4.5.

4.5. A primal-dual interior-point method with filter line search

.

Interior-point methods, also called barrier methods, were already considered in the 1950s, but it was much later that they received attention from researchers in the field of mathematical programming and optimization (Potra and Wright, 2000). Initially, interior-point methods were applied to linear programming problems. The introduction of the primal-dual approach by Kojima et al. (1993) allowed for extension of the algorithm to other convex programming problems such as semi-definite or quadratic programming problems.

The mathematical programming problem for this research is a non-convex optimization problem with linear equality and inequality constraints. Various methods have been developed to apply interior-point to non-convex nonlinear programs by Byrd et al. (1999) and Conn et al. (1999). Examples of these methods are primal-dual steps, barrier and merit functions and scaled trust regions (Potra and Wright, 2000). The nonlinear program in this research is solved with a primal-dual interior point method with filter line search as implemented in the Matlab IPOPT implementation (Wächter and Biegler, 2005b). This method can be applied to problems with general inequality constraints, but the algorithm will be explained for a problem with linear inequality constraints written in general form:

$$\begin{aligned} \underset{x}{\text{minimize}} \quad & f(x) \\ \text{subject to} \quad & A_e x - b_e = 0 \\ & A_i x - b_i \geq 0, \end{aligned} \tag{4.34}$$

where f is a function $f : \mathbb{R}^n \to \mathbb{R}$ defined by $x \mapsto f(x)$. A_e and A_i are an $m \times n$ matrix and $p \times n$ matrix respectively. The vectors b_e and b_i are vectors in $\mathbb{R}^m$ and $\mathbb{R}^p$ respectively. Note that variable bounds can be represented by $A_i x - b_i = x - \text{lb}$ for lower bounds and $A_i x - b_i = \text{ub} - x$ for upper bounds.

4.5.1. The barrier problem

The concept of interior point methods, or barrier methods, is that the optimization problem can be solved by solving a sequence of barrier problems subject to equality constraints for which the inequality constraints are included in the objective problem as follows:

$$\begin{aligned} \underset{x}{\text{minimize}} \quad & \phi_{\mu_i}(x) := f(x) - \mu \sum_{j=1}^{p} \ln\left((A_i x - b_i)^{(j)}\right) \\ \text{subject to} \quad & A_e x = b_e, \end{aligned} \tag{4.35}$$

where $(A_i x - b_i)^{(j)}$ is the j-th element of the vector $A_i x - b_i$, or in other words, it is the value of the j-th inequality constraint. The barrier parameter μ_i is decreasing to zero in the sequence of barrier problems. The solution of the barrier problem for a fixed μ_i is called the inner loop. The sequence of barrier problems with decreasing μ_i is referred to as the outer loop (Wächter and Biegler, 2005b). Appendix B describes the steps for solving the barrier problem in detail. For readers unfamiliar with the method of Lagrangian Multipliers and the Karush-Kuhn-Tucker (KKT) conditions, Appendix A provides background information.

4.5.2. The scaling of the objective function

Wächter and Biegler (2005b) state that scaling the problem statement can improve the performance of the algorithm. Hogg and Scott (2013) found that matrix scaling can reduce the computational time and increase the accuracy of solutions by Ipopt. Both authors mention that no standard method is available for nonlinear problems. The default scaling procedure for IPOPT is conservative, only performing automatic scaling if the maximum gradient is larger than a specified number (100, by default). Hogg and Scott (2013) recommend applying additional problem specific scaling to increase the performance of the algorithm. The authors recommend scaling elements such that function gradients are all in the same order of magnitude. For the unscaled version of our problem statement, where β_1, β_2, ρ_1 and ρ_2 are between 0 and 1, the gradients of the constraints and the objective function differ by several orders of magnitude.

Appendix C gives the gradient of the objective and the Jacobian of the constraints for stage 1. Note that the non-zero terms in A_i^T and A_e^T are either 1 or -1. The non-zero terms in the gradient vector of the objective function are

$$\hat{\beta}\beta_1 \frac{1}{T_{\text{opt}}\overline{S_{\text{res}}}Q_{\text{c}}} Q_{\text{c}}^k, \quad \hat{\beta}\beta_1 \frac{1}{T_{\text{opt}}\overline{S_{\text{res}}}Q_{\text{c}}} S_{\text{res}}^k \quad \text{and} \quad \hat{\beta}\beta_2 \frac{1}{\sum_{k=1}^{T_{\text{opt}}} \overline{Q_{\text{ir}}}^k}. \tag{4.36}$$

The first two terms range from 0 to $\hat{\beta}\beta_1(T_{\text{opt}}\overline{S_{\text{res}}})^{-1}$ and from 0 to $\hat{\beta}\beta_1(T_{\text{opt}}\overline{Q_{\text{c}}})^{-1}$, respectively. Table F.1 in Appendix F contains the values of $\overline{S_{\text{res}}}$ and $\overline{Q_{\text{c}}}$ for all reservoirs. The last term of 4.36 is constant. The yearly average irrigation demand is also in table F.1. It is clear that the terms in the gradient of the objective differs many orders of magnitude from the terms in the gradient of the constraints. Scaling the objective function with a constant improves algorithm performance as will be shown in subsection 5.1.1.

In stage 2, the spillway term and the flood term are included in the objective function and therefore appear in the gradients (see Appendix D). For these two terms no clear upper bound can be defined. The flood term is normalized by an approximate upper bound, as discussed in subsection 4.4.2. This causes the gradient of this term to have a value in the order of 10^{-5} (see subsection 5.2.1). This is the same order of magnitude as the gradient of the term for hydropower. The spillway term was not 'normalized'. The aim is to let this term approach zero by introducing an iteratively increasing penalty ρ_2. The choice of a penalty value for the spillway constraint is discussed in section 5.2.2.

It is expected that scaling the objective function has a positive effect on the performance of the algorithm. In subsection 5.1.1 the effect of the scaling parameters on the results is analyzed.

4.5.3. The termination criteria for IPOPT

Termination criteria for IPOPT can be defined by the user. In this section the various termination criteria and the values used in the implementation in this research are be discussed. Appendix B shows that each barrier problem is solved by solving equations 4.37 to 4.39.

$$\nabla_x f(x) + A_e^T y - A_i^T z = 0 \tag{4.37}$$
$$A_e x - b_e = 0 \tag{4.38}$$
$$\text{diag}\,(A_i x - b_i)\, z - \mu e = 0 \tag{4.39}$$

The termination criteria determine the thresholds for each of these terms at which the algorithm is terminated. The choice for this threshold depends on the required significance level of the final solution in the application. If all termination criteria are met, ipopt terminates with the message 'optimal solution found'.

The absolute tolerance on the constraint violation If the current solution is primal feasible, it means it does not violate the constraint. Equation 4.38 states that the primal infeasibility or the constraint violation should be zero. The desired absolute tolerance level for the constraint violation is set by constr_viol_tol for IPOPT. Besides the desired tolerance level, an acceptable level is defined by acceptable_constr_viol_tol. If after a predefined number of iterations the desired level is not achieved, the algorithm terminates if the acceptable level is reached with the message 'problem solved to an acceptable level'.

For stage 1 the primal infeasibility is the maximum violation of the constraint given by equation 4.11. The order of magnitude for the terms in this constraint are different per reservoir but vary from 4 (the conduit capacity of reservoir 20) to 9 (the storage capacity of reservoir) 18 (table F.1 appendix F). A desired absolute tolerance of 100 is therefore sufficient for this error term. The acceptable absolute tolerance was set to 1000.

For stage 2, the three equality constraints given by equation 4.30, equation 4.31 and equation 4.32 are included as well. Note that the inflows to the river sections are of the same order of magnitude as of the outflows of the subcatchments and the reservoirs. As are the storages and the outflows of the river sections. These variables are multiplied by $\frac{\Delta t}{2} = \frac{1}{2}$ or c_1, c_2, c_3 which are all values between -1 and 1 (table G.1 appendix G). This means that a desired absolute tolerance of 100 and an acceptable absolute tolerance of 1000 the constraint violation suffice for stage 2 as well.

The absolute tolerance on the dual infeasibility Equation 4.37 expresses the dual infeasibility of the problem. If the current solution is primal feasible but not dual feasible, it is not yet the optimal solution to the problem. The desired and acceptable tolerance levels are set by dual_inf_tol and acceptable_dual_inf_tol. Appropriate choices for the termination criteria depend on the objective function, constraints, gradient of the objective function and Jacobian of the constraints given in appendix C and appendix D. The choice of tolerance level for the dual infeasibility is less intuitive than for the constraint violation due to the presence of the Lagrange and KKT multipliers y and z in its definition. The desirable and acceptable tolerance levels were set to 100 and 1000.

The absolute tolerance on the complementarity Finally, the desired and acceptable absolute tolerance for the complementarity as given by equation 4.39 are set by compl_inf_tol and acceptable_compl_inf_tol. The complementarity is partially defined by the inequality constraints. For both stages the various terms of the inequality constraints are of the same order of magnitude as the terms of the equality constraints. Just like the tolerance for the dual infeasibility it is less intuitive, because of the KKT multipliers. The desirable and acceptable tolerance levels were set to 100 and 1000.

The tolerance level for the overal NLP error Wächter and Biegler (2005b) define the optimality error of the barrier problem. Rewritten for linear constraints it is defined as

$$E_\mu(x,y,z) = \max\left(\frac{\left\|\nabla_x f(x) + A_e^T y - A_i^T z\right\|_\infty}{s_d}, \|A_e x - b_e\|_\infty, \frac{\left\|\text{diag}\,(A_i x - b_i)\, z - \mu e\right\|_\infty}{s_c}\right) \tag{4.40}$$

The parameters s_c and s_c are scaling parameters defined by

$$s_d = \frac{1}{s_{\max}} \max\left\{ s_{\max}, \frac{\|y\|_1 + \|z\|_1}{(m+n)} \right\} \tag{4.41}$$

and

$$s_c = \frac{1}{s_{\max}} \max\left\{ s_{\max}, \frac{\|z\|_1}{n} \right\}. \tag{4.42}$$

The scaling means that for the optimality error the dual infeasibility is considered relative to the average size of the Lagrangian Multipliers y and the KKT multipliers z over $s_{\max}$ unless this becomes smaller than 1, in which case the scaling parameter is set to 1. The term for the complementarity is considered relative to the average size of the KKT multipliers z over $s_{\max}$, unless this becomes smaller than 1. The default value for $s_{\max}$ is 100.

The overal NLP error is the optimality error for the original problem where the barrier parameter $\mu = 0$. The tolerance level ϵ_{tol} for the overal NLP error is defined as

$$E_0(x^*, y^*, z^*) \leq \epsilon_{\text{tol}}. \tag{4.43}$$

The sensitivity of the final solution and the effect of the choice of tolerance levels for the overal NLP error was investigated. The results are presented in subsection 5.1.2 of chapter 4.

5

The results for the two-stage model predictive control system

The performance of the two-stage MPC method is discussed and the capacity of the reservoir system with respect to the different objectives is analyzed. Section 5.1 contains a description of the results for MPC stage 1: the optimization for hydropower and irrigation for each reservoir separately. Section 5.2 presents the results of stage 2, in which the complete system is considered in the optimization to reduce flooding.

5.1. The results for the MPC stage 1

In stage 1 the reservoir operation was optimized separately for irrigation water supply and hydropower generation for each reservoir. First, an analysis of appropriate choices for the objective function scaling factor, the tolerance level for the overall NLP error and the optimization horizon are presented in subsection 5.1.1, subsection 5.1.2 and subsection 5.1.3, respectively. For stage 1, the optimal values (maximizing hydropower generation and meeting irrigation demand) for these parameters were found to be: $365 \cdot 10^5$ for the objective function scaling factor objective function, 1 for the tolerance level of the overall NLP error, and 365 days for the optimization horizon. Unless explicitly stated otherwise, these are the settings used for the results shown in this section. Increasing the scaling factor of the objective function or the optimization horizon or decreasing the tolerance for the overall NLP error did not improve final results, but did increase the number of iterations and total CPU time to find the optimal solution. In section 5.1.4, the optimal operation as determined by MPC stage 1 is compared to the actual operation during that period for the Paunglaung reservoir. Section 5.1.5 contains a discussion on the trade-off between hydropower and irrigation.

5.1.1. The scaling the objective function

In section 4.5.2 it was discussed that the unscaled gradient of the objective function is many orders of magnitude smaller than the gradients of the constraints. Therefore, it was investigated whether scaling the objective function improved the performance of the optimization algorithm in terms of final solution and computation time. Seven different values for the objective function scaling factor, between $3.65 \cdot 10^4$ and $3.65 \cdot 10^{14}$, were tested for the 21 reservoirs in stage 1. The results showed that the total hydropower produced increases when the objective function scaling factor increases, indicating that no global optimum was reached for objective function scaling factors below $3.65 \cdot 10^7$. For each of the reservoirs there is an objective function scaling factor that results in the best performance of the algorithm in terms of final solution and computation time. This value is not necessarily the same for each reservoir. Increasing the objective function scaling factor beyond this value does not further increase the produced hydropower, but does increase the number of iterations and the computation time. Figure 5.1 shows the total hydropower produced in each of the reservoirs, divided by the total hydropower generation in that reservoir when scaling factor $3.65 \cdot 10^9$ is applied. The scaling factors $3.65 \cdot 10^{11}$ and $3.65 \cdot 10^{14}$ did not result in further improvement of the solution and are therefore disregarded. The bars represent different reservoirs and are ordered by increasing storage capacity from left to right. The

reservoir number is indicated above the bars. The maximum hydropower production for reservoirs 20, 17, 10 and 16 was found with a scaling factor of $3.65 \cdot 10^4$. The reservoirs 8, 15, 13, 12, 11, 6, 9 reached maximum hydropower production with a scaling factor of $3.65 \cdot 10^5$. Reservoirs 14, 7, 19, 3, 5, 2, 21, 4 and 1 reached maximum hydropower production with a scaling factor of $3.65 \cdot 10^6$. Finally, the hydropower production in reservoir 18 reaches its maximum with a scaling factor of $3.65 \cdot 10^7$.

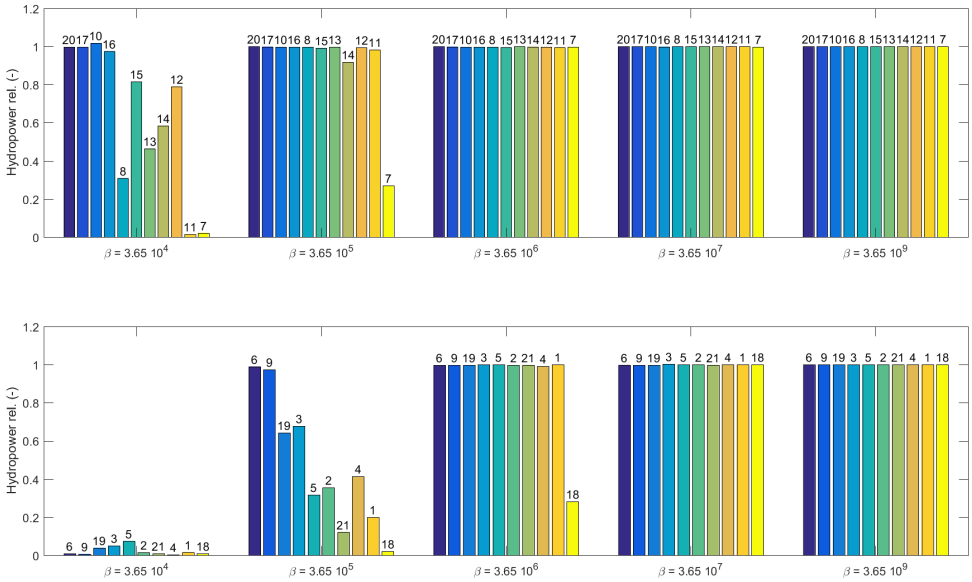

Figure 5.1: Hydropower generation per reservoir for several values for the objective function scaling factor, varying from $3.65 \cdot 10^4$ to $3.65 \cdot 10^9$. The hydropower generation for each reservoir is divided by the generated hydropower with a scaling factor $3.65 \cdot 10^9$. The reservoirs are ordered by increasing reservoir capacity and the number of the reservoir is indicated above the bar.

Table 5.1 shows total hydropower production in (GWH), irrigation deficit as a percentage of the total demand and total CPU time [1] in minutes for the different objective function scaling factors. Note that the total hdyropower production in the basin increases until a scaling factor $3.65 \cdot 10^7$ is applied. The solution for most reservoirs reached the maximal total hydropower for lower scaling factors, but because reservoir 18 is a large reservoir, its contribution to the total generated hydropower is significant. Increasing the objective function scaling factor from $3.65 \cdot 10^7$ to $3.65 \cdot 10^9$ does not further increase power production or decrease irrigation deficit, but does increase the total CPU time. For this reason, a scaling factor of $3.65 \cdot 10^7$ is preferred for stage 1.

Table 5.1: Total hydropower production in (GWH) for the basin, irrigation deficit as a percentage of the total demand in the basin and total CPU time in minutes for scaling factors $3.65 \cdot 10^4$, $3.65 \cdot 10^5$,$3.65 \cdot 10^6$,$3.65 \cdot 10^7$ and $3.65 \cdot 10^9$ for the objective function.

	Objective function scaling factors				
	$3.65 \cdot 10^4$	$3.65 \cdot 10^5$	$3.65 \cdot 10^6$	$3.65 \cdot 10^7$	$3.65 \cdot 10^9$
Hydropower (GWH)	34	400	693	721	721
Irrigation Deficit (%)	5	2	1	1	1
CPU (min)	16	22	29	54	116

Figures 5.2a to 5.2d show the operation of reservoir 18 for various scaling factors. From top to bottom each figure shows the storage in the reservoir (blue area) and the storage capacity (dashed line), the outflow through the conduit (red area) and the conduit capacity (dashed line), the offtake for irrigation (green area) and the demand (dashed line), the outflow through the spillway (yellow area) and finally, at the very bottom, the number of iterations used to solve the optimization problem at that timestep (blue line). The red vertical

[1] PC: intel i7 with 6 cores 12 threads on 4.3GHz, with 16GB ram

lines show the timestep for which the performance of the algorithm will be discussed in more detail later in this section.

Note that the y-axis for the plot with the number of iterations is presented on a logarithmic scale, because the number of iterations for the first few timesteps is 1 to 2 order of magnitudes larger than the number of iterations for the following timesteps. This is due to the warm-starting of the algorithm as discussed in chapter 4. These figures show that warm-starting reduces the number of iterations significantly.

Remember that hydropower generation is larger for larger storage in the reservoir and larger flows through the conduit. Clearly, the operation for scaling factor $3.65 \cdot 10^7$ is best in terms of irrigation supply as well as hydropower generation. Note that for this solution, the flow through the spillway is zero. This is expected, because flows through the spillway do not produce power. When optimizing for hydropower and irrigation without other objectives, spilling only occurs in the optimal solution when it is otherwise unavoidable, as discussed in chapter 4.

(a) Scaling of the objective function by a factor $3.65 \cdot 10^4$.

(b) Scaling of the objective function by a factor $3.65 \cdot 10^5$.

(c) Scaling of the objective function by a factor $3.65 \cdot 10^6$.

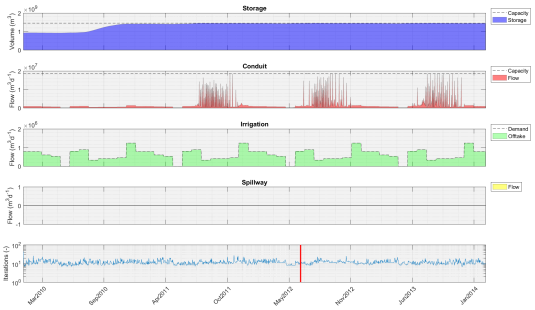

(d) Scaling of the objective function by a factor $3.65 \cdot 10^7$.

Figure 5.2: Operation for reservoir 18. The figures show the storage, flows through the conduit and spillways, irrigation offtakes and the number of iterations at each timestep. The results were obtained for stage 1, with equal weights on hydropower and irrigation. The scaling factor is different for each figure and indicated under the figure.

Figures 5.3a to 5.3c show the performance of the algorithm for the various scaling factors. Each set of three graphs shows the development of the unscaled objective function value, the unscaled primal infeasibility (eq. 4.38) and the scaled dual infeasibility (eq. 4.37) over the iterations for timestep 900. Note that in the last two figures (e and f), the number of iterations is much larger, so the x-axes are scaled differently. The y-axes for the primal and dual infeasibility are on a logarithmic scale.

The graphs show that scaling the objective function changes the balance between improving the objective function and decreasing constraint violation (primal infeasibility) in the algorithm, as was explained in subsection 4.5.2. The objective function value increases and stabilizes after a certain number of iterations for all of the scaling factors. The maximum value of the objective function is larger with scaling factors between $3.65 \cdot 10^7$ and $3.65 \cdot 10^{14}$ as compared to the lower scaling factors. The primal infeasibility is initially small for the scaling factors $3.65 \cdot 10^4$ and $3.65 \cdot 10^5$. In other words, the max-norm of the constraint violation is already small for the initial solution at this timestep. The primal infeasibility is initially larger, but decreases with the number iterations for the four larger scaling factors. The final value of the primal infeasibility is larger for the scaling factors $3.65 \cdot 10^{11}$ and $3.65 \cdot 10^{14}$ than for the scaling factors $3.65 \cdot 10^7$ and $3.65 \cdot 10^9$. This supports

the analysis in subsection 4.5.2, stating that the objective function needs to be scaled so that the gradients are of the same order of magnitude as the derivatives of the constraints. If the scaling factor applied to the objective function is too small, the constraint violation is reduced but the objective function does not reach the optimal value. If the scaling factor is too large, the objective function value improves but the constraint violation remains large. The scaling factor $3.65 \cdot 10^7$ improves both the objective function value as well as the constraint violation.

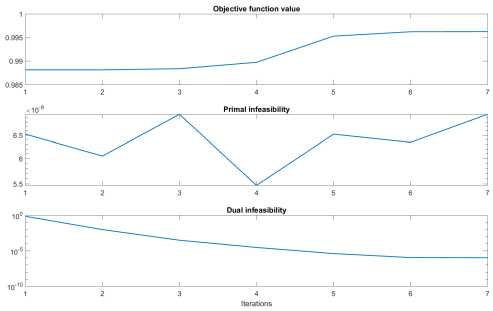

(a) Scaling of the objective function by a factor $3.65 \cdot 10^4$.

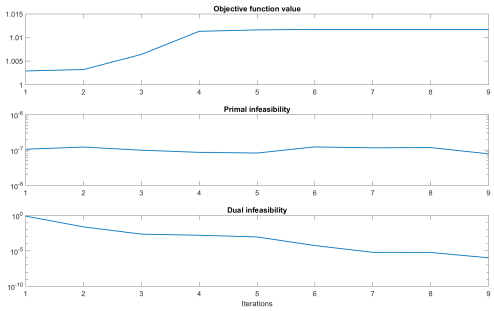

(b) Scaling of the objective function by a factor $3.65 \cdot 10^6$.

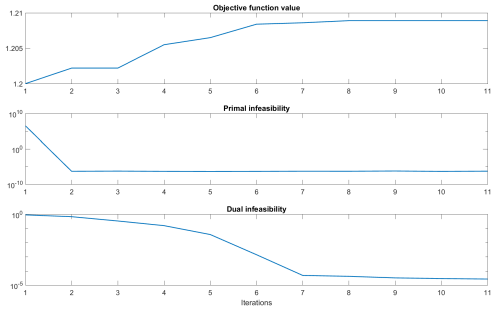

(c) Scaling of the objective function by a factor $3.65 \cdot 10^7$.

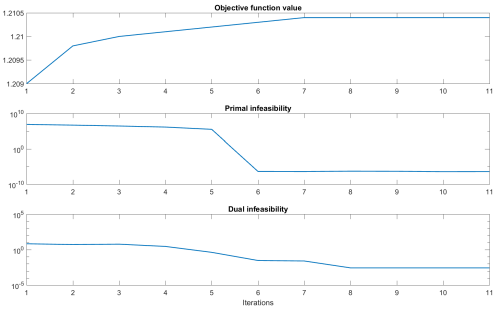

(d) Scaling of the objective function by a factor $3.65 \cdot 10^9$.

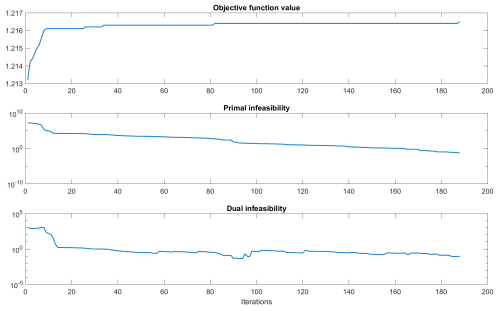

(e) Scaling of the objective function by a factor $3.65 \cdot 10^{11}$.

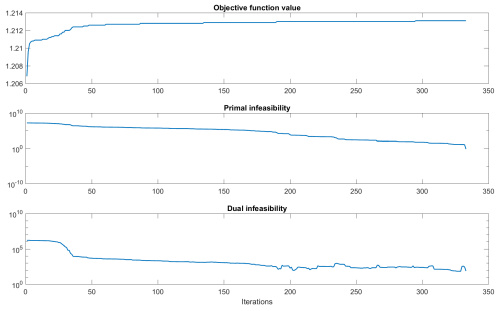

(f) Scaling of the objective function by a factor $3.65 \cdot 10^{14}$.

Figure 5.3: Performance of the algorithm for scaling factors $3.65 \cdot 10^4$, $3.65 \cdot 10^6$, $3.65 \cdot 10^7$, $3.65 \cdot 10^9$, $3.65 \cdot 10^{11}$ and $3.65 \cdot 10^{14}$ for reservoir 18 at timestep 900. The unscaled value of the objective function, the unscaled primal infeasibility and the scaled dual infeasibility at each iteration are presented.

5.1.2. The tolerance level for the overall NLP error

In subsection 4.5.3 the termination criteria are discussed. It was discussed that the choice for the tolerance level for the overal NLP error is less intuitive than the choice for the tolerance levels for absolute primal, dual and complementarity infeasibility. A comparison was made between the performance of the algorithm for different tolerance levels. The selected tolerance levels were 100, 1, 10^{-2}, 10^{-4} and 10^{-6}. Table 5.2 shows that total hydropower generation (GWh) and irrigation deficit (%) do not change for different tolerance levels. Howeverm, the CPU time increases from 28 minutes to 245 minutes when the tolerance level is decreased

from 100 to 10^{-6}. Therefore, a tolerance level of 100 is preferred for stage 1.

Table 5.2: Total hydropower production in (GWH) for the basin, irrigation deficit as a percentage of the total demand in the basin and total CPU time in minutes for tolerance levels 1, 10^{-2}, 10^{-4}, 10^{-6} for the overal NLP error for a scaling factor of the objective of $3.65 \cdot 10^7$, .

	100	1	10^{-2}	10^{-4}	10^{-6}
Hydropower (GWH)	721	721	721	721	720
Irrigation Deficit (%)	1	1	1	1	1
CPU (min)	28	54	93	177	245

5.1.3. The choice of an optimization horizon

The results shown in the subsections 5.1.1 and 5.1.2 were solutions for the optimization problem with an optimization horizon set to 365 days. This means that the algorithm searched for the optimal solution while looking 365 days into the future. Recall that the prediction horizon was set to 3 days and that for the remaining period of the optimization horizon, information on seasonality was provided to the MPC system. The optimization horizon determines the size of the optimization problem because each variable is included in every timestep of the optimization horizon in the optimization problem which means that increasing the optimization horizon increases CPU time. The influence of the optimization horizon is presented in table 5.3. The total hydropower generation, irrigation deficit and CPU time are given for several different optimization horizons between 60 and 365 days. Several objective function scaling factors were applied in the analysis because the optimal scaling factor is affected by the optimization horizon.

The total hydropower generation increases with an increasing optimization horizon and the best optimization horizon is different per reservoir. Figure 5.4 shows the generated hydropower for each of the reservoirs divided by the hydropower generated for an optimization horizon of 365 days. The irrigation deficit always remains below 1% of the total demand in the basin. Most reservoirs produce the same amount of energy with an optimization horizon of 120 or 365 days. For reservoir 7, 1 and 18 the generated hydropower increases until an optimization horizon of 250 days is implemented. Finally, reservoir 14 produces the most hydropower with an optimization horizon of 365 days. Therefore, an optimization horizon of 365 days is used for stage 1. Note the CPU time increases nonlinearly with the size of the optimization problem.

Table 5.3: Summary of the results for the optimization horizons of 60, 120, 180, 250 and 365 days for MPC stage 1. Total hydropower for the basin in (GWh), irrigation deficit as percentage of the total demand and the CPU time in minutes is given for each of the optimization horizons with the objective function scaled by a factor $3.65 \cdot 10^7$, $3.65 \cdot 10^{12}$ and $3.65 \cdot 10^{14}$.

Scaling objective		60	120	180	250	365
$\beta = 3.65 \cdot 10^7$	Hydropower (GWH)	598	688	715	721	721
	Irrigation Deficit (%)	1	1	1	1	1
	CPU time (min)	8	9	11	14	54
$\beta = 3.65 \cdot 10^{12}$	Hydropower (GWH)	623	697	718	722	-
	Irrigation Deficit (%)	1	1	1	1	1
	CPU time (min)	25	44	72	117	-
$\beta = 3.65 \cdot 10^{14}$	Hydropower (GWH)	621	697	718	722	721
	Irrigation Deficit (%)	1	1	1	1	1
	CPU time (min)	38	75	118	176	410

5.1.4. Comparing the actual and the MPC operation for the Paunglaung reservoir

Figure 5.5 shows the MPC operation and the actual operation for the Paunglaung reservoir. A comparison is made between the optimized and the actual operation for this specific reservoir because the inflow timeseries used in the model was derived from measurements in this reservoir. The storage of the reservoir at the start of the optimization is set to the storage provided in the data on that date to make a fair comparison. No

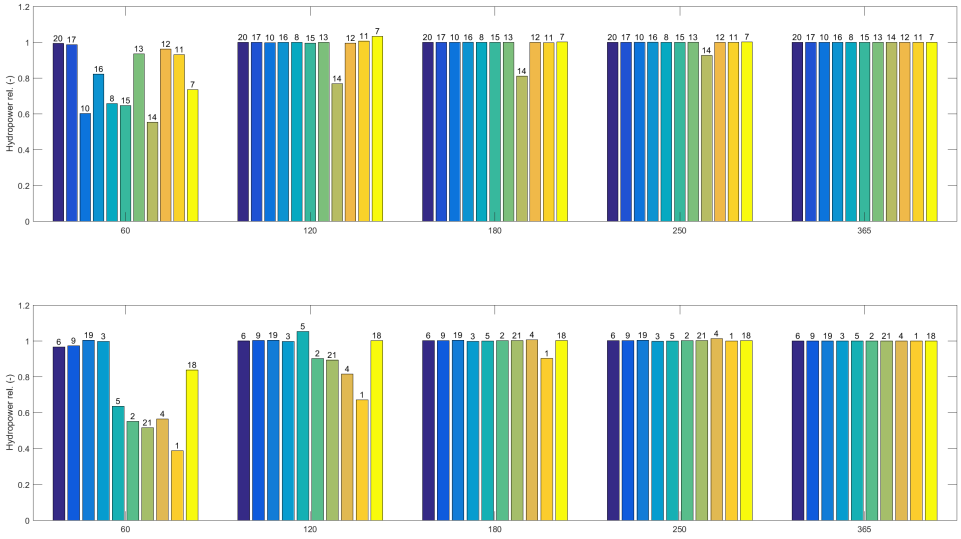

Figure 5.4: Hydropower generation per reservoir for optimization horizons 60, 120, 180, 250 and 365 days. The hydropower generation for each reservoir is divided by the generated hydropower for the run with optimization horizon of 365 days. The reservoirs are ordered by increasing reservoir capacity and the reservoir number is indicated above the bar.

information is available regarding irrigation off-takes, so the irrigation off-takes in the optimization cannot be compared to actual operation. In the optimization precipitation on the reservoir is neglected, which is reasonable as its volume is only 0.4 % of the total inflow to the reservoir; the waterspread area of the reservoirs is much smaller than the area of the reservoir catchment. Evaporation and outflows other than those through the spillway and conduit are neglected as well, as these volumes are less than a permille of the total outflow.

From top to bottom, the plots in figure 5.5 show the storage in the reservoir, the outflow through the conduit, the outflow through the spillway, the sum of the outflow through the conduit and the spillway and the reservoir inflow over time. The black lines show the actual operation of the reservoir and the coloured areas represent the operation recommended by MPC stage 1.

An important difference between the optimization and the actual operation is that in the optimization, the reservoir is filled up to maximum capacity and remains close to maximum capacity over the entire period (blue area, first plot in figure 5.5). In the actual operation, the reservoir storage reaches maximum capacity in the wet season but drops to dead storage capacity in the dry season. Keeping the storage in the reservoir high is clearly beneficial in terms of hydropower generation, but is risky in case floods are considered and if there is a large uncertainty in predicted reservoir inflows. In this stage of the optimization floods were not taken into account, which may explain the difference between optimized operation and the actual operation.

The conduit releases (red area, second plot in figure 5.5) of the MPC operation follow the pattern of the actual operation. In the wet season, during the actual operation, the conduits did not release water at full capacity even though spilling did occur in these periods (third plot). The MPC operation does release at full capacity at those moments, which is clearly beneficial in terms of hydropower generation. It is not known why the operator decided to keep the conduit partially closed. A potential reason could be the limited capacity of the electricity network, which was not considered in this study. The volume spilled (yellow area, third plot) is much lower in the MPC operation than in the actual operation. The sum of the outflows from the reservoirs (fourth plot) is comparable in the actual and the MPC operation, though the MPC operation has fewer peaks in the wet season.

Figure 5.6 shows the water level in the reservoir, the outflow through the conduit and the generated hydropower for both the actual operation and the MPC operation. In order to calculate the amount of produced hydropower, the storage in the reservoir was converted to a water level assuming a linear reservoir instead of

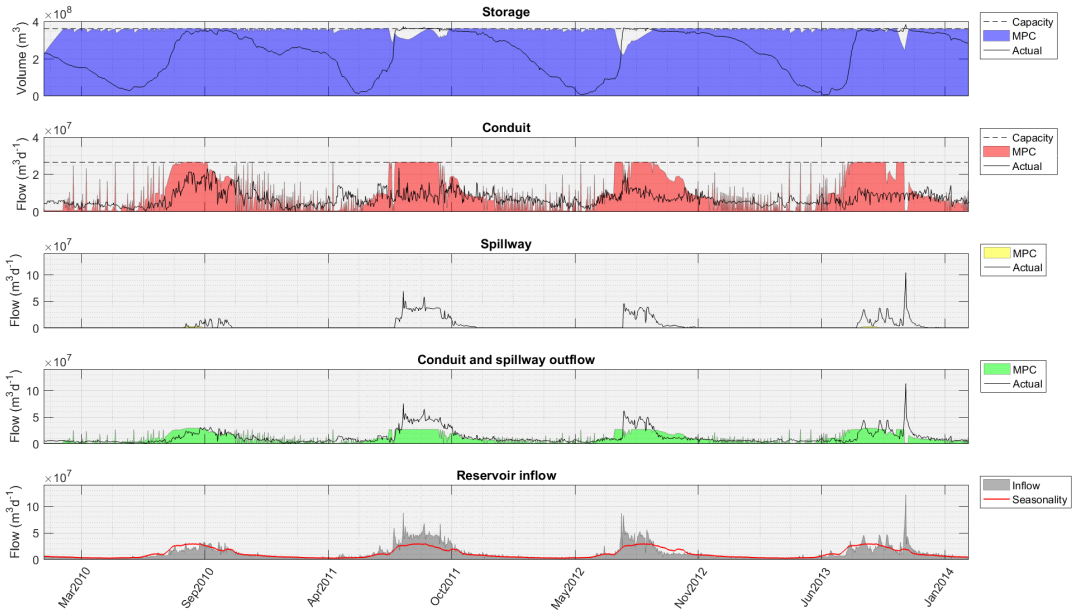

Figure 5.5: MPC stage 1 operation and actual operation of the Paunglaung reservoir between January 1, 2010 and February 8, 2014. Plots from top to bottom: the storage in the reservoir, the flow through the conduit, the flow through the spillway, the total outflow from the reservoir, the inflow to the reservoir.

using the reservoir curve which introduces an error, as discussed in section 3.5. The first plot shows the water level derived from the storage in the MPC operation (blue area), the water level derived from the storage given in the data using the linear reservoir assumption (black line), and the water level given in the data (black dashed line). The maximum absolute difference between the linearized water level of the actual operation and the measured water level of the actual operation is 5.5m, which is a relative difference of 21%. The second plot in the figure shows the release through the conduit for the MPC operation (red area) and the actual operation (black line). The bottom plot shows the generated hydropower calculated for the MPC (yellow area) and actual operation (black line). The generated hydropower for the actual operation is calculated based on the linearized water level to make a fair comparison of the produced hydropower.

The total amount of hydropower produced in the MPC operation, 349 GWH, is 67% larger than in the actual operation, 209 GWH, for the period between January 1, 2010 and February 8, 2014. Note that the fluctuation in production is much larger for the MPC operation and that the production in the dry season is lower than for the actual operation. This is a consequence of the formulation of the optimization problem in which no penalty on fluctuations was included whereas the operator is likely to aim for a relatively constant generation of hydropower.

5.1.5. The trade-off between hydropower and irrigation supply

Table 5.4 shows the total amount of hydropower produced, the total deficit of irrigation water, the number of days there was an irrigation deficit, the total volume spilled and the number of days for which spilling occured for the whole system. The selected weights when optimizing only for hydropower were $[\beta_1 \beta_2] = [1 \quad 0]$, when optimizing only for irrigation they were $[\beta_1 \beta_2] = [1 \quad 0]$ and when optimizing for both they were $[\beta_1 \beta_2] = [1 \quad 1]$.

Note that the total generated hydropower production does not decrease significantly when including irrigation demands in the objective function. The total amount produced by all reservoirs together is 739 GWH when optimizating only for hydropower generation and drops to 721 MWH for the multi-objective case, a decrease of 2.4%.

It is interesting that the irrigation deficit for the sinlge-objective optimization for irrigation is larger than the

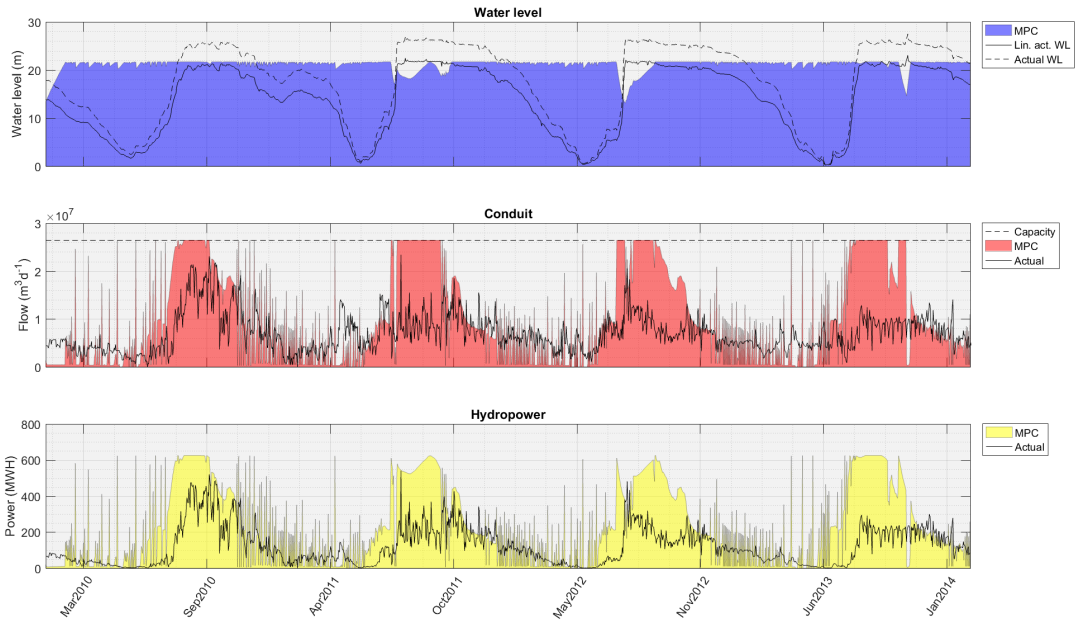

Figure 5.6: Comparison of the hydropower generation for the MPC stage 1 and actual operation of the Paunglaung reservoir between January 1, 2010 and February 8, 2014. Plots from top to bottom: the water level in the reservoir, the flow through the conduit of the reservoir, the generated hydropower.

irrigation deficit of the multi-objective optimization, 284 million m^3 and 115 million m^3 respectively, which is 1% and 3% of the total demand in the basin. This can be explained by the fact that no uncertainty in reservoir inflows was assumed. The MPC operation releases through the conduit such that sufficient water remains in the reservoir to meet the irrigation demands for the entire optimization horizon. There is no incentive to store more water in the reservoir. However, the prediction horizon of 3 days means that only inflows for the next three days are known. The inflows on the remaining 362 days of the year are seasonality predictions. When the actual inflow to the reservoir is lower than the seasonality, the MPC operator only knows this 3 days in advance and has no time to save extra water to meet the irrigation demand. In the multi-objective case, the MPC controller has an incentive to keep the storage in the reservoir larger than the demand for irrigation, as a higher water level results in more energy production. A positive side effect is that the MPC operator can easily adjust to unexpected lower inflows to the reservoir and always meet the demand for irrigation. A way to deal with this is to incorporate uncertainty of the predicted inflows in the MPC method, which is discussed in chapter 6.

The total spilled volume for the multi-objective optimization is similar to the single-objective hydropower optimizition, 2850 million and 3000 million m^3 respectively. This amount is much larger in the single-objective irrigation optimization . Part of the spilling occurs at moments when the storage in the reservoir does not exceed maximum capacity, which would never happen in reality. This behaviour can be prevented by including a spillway constraint as discussed in chapter 3. The spillway constraint does not need to be included for optimizations including hydropower generation, since the optimal operation will never unnecessarily spill water. The irrigation demands are so low that there is no incentive in the problem statement to prevent unnecessary spilling.

The irrigation supply and hydropower generation are not competing objectives in this case because the irrigation demands are much smaller than the reservoir and conduit capacities for most of the reservoirs. If the demands for irrigation supply would be larger, results could show a different outcome.

Finally, 5.5 shows for each reservoir the absolute produced hydropower (GWh) and the production as a percentage of the total system for the multi-objective optimization with equal weights. The hydropower in the catchment is mainly produced by reservoir 3, 19, 1, 2, 4, 5, 18 and 21. The table also shows the irrigation deficit for each reservoir as a percentage of the demand per reservoir and the total irrigation deficit relative to the total demand. Note that only reservoir 14 and 20 suffer an irrigation deficit. The estimated demands

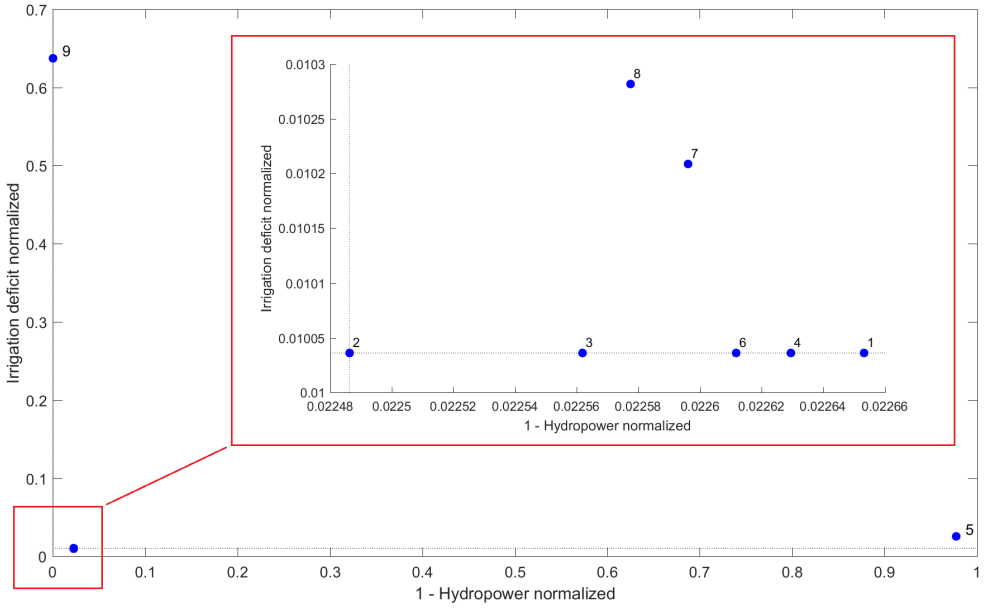

Figure 5.7: Pareto plot for the trade off between hydropower and irrigation in MPC stage 1. The numbers 1-9 represent runs with different weight factors for hydropower (β_1) and irrigation (β_2). Run 1: [1 1], run 2: [0.75 1], run 3: [0.5 1], run 4: [0.25 1], run 5: [0 1], run 6: [1 0.75], run 7: [1 0.5], run 8: [1 0.25], run 9: [1 0]. For all runs the objective function was scaled with factor 10^7.

Table 5.4: Summary of the results for the multi-objective (equal weights) and single-objective hydropower and irrigation optimization for MPC stage 1 The total hydropower (GWh) for the basin, the irrigation deficit as a percentage of the total demand, the volune spilled in m^3 and the number of days on which spilling occurs are given for each of the three scenarios.

	Both	Hydr.	Irr.
Hydropower (GWH)	721	739	187
Irrigation deficit (%)	1	64	3
Spilled volume (m^3)	2850	3000	20400
Number of spilling days	3519	3697	26757

for these reservoirs are 2% and 0.1% of the total estimated demand for the basin and the reservoir catchment areas are less than 1% of the basin area for both reservoirs. The irrigation deficit for the total basin is 1%, indicating that these reservoirs do not play an important role in the basins irrigation supply. The irrigation deficit for reservoir 20 is caused by the fact that for some periods the irrigation demand is larger than the conduit capacity. This is due to an error in the estimation of the irrigation demand or the assumed value for the conduit capacity of this reservoir. In Appendix H the estimations for the irrigation demands are compared to actual average daily irrigation offtakes at reservoir 14, 6 and 12. This shows that the estimated irrigation demands were much larger than the average offtakes for these reservoirs. The actual daily offtake for reservoir 14 is 99 $\cdot 10^3$ $m^3 d^{-1}$ while the average estimated daily demand is 150 $\cdot 10^3$ $m^3 d^{-1}$. Chapter 6 will discuss the uncertainty in estimations of irrigation demands, dimensions of the reservoirs and inflows to the reservoirs on the results.

5.2. The results for the MPC stage 2

In stage 2 of the optimization, the aim was to prevent or reduce floods. Based on the results obtained in stage 1, it was concluded that when irrigation demands are met, hydropower generation only decreases by 2.4%. Therefore, the weight of the irrigation term was set to zero in the objective function in stage 2 and irrigation offtakes were set to the irrigation demand or conduit capacity, when the irrigation demand exceeded conduit capacity. The river dynamics were also included in the optimization in stage 2, which led to an increase in

Table 5.5: Total hydropower generation per reservoir (GWh) and as a percentage of the total production, irrigation deficit for each reservoir as a percentage of the demand per reservoir and the total irrigation deficit relative to the total demand in the basin for optimal stage 1 operation.

Reservoir	Hydropower generation (GWh)	Percentage of total hydropower generation (%)	Irrigation deficit relative to demand (%)
1	29.80	4.13	0
2	36.41	5.05	0
3	349.48	48.44	0
4	45.20	6.26	0
5	40.76	5.65	0
6	10.92	1.51	0
7	3.59	0.50	0
8	0.68	0.09	0
9	20.89	2.90	0
10	0.24	0.03	0
11	5.78	0.80	0
12	4.60	0.64	0
13	3.17	0.44	0
14	0.40	0.06	48.42
15	1.96	0.27	0
16	0.35	0.05	0
17	0.10	0.01	0
18	37.63	5.22	0
19	90.74	12.58	0
20	0.06	0.01	2.74
21	38.68	5.36	0
Total	721.46	100	1.00

computation time. Therefore, results were considered for one year only, from April 1st, 2010 until March 31st 2011.

In the following subsections, the flood mitigating capacity of the reservoir system is analysed. Also, the trade off between hydropower and flood mitigation is studied. Subsection 5.2.1 presents an analysis of the systems flood mitigating capacity with respect to the river inflows and the reservoirs' storage capacities. In subsection 5.2.2 the behaviour of the spillway is investigated. The results for various flood levels are discussed in subsection 5.2.3. Finally, subsection 5.2.4 discusses the trade off between hydropower and flood mitigation. All results in this section are generated with a scaling factor for the objective function of 10^{12}, a tolerance level for the overall NLP error of 1, and an optimization horizon of 30 days.

The water levels near Taungoo for stage 1 operation Figure 5.8 shows the water level in the river section near Taungoo city if the system was operated according to the stage 1 multi-objective optimal operation. The period considered for stage 2 is the area between the red vertical lines. The blue area is the modelled water level, the black line is the measured water level near Taungoo by Rest (2015). Water level measurements near Taungoo are only available from January 1st, 2013 till December 31st 2015. This means that there is one year overlap between the modelled and the measured water levels. The figure shows that the water levels are underestimated, which is most likely due to an underestimation of the river inflows as will be discussed in chapter 6. The timing of the peak water levels is similar for the modelled and measured water levels, which is expected because the semi-synthetical inflow series is based on actual inflows to the Paunglaung reservoir as discussed in chapter 3. These simplications of the river morphology do not influence the routing in the river, as the Muskingum routing method is based on storage, inflows and outflows. The choice of cross-section shape and width only influences the conversion from storage to water level. For this reason, a flood level is determined based on the water level in figure 5.8. Water levels above this flood level are considered to cause flooding, which ideally should be prevented or reduced through operational choices. In section 5.2, flood mitigation is analysed for selected flood levels of 40.6m, 40.9m and 41.2m. The flood level determined by Rest (2015) for this location is 43m. The underestimation of the water levels in 2014 is approximately 1.5 meters, so the flood levels of 40.6-41.2 m are considered to be conservative with respect to the real system.

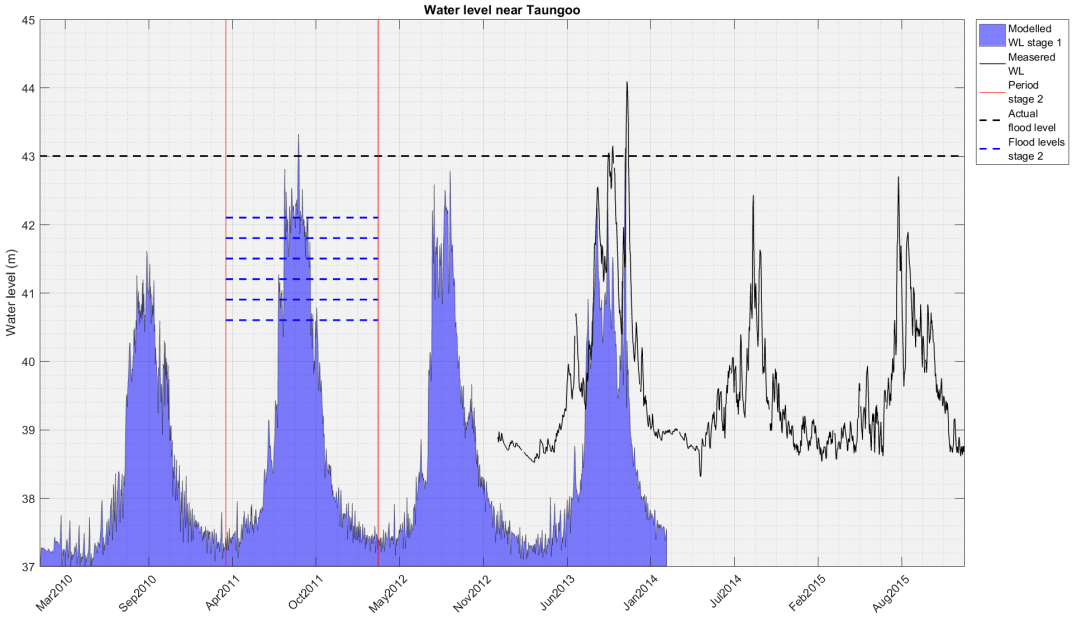

Figure 5.8: Water level near Taungoo city for MPC operation resulting from stage 1 (blue area) and the measured water levels at the nearby measure station Ohn pin (black line). The red vertical lines indicate the period considered for the section about results for MPC stage 2. The dashed horizontal lines indicate flood levels discussed in the section about results for MPC stage 2.

5.2.1. The flood mitigating potential with respect to the reservoir storage capacities

This section contains an initial analysis of the storage capacity of the reservoirs to determine to what extent floods can potentially be mitigated. Another relevant factor that is considered is the ratio between controlled and uncontrolled flow to the river, i.e. what percentage of flow passes through the reservoir.

The total storage capacity of the reservoirs upstream of the flood location is 1500 10^6 m^3. If all reservoirs would be empty on the first day of floods, this is the amount of water the reservoirs would be able to store. If the flood period is uninterrupted, the reservoirs have no time to release water between flood events. Figure 5.8 shows that this is approximately the case for most flood levels. Table 5.6 shows the total discharge in the river section above flood level in m^3 for the entire year for the flood levels 40.6m, 40.9m, 41.2m, 41.5m, 41.8m and 42.1m. If all reservoirs are empty at the beginning of the flood, the total storage of the reservoirs is sufficient for storing all discharge responsible for floods.

Table 5.6: Discharge above flood level in M m^3 and as a percentage of the total discharge in the flood period for river section 7 for flood levels 40.6-42.1 m. The normalization factor for the flood term in the objective function calculated based on these flood levels is given.

Flood level (m)	40.6	40.9	41.2	41.5	41.8	42.1
Discharge above flood level (10^6 m^3)	173	135	99	66	37	15
% of total discharge in period of flood	26	22	17	12	8	6
$\overline{f_{\text{fl}}}$ $(\cdot T_{\text{opt}} \cdot 10^4)$	47	37	27	18	10	4

Part of the inflow to the river does not pass through the reservoirs but flows directly into the river. Around 40% of the basin area upstream of the river segment near Taungoo city is not part of the reservoir catchment areas. Outflows from this part of the basin are uncontrolled. This means that in the model used, 40 % of the river inflow is uncontrolled. Table 5.6 also shows the discharge above flood level as a percentage of the total flow in the period of flood. This percentage is lower than the percentage of flow flowing through the reservoir. The discharge causing floods near Taungoo can be controlled because it flows through the reservoirs. The reservoir storage capacity is not expected to be a limiting factor for flood mitigation for any of the considered flood levels.

The choice of a normalization factor for the flood term in the objective function The normalization factor for the flood term was defined in equation 4.17 - 4.18 as

$$\overline{f_{\text{fl}}} = \frac{T_{\text{opt}}}{365} \sum_{k=1}^{365} \overline{x_{\text{fl}}}^k, \tag{5.1}$$

with $\overline{x_{\text{fl}}}^k$,

$$\overline{x_{\text{fl}}}^k = \left(\left(S_{\text{riv}}^k \right)_7 - A_{\text{riv}} L_{\text{flood}} \right)^+. \tag{5.2}$$

A normalization factor calculated based on the results of stage 1 and the same value was used for all flood levels. Table 5.6 shows the value of $\overline{x_{\text{fl}}}^k$ for all flood levels. The normalization factor for a flood level of 40.9 m was selected, $T_{\text{opt}} \cdot 37 \cdot 10^4$, because it is average for the flood levels 40.6m - 41.2m considered in this research.

Stage 2 operation without spillway constraints Travel times were neglected because, these are in the order of hours to days and not expected to impact the results. The system's flood mitigating capacity without the presence of spillway constraints is considered to verify this. When the optimization is performed without the spillway constraint, the system is allowed to spill whenever and as much as is needed to prevent floods.

Figure 5.9 shows the water levels when optimizing stage 2 for only hydropower (top), for hydropower and floods both with weight 1, for flood levels 41.2 m (second plot), 40.9 m (third plot) and 40.6m (bottom). The

water level for stage 2 operation for only hydropower is lower than the water level in stage 1, because the optimization horizon of 30 days is used in this stage. Water levels above a level of 41.2 m, 40.9 m or 40.6 m can be avoided if no spillway is present. This confirms the analysis based on table 5.6.

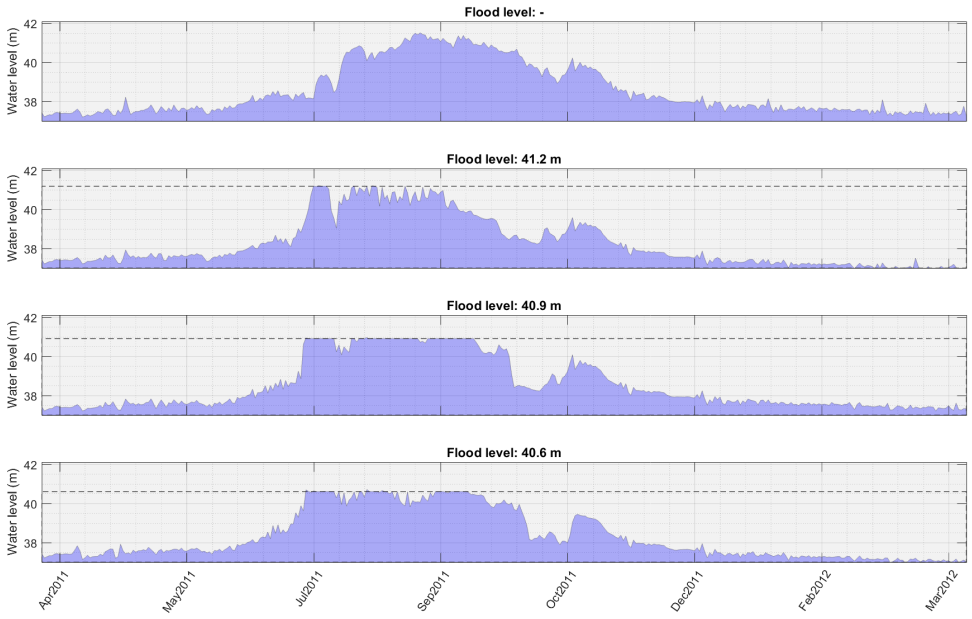

Figure 5.9: Water levels near Taungoo city for MPC stage 2 without spillway constraint. The plots from top to bottom are generated for optimization without floods included in the objective, with a flood level of 41.2 m, with 40.9m and with 40.6m. The weight on hydropower was 1 in all four cases. Hydropower and flood mitigation are both given weight 1.

It can be concluded that it is not the storage capacity of the reservoirs that limits flood prevention. However, the situation in which the reservoirs can spill whenever and as much as required is not realistic. Section 3.2 explained that the spillways in the Sittaung basin are not controllable. Water flows through the spillway if and only if the storage in the reservoirs exceeds the maximum capacity. The amount spilled is the exactly the exceeding amount. When including the spillway constraint in the objective function, the flows through the spillway are forced to behave this way. The outflow that can be released from the reservoir is then limited by the capacity of the conduit when the reservoir is not overflowing. Table 5.7 shows the storage capacity, the conduit capacity and the ratio of these two terms for all the reservoirs upstream of the flood point. Completely emptying the reservoirs takes more than 120 days for most reservoirs. If the reservoirs are full when a flood is expected by the MPC system, the buffer that can be created by the reservoir is at maximum the duration of the optimization horizon times the conduit capacity.

Table 5.7: Storage capacity (m^3), conduit capacity (m^3/day) and the ratio between storage and conduit capacity (days) for the reservoirs upstream of the considered location near Taungoo city. The ratio between the storage and conduit capacity is the minimum time needed to empty a full reservoir by releasing water from the conduit.

Reservoir	3	6	9	10	11	12	13	14	15	17	19
Storage capacity (m^3)	360	176	267	19	113	93	45	90	38	12	295
Conduit capacity (m^3/day)	26	1.5	1.8	0.16	0.61	0.75	0.69	0.72	0.31	0.10	18
Ratio (days)	14	120	145	121	185	124	66	124	124	124	16

5.2.2. The implementation of a penalty method for the spillway constraint

The spillway constraint is added iteratively with an increasing penalty to the objective function. There is no obvious normalization factor for this term, as the constraint has to be minimized and there is no clear reference value. The spillway behaviour in stage 1 may be very different from the spillway behaviour in stage

2. Also, spillway behaviour is different when optimizing for hydropower generation, flood control or both. Therefore, the spillway constraint was not normalized in the objective function. The value of the penalty applied to the spillway term was determined empirically. Choosing an appropriate value for the spillway constraint is not obvious. If the value is chosen too small, the solution will use the spillway in a physically impossible way. If the penalty on the spillway is too large, the spillway term in the objective function will become very large with respect to the other terms in the objective. This occurs because the spillway term often does not reach zero exactly. The spillway penalties with best performance differ per reservoir. The spillway penalty was increased in three steps from 0 to 10^{-15} to 10^{-14}. This resulted in the best performance in terms of final solution for most of the reservoirs. For some reservoirs, the spillway constraint showed correct behaviour after the first iteration already, for other only at the final iteration.

Figures 5.10a to 5.10c show the spilling behaviour for the three iterations of the penalty for reservoir 6. When the penalty is zero, the reservoir is emptied completely before the wet season to prevent floods. With a penalty of $\rho = 10^{-15}$ the spillway constraint works well. Increasing the penalty further to 10^{-14} leads to negligible improvement in spillway behaviour, and reduces the amount of hydropower produced.

Figures 5.10d to 5.10f show the spillway behaviour for reservoir 17. In this reservoir, the penalty needed to increase to 10^{-14} before it behave as required.

In Appendix I, the details of the behaviour of the spillway are presented for all reservoirs. The number of days that spilling occurs when the reservoir is not full is calculated with a 5 % margin. This means that if spilling occurred when storage exceeded 95% of the storage capacity, this spilling was considered legitimate. The spillway behaves as required with a penalty of 10^{-15} for all reservoirs except reservoir 3, 6 and 17. The decrease in number of spilling days for reservoir 3 is only one day, but for reservoir 17 it is 10 days. For reservoirs 14 and 19, the generated hydropower decreases with 7% and 8%, when the penalty for the spillway is increased from 10^{-15} to 10^{-14}. At the same time, the flood discharge for these reservoirs decreases with 5 % and 17% respectively. For all other reservoirs, the hydropower generated and flood discharge change by less than 1.5%.

5.2.3. The choice of a flood level

Subsection 5.2.1 shows that when the spillway constraint is not included, floods can be prevented for flood levels of above 40.6 m. When the spillway constraint is included, the reservoirs are limited by the capacity of the conduit to create a buffer zone to prevent floods. Figure 5.11 shows the water level after stage 2 for the flood levels 41.2m, 40.9m, and 40.6m. The penalty constraint is included with increasing penalty from 0 to 10^{-15} to 10^{-14}. The results in the figure are results for multi-objective scenario with weights of 1 for the hydropower and flood terms. The water level when not optimizing for floods in stage 2 is also presented in the figure for comparison. Floods can be prevented completely for a flood level of 41.2 m. When the flood level is defined at 40.9 m and 40.6 m, the water level exceeds the defined flood level. The maximum water level in this case is 41.2m, which is higher than in the optimization with a flood level of 41.2 m. This is because more water needs to be stored at the beginning of the wet season to keep the water levels below 40.9 and 40.6 meter instead of 41.2 m. Later in the wet season, less free storage is available in the reservoirs, resulting in higher water levels for a defined flood level of 40.6 and 40.9 meters than for 41.2 meters.

Table 5.8 shows the maximum water level, the total flood discharge, the total discharge above 40.6 m, the number of flood days and the hydropower generated for the four different scenarios. Additionally, the CPU time is given. For the optimization without the flood term, the flood discharge and number of flood days are calculated with a flood level of 40.6 m. The table shows that the maximum water level is lowest when optimizing for a flood level of 41.2 m, shown in figure 5.11. The total discharge above flood level decreases from 26.9 m^3 for flood level 40.6 m to 0.1 m^3 for flood level 41.2 m. This was the term that had to be minimized in the objective function. However, the total flood discharge increases when increasing the flood level from 40.6 m to 41.2 m. This can also be seen in figure 5.11. For a flood level of 41.2 m, the water level increases at other moments compared to the original water level. Even though floods cannot be prevented completely for flood levels of 40.6 m, the number of flood days can be decreased from 50 to 40 days and the flood discharge can be decreased from 36.8 m^3 to 26.9 m^3. The total hydropower produced in the basin decreases from 180 GWh to 160 GWh or 159 GWh, when changing from single-objective hydropower optimization to optimization for both hydropower and flood mitigation. This is a decrease of 11 % to 12%. In the next section, the trade-off between hydropower generation and flood mitigation is discussed in more detail.

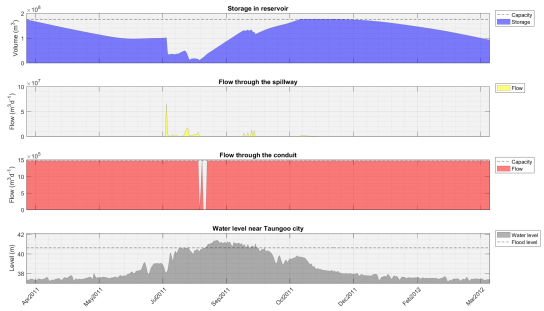

(a) Reservoir 6, penalty for spillway (ρ_2)0.

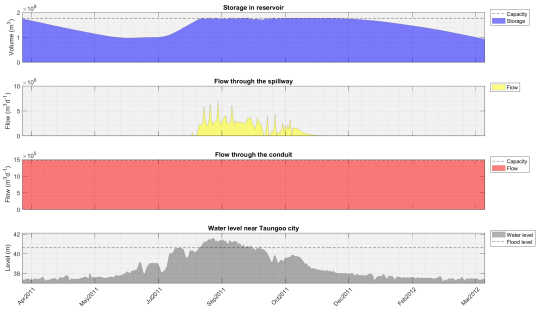

(b) Reservoir 6, penalty for spillway $\rho_2 = 10^{-15}$.

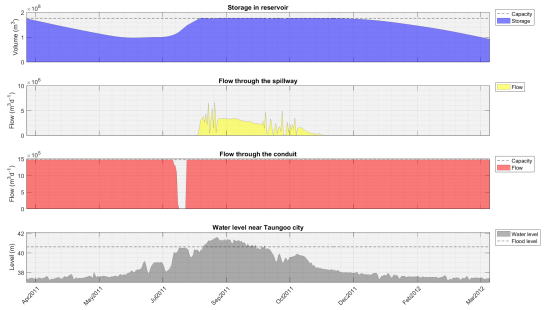

(c) Reservoir 6, penalty for spillway $\rho_2 = 10^{-14}$.

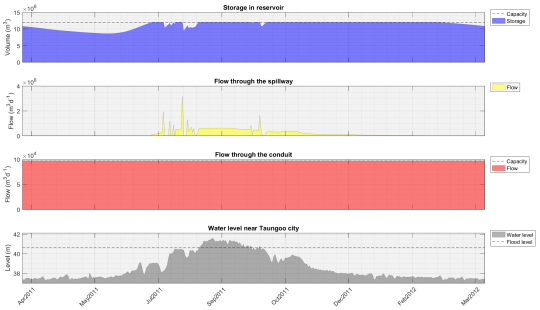

(d) Reservoir 17, penalty for spillway $\rho_2 = 0$.

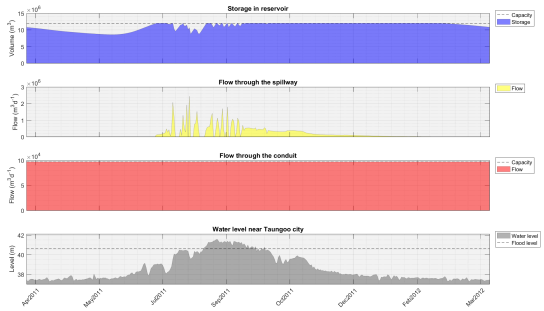

(e) Reservoir 17, penalty for spillway $\rho_2 = 10^{-15}$.

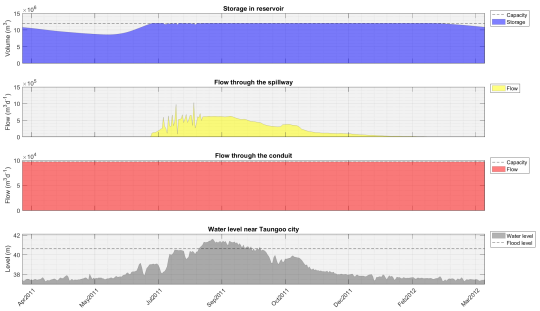

(f) Reservoir 17, penalty for spillway $\rho_2 = 10^{-14}$.

Figure 5.10: Behaviour of the spillway for iteratively increasing penalty for the spillway term in the objective function. The storage in the reservoir, flow through the spillway, flow through the conduit and the resulting water level near Taungoo city are shown for the penalty increasing from 0 to 10^{-15} to 10^{-14} for reservoir 6 and 17.

5.2.4. The trade off between hydropower generation and flood prevention

Figure 5.12 shows the pareto plot for results of stage 2. The result for each run is labelled with a number in the figure. Number 1 indicates the result for the single-objective hydropower optimization. The other numbers represent runs with different flood levels, indicated by the first two digits, and weight factors for flood mitigation and hydropower, indicated by the last two digits. The first two digits are 12, 13, or 14, indicating the flood levels 40.6m, 40.9m, and 41.2m. The last two digits indicate the weights [HP FL], run XX00: [1 1], run XX01: [1 0], run XX02: [1 0.5], run XX03: [0 1], run XX04: [0.5 1]. The filled circles are points that are pareto optimal for the considered set of points.

The total amount of hydropower generated is normalized by the amount generated in run 1, so it is scaled by 180 GWh hydropower. The flood discharge is normalized for the discharge above the considered flood level for run 1. For example, when optimizing for a flood level of 40.9 meter, the total discharge above that level is calculated and divided by the total discharge above 40.9 meter for run 1. This means that the flood discharge for run 1400 is normalized with a different factor than run 1300 or 1200. Runs with different flood levels should only be compared in terms of hydropower generation. Runs with the same flood level can also

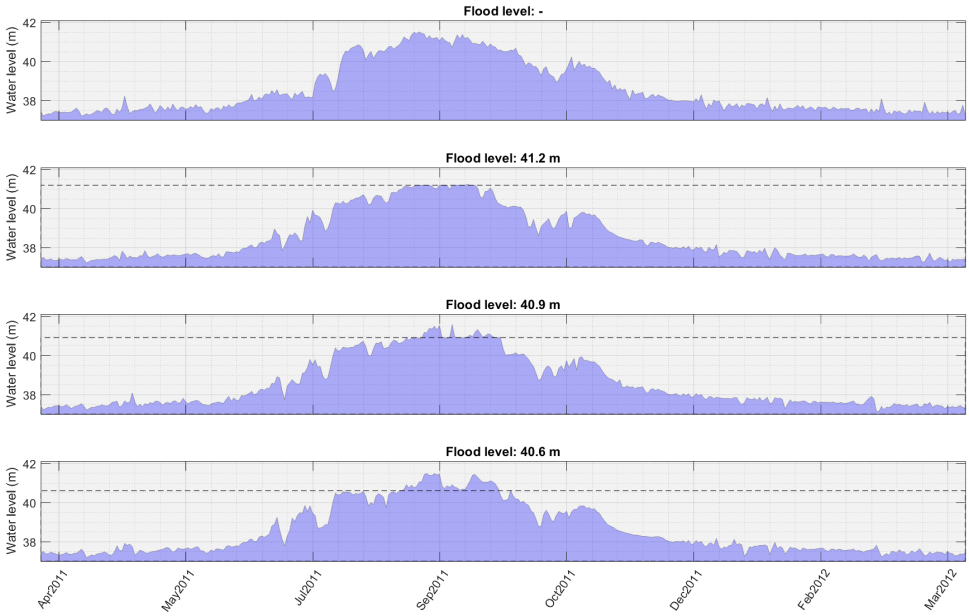

Figure 5.11: Water levels near Taungoo city for MPC stage 2 with spillway constraint. The plots from top to bottom are generated for optimization without floods included in the objective, with a flood level of 41.2 m, with 40.9m and with 40.6m. The weight on hydropower was 1 in all four cases. The weight on flood mitigation was 0 in the first and 1 in the second, third and fourth plot.

be compared in terms of flood discharge.

Note that the runs 1200,1202, 1300, 1302, 1400 and 1402 resulted in better final solutions in terms of both objectives than the runs 1201, 1301 and 1401. This means that the multi-objective optimization for floods and hydropower not only results in more hydropower, but also in more flood reduction than the single-objective flood optimization. This can be explained by looking at the reservoir operation for both scenarios. Figure 5.13a shows the operation of reservoir 6 for the single-objective flood optimization and figure 5.13b shows the operation for the optimization with equal weights on floods and hydropower. Recall that the optimization horizon is 30 days. When starting in April 2011, the MPC system does not foresee floods in the optimization horizon. In the multi-objective optimization, the reservoir releases water through the conduit to produce hydropower at maximum capacity. In the single-objective optimization, there is no incentive to release water causing the waterlevel drop slower than in the multi-objective optimization. When the MPC system foresees floods within 30 days, the reservoir in the single-objective case has less free storage available than the reservoir in the multi-objective case. This only occurs because the reservoirs are full at the start of stage 2. If the storage in the reservoir is low at the start of stage 2, the single-objective reservoir has no incentive to increase

Table 5.8: The maximum water level (m) in the river section near Taungoo city. The flood discharge (10^6 m^3), that is the total discharge above flood level, and the discharge above 40.6 m (10^6 m^3) are given for each of the defined flood levels. The number of flood days, total hydropower generation for the basin (GWh) and the CPU time (min) for running stage 2 are given as well. The first row containts the results for single-objective hydropower optimization. The second, third and fourth row show the results for the multi-objective optimization with equal weights for hydropower and flood mitigation.

Flood level (m)	Maximum WL (m)	Flood discharge (10^6 m^3)	Discharge above 40.6 m (10^6 m^3)	Flood days	Total hydro-power (GWh)	CPU time (min)
-	41.5	36.8	36.8	50	180	101
40.6	41.5	26.9	26.9	40	160	694
40.9	41.6	9.2	29.7	30	160	689
41.2	41.2	0.1	34.2	14	159	702

the storage in the reservoir, whereas the multi-objective optimization does. In that case, the opposite result would be observed, the single-objective optimization probably would result in more flood reduction than the multi-objective optimization. The set-up of the two-stage MPC method was to run stage 2 of the optimization only for a period with a risk of floods. Stage 2 often starts with full reservoirs, because stage 1 optimizes for hydropower and irrigation supply and has an incentive to keep the reservoirs full. Therefore, the multi-objective optimization for stage 2 performs better in terms of both objectives than the single-objective flood optimization.

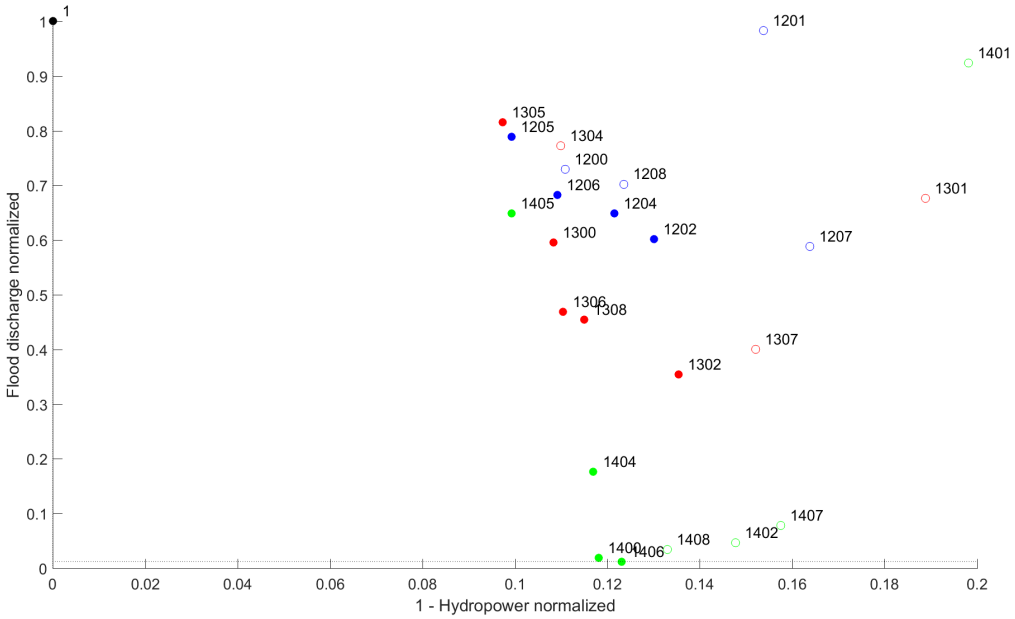

Figure 5.12: Pareto plot for the trade-off between hydropower and flood mitigation in stage 2. Number 1 indicates the result for the single-objective hydropower optimization. The other numbers represent runs with different flood levels, indicated by the first two digits, and weight factors for flood mitigation and hydropower, indicated by the last two digits. The first two digits are 12, 13, or 14, indicating the flood levels 40.6m, 40.9m, and 41.2m. The last two digits indicate the weights [HP FL], run XX00: [1 1], run XX01: [1 0], run XX02: [1 0.5], run XX03: [0 1], run XX04: [0.5 1].

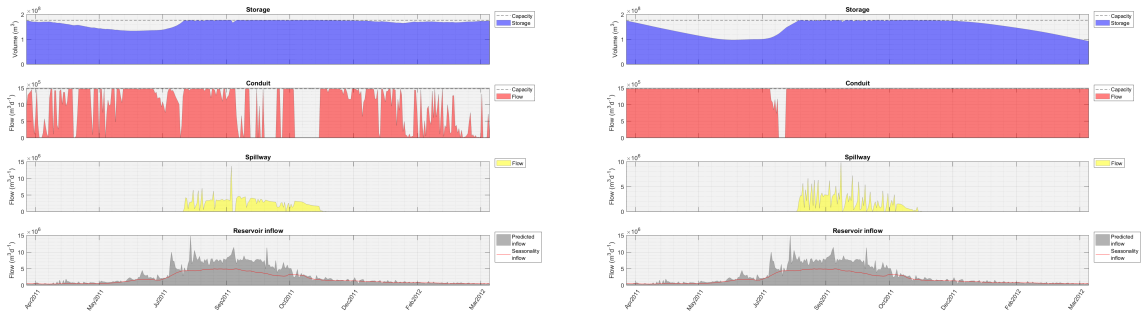

(a) Single-objective flood optimization.

(b) Multi-objective flood and hydropower optimization.

Figure 5.13: Operation of reservoir 6 for the single-objective flood optimization and the multi-objective optimization with weight 1 on hydropower and flood mitigation.

The best performance in terms of flood reduction is the multi-objective case. In this case, the decrease in hydropower is 11 % for a flood level of 40.6 m and 40.9 m, and 12 % for a flood level of 41.2 m. Even though this decrease is significant, it also means that flood mitigation does not come fully at the expense of hydropower generation. For longer optimization horizons, flood mitigating capacity of the system is expected to be larger. A side effect of this may be that hydropower generation is reduced more, as the storages in the reservoirs can be lowered more.

6

Discussion

In this chapter the effects of used methods, assumptions and other choices on the results will be discussed. The affects of choices made in the model for the system dynamics are discussed in . Effects of estimations of irrigation demands and calculation of hydropower generation are described in section 6.2 and section 6.3. Section 6.4 discusses the effect of assumptions about reservoir characteristics. The external disturbances are considered in section 6.5. The effect of uncertainties on the performance of the MPC system is discussed in section 6.6. Finally, the effects of choices made for the structure of the MPC method are discussed in section 6.7.

6.1. The effects of choices made when modelling the river dynamics

The choice for the Muskingum routing method The Muskingum routing method was used for flood routing in the river for two reasons. First, not enough hydro-morphological data was available to estimate the parameters for the Saint-Venant equations. The second reason is that fewer variables are used in the Muskingum routing method than in the discretized Saint-Venant equations. A larger number of state variables results in a larger optimization problem. The number of optimization variables turned out to be a limiting factor for the implementation of the MPC system. If the appropriate variables are used, the Saint-Venant equations describe the propagation of a flood wave in a physically more realistic way. However, when the appropriate parameters for the Muskingum method are used, the estimation of the timing of flood waves and the maximum water levels is reasonable. An approximate estimation of timing and size of the flood wave is sufficient for the application of flood control. An operator is likely to select a conservative operation for flood management. A more detailed estimation of the water levels is not required. Considering the fact that the control actions are performed on a daily basis, better estimation of the timing of flood peaks is also not expected to improve the performance of the MPC system.

The estimation of parameters for the Muskingum routing method The parameters x and K, the weighting factor for inflow versus outflow and the storage-time coefficient, are usually calibrated on historical flood data. Since water level and discharge measurements were only available per day, a commonly used value for the parameters was assumed. The effect of these parameters on the results should be investigated.

The conversion from storage to water level and the choice of a flood level The cross-section of the river was assumed to have a rectangular shape with a width of 200 meter for the entire cross-section near Taungoo. The length of that segment is 7 km and the shape of the cross-section probably varies over this distance. This would change the conversion from storage to water level. It does not influence the flood routing because the Muskingum method is based on storage and not on water depths. It does influence the comparison of simulated water levels and flood levels with the actual water and flood levels. Figure 5.8 shows the water levels are underestimated in comparison to the measured water levels, especially for low flow periods. The variation of the simulated water level over a year is similar to the variation of the measured water levels. Flood mitigation

is analysed for selected flood levels of 40.6m, 40.9m and 41.2m. The flood level near Taungoo determined by Rest (2015) is 43m. The underestimation of the water levels in 2014 is approximately 1.5 meters, so the flood levels of 40.6-41.2 m are considered to be conservative with respect to the real system.

6.2. The estimation of irrigation demands

Appendix H describes how the irrigation demands are estimated. The irrigation demands are likely overestimated. This is probably due to an optimistic estimation of the irrigated area, which was assumed to be equal to the irrigable area. Also, the water demands of the crops were used as irrigation demand, without taking precipitation into account. The model resukts show that the irrigation demands can almost always be satisfied, which would still hold if actual irrigation demands were lower. The irrigation demands for the Yezin (14) and Minye (20) reservoir are not always met. This irrigation deficit is not due to a lack of available water, but due to the limitation of the conduit capacity. It is likely that this deficit is a result of the overestimation of the irrigation demand. Finally, it was concluded that hydropower generation and irrigation supply are not competing objectives in the basin. This conclusion remains valid if actual irrigation demands are lower than the estimated irrigation demands.

6.3. The estimation of hydropower generation by the reservoirs

The water level and the storage were assumed to be linearly related for the calculation of the hydropower generation. This leads to an underestimation of the generated hydropower. Hydropower is calculated for discrete timesteps using a first order Taylor approximation, which introduces an error in the estimation. Finally, the average efficiency of the reservoirs was estimated to be 40 % (Kyi, 2015), but are actually different per reservoir. The generated hydropower in the reservoirs should be verified with data. For the MPC method a rough estimation of hydropower generation is sufficient to optimize reservoir operation.

6.4. The influence of the assumed reservoir dimensions

For some reservoirs in the model the storage capacity, conduit capacity, irrigable area, waterspread area are unknown. Values were assumed based on typical relations between storages, conduits, waterspread area, irrigable areas and reservoir catchment area. Variations in these relations are large the assumed values are uncertain. When implementing the MPC system, the actual dimensions of the reservoirs should be included in the model. The influence of these assumptions on the results presented in this study are considered.

The estimated hydropower generation is based on the storage capacity, the conduit capacity and the waterspread area. For reservoirs Kawliya (7), Bawni (8), Yanaungmyin (10), Ngalaik (12), Yezin (14), Chaungmagyi Pyi (17), Swegyin (18), Thaukyegat (19), Minye (20) and Kunchaung (21), one or more of these values had to be assumed. The reservoirs 7, 8, 10, 12, 14, 17 and 20 each contribute less than 1% to the total hydropower generation in the system (table 5.5), so the impact of the assumptions for these reservoirs on hydropower generation is negligible. Reservoir 18 and 21 contribute 5 % and reservoir 19 contributes 13 % to the total hydropower generation. The conduit and storage capacities for these reservoirs were known, only the waterspread area was assumed. The waterspread area is not used in the optimization. It is only for the calculation of the amount of hydropower production. The assumption for these areas does not influence the optimal operation of the reservoirs, but may influence the estimated absolute amount of hydropower produced.

The effect of assumed values for reservoir dimensions on the irrigation supply are only related to storage, conduit capacity and irrigable area. Irrigable areas affect the estimated irrigation demands, which were found to be overestimated. The only reservoir for which there was an irrigation deficit, was reservoir Miny (20). This irrigation deficit is not related to the reservoirs capacity but due to the limited conduit capacity. This may indicate that the conduit capacity is underestimated, but it is more likely that the irrigation demand was overestimated.

For flood control, the values for storage and conduit capacity are important. These values were assumed for reservoirs Yanaungmyin (10), Ngalaik (12), Yezin (14) and Chaungmagyi Pyi (17) upstream of Taungoo. The reservoir catchment areas of these reservoirs are 28 km^2, 328 km^2, 33 km^2 and 119 km^2, which is less than 1 % of the Sittaung river basin area. Their influence of flood control is negligible.

Uncertainties in the assumed values do not affect the optimal operation of the reservoirs and conclusion related to trade-off between the different objectives. Assumptions for the waterspread area may affect the reported absolute amounts of hydropower for some reservoirs and for the total system.

6.5. The model for the external disturbances

At the start of this research, a rainfall-runoff model was developed for the predicted inflows to the reservoirs and river. There was insufficient (reliable) data available to calibrate a model that predicts flood peaks in the basin accurately. Instead, a semi-synthetic series of inflows to the reservoirs and rivers was used in this study. No spatial variability of the external disturbances throughout the basin was taken into account.

The spatial variability of external disturbances Outflows from all subcatchments were assumed to have the same pattern as the inflow series to the Paunglaung reservoir, multiplied by a factor related to the size of the subcatchment. This means that the spatial variability of climate, geography and vegetation in the basin were not taken into account. This spatial variability is known to be large in the Sittaung basin. The Paunglaung reservoir is located in the north of the basin, where the annual precipitation (890 mm y^{-1} is smaller than in the south of the basin (3800-5000 mm y^{-1}). It is likely that the inflows to the river are underestimated,(see figure 5.8). Effects on the results with respect to irrigation supply are expected to be negligible. The irrigation demands were likely overestimated and the inflows to the reservoirs likely underestimated and still irrigation demands could be met. Effects on the results with respect to hydropower are expected to be larger. When optimizing for hydropower in stage 1, most reservoirs do not use the full capacity of the conduits to generate hydropower. The outflow through the conduit and the water level in the reservoir need to be maximized to maximize hydropower generation. If inflows to the reservoir are low, the optimal strategy is to release water through the conduit at a lower rate than the conduit would allow in order to keep water levels high. If inflows are larger, the outflows through the conduits could be increased while keeping the water levels in the reservoir high, increasing the hydropower generation. The underestimation of inflows to the reservoirs results in an underestimation of the potential hydropower generation in the basin. The results for stage 1 operation suggest that this effect is significant.

The capacity to mitigate flood is likely overestimated if inflows to the reservoirs and rivers are underestimated. On the other hand, the flood location that was considered is Taungoo city, which located in the center of the basin. This means that only the spatial variability for the upper part of the basin is relevant for the results with respect to flood control in this study. Furthermore, figure 2.3 shows that the area of the Paunglaung reservoir catchment covers around 30 % of the basin upstream of Taungoo city. This explains why the simulated peaks based on Paunglaung data, in water levels near Taungoo showed a correspondence with peaks in the measured water levels near Taungoo (see figure 5.8). It is expected that better estimation of the external disturbances decrease the flood mitigation capacity of the system. The effect on flood mitigation near Taungoo city is expected to be lower than for sections of the river downstream of Taungoo. For the practical implementation of this system, a better prediction model for external disturbances should be developed.

The uncertainties in the predicted future external disturbances Uncertainties in the predicted future external disturbances were not taken into account. In the experimental set-up the predicted external disturbances were equal to the actual past external disturbances used as input to the model. In a practical implementation of the MPC system, the predictions of future external disturbances result from a model, whereas past external disturbances would be measured in the real system. The effects of these uncertainties on the performance of the MPC system in the Sittaung basin should be investigated. Methods to handle these uncertainties have been investigated intensively Camacho et al. (2007) Raso (2013), but were beyond the scope of this research.

Seasonality of the external disturbances Beyond the prediction horizon, seasonality of the external disturbances was provided to the MPC system. The seasonality series was derived as the 4-year average of the input series for the external disturbances. The seasonality series in the model likely includes more information about the actual external disturbances than seasonality information would in reality. This results in an

overestimation of the control system's performance in the experiments. Together with the assumption of perfect predictions within the prediction horizon, the system's performance presented in this research should be considered a hypothetical optimal performance. For implementations in the real world, the performance of the system especially in terms of flood control and hydropower generation will likely be lower.

6.6. The effect of uncertainties on the performance of the MPC system

The previous sections discuss the uncertainties in the model for the internal system dynamics and in the predictions of future external disturbances. In practical implementations, actual external disturbances, control actions and system outputs are measured in the real system and used as input for the model. These measurements also include uncertainties that were not taken into account in the experimental set-up for this research. The effect of these uncertainties on the performance of the MPC system should be investigated. This was beyond the scope of this research.

6.7. The structure of the MPC method

The two-stage approach of the MPC method was developed to reduce the problem size by dividing it into subproblems. In this section the choices made for the two-stage optimization will be discussed.

The decentralized approach for stage 1 Stage 1 was implemented with a decentralized approach, in which hydropower and irrigation are considered per reservoir. This approach is possible because the objective of the control problem was to maximize hydropower generation in the basin. If the aim were to meet an electricity demand for the entire basin, the decentralized approach is not possible. A reason to define the aim of meeting a demand instead of maximizing production could be related to the limitations of the electricity network. In that case, a coordinated approach could be implemented similar to the stage 2 implementation. The aim to maximize hydropower generation is an appropriate choice for considering the potentials of the reservoir system in the Sittaung basin. In a practical implementation of an MPC system, the capacity of the electricity network should be considered.

The coordinated appraoch for stage 2 A coordinated approach is implemented in stage 2 of the MPC control. In this approach the problem is divided into subproblems, in which for each subproblem the optimal operation of a reservoir is determined with respect to the system-wide objective of flood mitigation and hydropower generation. It is possible that the coordinated approach does not achieve the results that a centralized MPC controller would be able to achieve for the system. There are several reasons for which the coordinated approach could have a lower performance in terms of final solution than the centralized approach. The operation of reservoirs at a specific timestep is included in the optimization of other reservoirs for that timestep only if their optimization if performed later in the stage 2 loop. The order in which reservoirs are optimized could therefore influence the final solution. When optimizing the subproblem for one reservoir in stage 2, its objective is to prevent floods if possible. It may be more efficient if the flood were prevented by another reservoir, when the entire system is considered. When solving the optimization in a centralized way, this option is considered in the optimization. Rawlings and Stewart (2007) mention that the extent to which a coordinated approach results in system-wide optimal solutions mainly depends on the level of interaction between the subsystems. The level of interaction between the reservoirs is limited, their only interaction is that they affect the same objective. It is expected that the coordinated approach leads to similar results as the centralized approach, but this should be investigated further.

A disadvantage of the coordinated approach as presented in this study, is that solution of the optimization problems for each reservoir cannot be performed in parallel. The MPC system would be much faster if all subproblems could be optimized in parallel. The effect of performing the optimization of the subproblems in parallel, thereby loosing the information exchange between the sub-problems, was not investigated in this research. If performing the optimization in parallel results in final solutions similar to the approach in series, the parallel approach would be an improvement of the system.

The switching decision from stage 2 to stage 1 The MPC system switches to stage 2 if a flood is predicted by the simulation model within the optimization horizon of stage 2. After optimization for stage 2, the maximum simulated water level until the optimization horizon is considered. If that water level is lower than a specified flood level minus an offset, the MPC system will switch back to stage 1. If the maximum water level is higher than the specified flood level minus offset, the MPC system will continue in stage 2. This mechanism was not studied in this research. The offset needs to be determined and the appropriate value for this offset depends on the defined flood levels and uncertainties in the model. If the offset is chosen too small, the system switches back to stage 1 when the flood risk is not yet over. If the offset is chosen too large, the system continues in stage 2 for too long, leading to unnecessary computation times and unnecessary irrigation deficits. This switching decision from stage 2 to stage 1 should be investigated further.

The implementation of the receding horizon in stage 2 The MPC system uses a three layer deep nested loop;a loop for the iteration over the sub-problems defined for the coordinated approach of stage 2 (sub-problem loop), a loop over the increasing penalties for the violation of the spillway constraint in the objective function (penalty method loop) and a loop shifting the optimization horizon and optimizing the next timestep (receding horizon loop). In this research the receding horizon loop was implemented as the inner loop, followed by the penalty method loop and the sub-problem loop as the outer loop. In practice the penalty method loop should have been implemented as the inner loop, followed by the sub-problem loop and the receding horizon as the outer loop. In practice, at each timestep the stage 2 optimization is performed for all reservoirs before continuing to the next timestep and using new observations from the real system. For the experimental set-up this difference in implementation does not significantly influence the results because no new information from the real system is used at new timesteps. The only difference in the approach is solution used for warm-starting the problem. Each optimization is warm-started with the solution of the previous optimization. This means that in the practical implementation, the solution of the optimization problem at timestep k for reservoir j for a value of the penalty is used to warm-start the next iteration of the penalty method loop for that same timestep and reservoir. In the implementation used in this research, algorithm proceeds over all timesteps for a fixed penalty and only proceeds to the next value for the penalty after the 'implemented' solution for all timesteps was determined. The effect of this incorrect implementation is expected to influence the computation time, because the warm-starting of the problem is further away from the optimal solution. The effect on the final solution is most likely limited. The receding horizon should be implemented as the outer loop, for practical implementation of the system.

Including a long-term strategy in the MPC method without increasing the optimization horizon The research showed that increasing the optimization horizon for MPC increases computational costs for solving the optimization problem. The system's flood mitigating capacity was found to be limited mainly by the conduit capacities and the optimization horizon. Most reservoirs need more than 120 days to empty completely when releasing water at maximum capacity through the conduits. The pattern of wet and dry seasons in the basin is strong and relatively predictable. Raso and Malaterre (2016) propose a strategy to include long-term strategies for reservoir operations in model predicive control systems. Including a strategy will likely improve the system's flood mitigating capacity.

6.8. The formulation of the optimization problem

Choices were made for the formulation of the optimization problem. Objectives and constraints could have been implemented in other ways, in this section the implications of these choices are considered.

The formulation of the hydropower objective In the previous section the formulated objective for hydropower was discussed in relation to the decentralized approach of stage 1. The implementation in this study works to maximize hydropower for a period until the optimization horizon. It was show that this leads to fluctuations in hydropower generation and large fluctuations in the conduit outflows. In reality, an operator is more likely to aim for a reliable constant hydropower generation. This could be included in the objective function by penalizing changes of the conduit outflows.

The implementation of spillway dynamics in the optimization problem The spillway constraint is defined as a complementarity constraint, stating that the product of the term α defined in equation 3.4 and the flow through the spillway Q_s should always be zero. In this research the spillways behave as required with this implementation. Finding appropriate values for the penalty was not trivial and inclusion of the spillway increases computation time for the optimization problem significantly. Celeste and Billib (2010) present a method, in which a similar term α is defined. Instead of minimizing the product of α and Q_s, the sum of α and Q_s is minimized in the objective function. The advantage of this method is that the term in the objective function is linear in terms of the optimization variables. Also, it is easier to determine a normalization factor for this term than for the product. This approach has not been investigated in this research but should be considered in future work. Another option is to apply relaxation for the complementarity constraint in which the lower and upper bounds on the complementarity constraints are set to $-\delta$ and δ and solving the problem iteratively for decreasing value of δ (Pecci et al., 2017). In this research initial tests were performed for this method and results were comparable to to the penalty method.

The scaling of the optimization problem The results showed that the optimization is sensitive to scaling of the optimization problem. In this research, the terms in the objective function were scaled with a normalization factor. The constraints and variables were not scaled. Betts (2010) states that no scaling method is uniformly successful for nonlinear optimization problems. The structure of the optimal control problem can be used to improve scaling of the related NLP problem. This approach was taken when scaling the objective function. Potentially, scaling the constraints and variables could further improve the robust and rapid convergence to a solution of the NLP. However, the scaling performed would always be tailor-made for the problem considered and would not be transferable to other problems. For this reason, further scaling of the optimization problem was not considered in this research. When implementing the MPC system in practice, the scaling of the NLP for the specific application can improve performance of the MPC system and therefore be useful to consider.

7

Conclusions and recommendations

This research follows the trend of increasing attention for the application of model predictive control on water systems and reservoir systems in particular (Van Overloop (2006), Tian et al. (2015), Raso (2013)). In the field of model predictive control more and more researchers focus on approaches such as disctributed, coordinated and hierarchical MPC (Maestre et al. (2011), Christofides et al. (2013), Rawlings and Stewart (2007), Scattolini (2009)). Application of these methods on multi-reservoir systems was studied by Anand et al. (2013), Breckpot et al. (2010), Doan et al. (2013) and Niewiadomska-Szynkiewicz et al. (1996). The considered systems in these studies consisted of two or three reservoirs and were optimized for flood control or hydropower generation. The reservoir system studied in this research has 21 reservoirs and is operated for hydropower, irrigation and flood management. One aim of this research was to develop an optimal control method for the operation of a large-scale multi-purpose multi-reservoir system.

The case study for this research was the reservoir system in the Sittaung river basin in Myanmar. The basin suffers from frequent floods causing large social and economic losses (Rest, 2015). Myanmar is a rapidly developing country with a rapidly increasing demand for energy (Hasman, 2014). Agriculture is a main source of income for Myanmar (Hasman, 2014). Optimal operation of the Sittaung's reservoir system in terms of hydropower, irrigation and flood management is a relevant topic. This leads to the second aim of this research, which was to investigate whether operation of the reservoirs in the Sittaung basin can be improved such that floods are prevented or reduced while taking hydropower generation and irrigation supply into consideration.

The research showed that irrigation demands could almost always be met for the scenario considered. In this scenarios the demands are expected to be overestimated and the inflows to the reservoirs underestimated, meaning that this conclusion probably holds for the real system as well. It was concluded that hydropower and irrigation are no competing objectives because the irrigation demands are much smaller than the dimensions of most reservoirs. Results showed that flood mitigation is possible for a modelled flood level of 41.2 meter near Taungoo city, but not for the defined flood levels of 40.9m or 40.6m. The flood levels 40.6m - 41.2m are conservative with respect to the real system, but better estimations of river inflows are needed to relate conclusions to the actual situation in the Sittaung basin. For the flood level of 41.2 m, reduction of hydropower generation for flood mitigation was approximately 12 %. This shows that there is a trade-off between hydropower and flood mitigation, but the trade-off is small. An analysis of the reservoir capacities showed that the limiting factors for flood mitigation are the conduit capacities and the optimization horizon, but not the storage capacity of the reservoirs. Stage 2 of the MPC method was performed with an optimization horizon of 30 days. It was shown that most reservoirs need to release water at full capacity for more than 120 days in order to completely empty the reservoirs. Computational costs for solving the optimization problem increase nonlinearly with increasing optimization horizons. The extent to which optimal operation of the reservoir system in the Sittaung river basin can reduce flooding mainly depends on the optimization horizon.

Considering the clear distinction between wet and dry season in the basin (Rest, 2015), the option to implement different strategies in the MPC method for long-term planning of reservoir management, is an inter-

esting direction for future research. Raso and Malaterre (2016) consider such a method. A better model for the external disturbances, including the spatial variability, needs to be developed to increase reliability of conclusions about the Sittaung river basin, a. This model is also required for the practical implementation of a model predictive control system in the basin. More reliable, frequent and spatially distributed measurements of discharges in the tributaries of the Sittaung river and the river itself, as well as precipitation and evaporation data are required to develop such a model.

The second research question was: 'How can model predictive control be applied for optimal operation of a multi-purpose reservoir system of 21 reservoirs?'. A two-stage MPC method was presented, dividing the optimization problem into sub-problems using the structure of the dynamic system (parallel connection of the reservoirs to the river) and periodicity of the external disturbances to the system (wet season and dry season). Switching to the decentralized approach of stage 1 in periods without flood risks decreases computation times because the optimization can be performed in parallel. The decentralized optimization for hydropower and irrigation in stage 1 results in a system-wide optimal solution as a results of the system's structure. The coordinated MPC method for stage 2 reduces computation time with respect to a centralized approach, because computation time for solving the nonlinear program increases nonlinearly with the size of the optimization problem. The nonlinear dynamics of flow through the spillways was modelled with a complementarity constraint and included in the objective function using the penalty method. The flow through the spillway behaved as required, but inclusion of the spillway term increases computation times and finding a normalization factor for the spillway term and appropriate values for the penalty parameter is not trivial. One of the challenges when solving the nonlinear optimization problem was that it was found to be highly sensitive to scaling of the problem. Defining normalization factors for the flood and spillway terms in the objective function was not trivial, especially because the order of magnitude of these terms are different for different system states. After normalization of the different terms in the objective function, a scaling factor was required for the convergence of the algorithm. Appropriate termination criteria for the interior-point method depend on scaling of the problem as well. All these aspects affect the performance of the interior point method in terms of computation time and final solution. Appropriate scaling of the NLP is very problem specific and was therefore only considered to a limited extent in this work. For implementation of a system in practice, scaling of the problem should be considered in more detail.

It was not investigated whether the coordinated MPC approach results in system-wide optimal solutions as would be found by a centralized approach. Based on Rawlings and Stewart (2007), it is expected that this is the case, because interaction between the subsystems is limited. Furthermore, the switching condition for switching from MPC stage 2 to MPC stage 1 was described but not studied in this research. It was discussed that consideration of prediction uncertainties within the MPC is necessary for implementation in practice. It is also important to consider when determining the potential performance of a MPC system in the basin. All these aspects of the MPC method should be investigated. Recommendations in terms of formulation of the optimization problem concerns the spillway term and the hydropower objective. It was discussed that for practical purposes a constant reliable energy production is more valuable than a fluctuating maximum production. It is recommended to penalize fluctuations of energy production in the formulation of the optimization problem. Finally, Celeste and Billib (2010) proposes a method for including spillway flows in the objective function is a linear way and suggests appropriate normalization factors for this term. This method is expected to lead to better performance in terms of computation time and it is recommended to consider this method in future research.

Appendix A

Karush-Kuhn-Tucker (KKT) conditions

The Karush-Kuhn-Tucker (KKT) conditions are necessary conditions for optimality of the solution of a non-linear program subject to equality and inequality constraints. To derive the KKT conditions, first the solution of an optimization problem without constraints will be discussed. Then the solution of an optimization problem with only equality constraints using the Method of Lagrangian Multipliers will be discussed. Finally, the KKT conditions will be derived.

For an optimization problem without constraints, the objective function would be minimized by finding the roots of the gradient of the objective function with respect to x.

$$\nabla_x f(x) = 0 \tag{A.1}$$

An optimization problem with only equality constraints can be solved with the method of Lagrangian Multipliers. In this method the equality constraints are included in the Lagrangian using Lagrangian multipliers y with $y \in \mathbb{R}^m$ (eq. A.2). The derivative of the Lagrangian with respect to a Lagrangian multiplier is equal to the corresponding equality constraint. A solution that is zero is all derivatives with respect to the Lagrangian multipliers satisfies the equality constraints (eq. A.4). Hence, finding the roots of the gradient of the Lagrangian with respect to x (eq. A.3) and y, results in a solution that minimizes the objective function while satisfying the equality constraint.

$$\mathscr{L}\left(x, y, z\right) = f(x) + (A_e x - b_e)^T y \tag{A.2}$$

$$\nabla_x \mathscr{L}\left(x, y, z\right) = \nabla_x f(x) + A_e^T y = 0 \tag{A.3}$$

$$\nabla_y \mathscr{L}\left(x, y, z\right) = (A_e x - b_e)^T = 0 \tag{A.4}$$

In case the optimization problem is defined equality and inequality constraints, the inequality constraints are included in the Lagrangian using Karush-Kuhn-Tucker (KKT) multipliers z with $z \in \mathbb{R}_+^p$ (eq. A.5). In this case, there are three necessary conditions for optimality, the KKT conditions. First, the solution is a root of the gradient of the Lagrangian function with respect to x (eq. A.6). Second, the solution is a root of the derivatives of the Lagrangian function with respect to y (eq. A.7). The third and final condition ensures that the inequality conditions are satisfied. This is called the complementary slackness condition (eq. A.8). In order to see why this condition works, the concept of active and inactive contraints is important. Let $(A_i(x) - b_i)^{(j)}$ denote the j-th constraint in the set of p constraints $A_i x - b_i \geq 0$. If for a solution x^* the constraint $(A_i(x^*) - b_i)^{(j)} = 0$, this constraint is at actively restricting the optimal solution. We call it an active constraint. If on the other hand, $(A_i x^* - b_i)^{(j)} > 0$, the constraint is said to be inactive as it is not restricting the optimal solution. For inactive constraints the corresponding KKT multipier $z^{(j)}$ is defined to be zero. This means that either $z^{(j)}$ or $(A_i x^* - b_i)^{(j)}$ is equal to zero if x^* satisfies the constraint and is optimal.

$$\mathscr{L}\left(x, y, z\right) = f(x) + (A_e x - b_e)^T y - (A_i x - b_i)^T z \tag{A.5}$$

$$\nabla_x \mathscr{L}\left(x, y, z\right) = \nabla_x f(x) + A_e^T y - A_i^T z = 0 \tag{A.6}$$

$$\nabla_y \mathscr{L}\left(x, y, z\right) = \left(A_e x - b_e\right)^T = 0 \tag{A.7}$$

$$\text{diag}(z)\left(A_i x - b_i\right) = 0 \tag{A.8}$$

The matrix diag(z) is defined as the diagonal matrix with the vector z on the diagonal elements. So, diag(z) $(A_i x - b_i)$ is of size $p \times 1$.

Necessarity of KKT optimality conditions The above conditions are necessary conditions for optimality of a solution, only if the optimization problem is regular at the solution x^*. The problem is regular at x^* if it satisfies regularity conditions, or in other words a constraint qualification (Eustaquio et al., 2008). For the problem defined in this thesis the Linearity Constraint Qualification is satisfied for all x, as all constraints are affine functions. Therefore, the KKT conditions are necessary conditions for optimality.

Sufficiency of KKT optimality conditions The KKT conditions are sufficient optimality conditions only in specific cases (Hanson, 1981). In general, additional conditions are required to have sufficient conditions for optimality.

Appendix B

The solution of the barrier problem

For the solution of the NLP formulated in section 4.5 the primal-dual interior point algorithm with a filter line-search method as implemented in IPOPT.m was used. In this appendix the steps for solving the barrier problem will be explained. For readers unfamiliar with the method of Lagrangian Multipliers and the Karush-Kuhn-Tucker (KKT) conditions, appendix A provides the necessary background information.

Solving the barrier problem for a fixed μ

The barrier problem as defined by equation 4.35 is an optimization problem with only equality constraints. For it to be solved the Lagrangian method can be applied, defining Lagrangian multipliers y with $y \in \mathbb{R}^m$. For the barrier problem the Lagrangian is defined as

$$\mathscr{L}\left(x,y\right) = f(x)) - \mu \sum_{j=1}^{p} \ln\left(\left(A_i x - b_i\right)^{(j)}\right) + \left(A_e x\right) - b_e)^T y. \tag{B.1}$$

The first condition for optimality formulated by equation A.3 applied to this barrier problem is:

$$\nabla_x f(x) - \mu \sum_{i=1}^{p} \left(\frac{(A_i)^{(j)}}{(A_i x - b_i)^{(j)}}\right)^T + A_e^T y = 0. \tag{B.2}$$

It can be rewritten with the vector e of length p with all elements equal to one and $\mathrm{diag}\left(A_i x - b_i\right)$ the $p \times p$ matrix with elements of the vector $A_i x - b_i$ on the diagonal to:

$$\nabla_x f(x) - \mu A_i^T \left(\mathrm{diag}\left(A_i x - b_i\right)\right)^{-1} e + A_e^T y = 0. \tag{B.3}$$

The second optimality condition (eq. A.4) for the barrier problem is

$$A_e x - b_e = 0. \tag{B.4}$$

Also

$$A_i x - b_i > 0 \tag{B.5}$$

is required. Gould et al. (2001) shows that this system of equations is equivalent to the system

$$\nabla_x f(x) + A_e^T y - A_i^T z = 0, \tag{B.6}$$
$$A_e x - b_e = 0, \tag{B.7}$$
$$\mathrm{diag}\left(A_i x - b_i\right) z - \mu e = 0, \tag{B.8}$$
$$\mathrm{diag}\left(A_i x - b_i\right) z > 0, \tag{B.9}$$

because from the last two equations it follows that $z = \mu \operatorname{diag}(A_i x - b_i)^{-1} e$. For μ decreasing to zero the equations above approximate the KKT conditions for the original nonlinear program given by equations A.6 to A.8.

Computing the search directions This system is solved using a damped Newton's method where the equations B.6 - B.10 are linearized around the current iterate (x_k, y_k, z_k) to derive the search direction (d_k^x, d_k^y, d_k^z) for the next iterate (Wächter and Biegler, 2005a). This linearization leads to te system

$$\begin{bmatrix} \nabla_{xx} f(x_k) & A_e^T & -A_i^T \\ A_e & 0 & 0 \\ \operatorname{diag}(z_k) A_i & 0 & \operatorname{diag}(A_i x_k - b_i) \end{bmatrix} \begin{bmatrix} d_k^x \\ d_k^y \\ d_k^z \end{bmatrix} = - \begin{bmatrix} \nabla_x f(x_k) + A_e^T y_k - A_i^T z_k \\ A_e x_k - b_e \\ \operatorname{diag}(A_i x_k - b_i) z_k - \mu e \end{bmatrix}. \tag{B.10}$$

From the linearization of the last equation, the lowest row of the matrix, it can be derived that

$$\begin{aligned} d_k^z &= \operatorname{diag}(A_i x_k - b_i)^{-1} \left(-\operatorname{diag}(A_i x_k - b_i)(z_k) + \mu e - \operatorname{diag}(z_k) A_i d_k^x \right) \\ &= -z_k + \mu \operatorname{diag}(A_i x_k - b_i)^{-1} e - \operatorname{diag}(A_i x_k - b_i)^{-1} \operatorname{diag}(z_k) A_i d_k^x \\ &= -z_k + \mu \operatorname{diag}(A_i x_k - b_i)^{-1} e - \mu \operatorname{diag}(A_i x_k - b_i)^{-1} \operatorname{diag}(A_i x_k - b_i)^{-1} A_i d_k^x \end{aligned} \tag{B.11}$$

so that the system van be written to the symmetric sytem:

$$\begin{aligned} &\begin{bmatrix} \nabla_{xx} f(x_k) + \mu A_i^T \operatorname{diag}(A_i x_k - b_i)^{-1} \operatorname{diag}(A_i x_k - b_i)^{-1} A_i & A_e^T \\ A_e & 0 \end{bmatrix} \begin{bmatrix} d_k^x \\ d_k^y \end{bmatrix} \\ &= - \begin{bmatrix} \nabla_x f(x_k) + A_e^T y_k - A_i^T z_k - A_i^T \left(-z_k + \mu \operatorname{diag}(A_i x_k - b_i)^{-1} e \right) \\ A_e x_k - b_e \end{bmatrix} \\ &= - \begin{bmatrix} \nabla_x f(x_k) + A_e^T y_k - \mu e \left(\operatorname{diag}(A_i x_k - b_i)^{-1} A_i \right) \\ A_e x_k - b_e \end{bmatrix}. \end{aligned} \tag{B.12}$$

These terms are the linearizations equations B.3 and B.4 around (x_k, x_y). Solving equation B.11 and equations B.12 gives the search directions (d_k^x, d_k^y, d_k^z).

Computing the step sizes The search directions (d_k^x, d_k^y, d_k^z) give directions for the next step in the algorithm. The step sizes $\alpha_k, \alpha_k^z \in (0, 1]$ determine the size of the steps in this direction. The step sizes are chosen such that the new iterate $x_{k+1}, y_{k+1}, z_{k+1}$ remains within the interior of the feasible domain. The maximum step size is defined such that the distance of the next iterate to the boundary is never smaller than a fraction of the distance of the current iterate of the boundary. This fraction is determined by the fraction-to-boundary parameter τ_i. The definition of the maximum step size as presented by Wächter and Biegler (2005b) for inequality constraints of the form $x \geq 0$ is adapted to the optimization problem in this research with inequality constraints of the form $A_i x - b_i \geq 0$. The step size in d_k^z direction is not a maximum but the actual step taken and it is the same as presented by Wächter and Biegler (2005b).

$$\alpha_k^{\max} = \max \left\{ \alpha \in (0, 1] : A_i \left(x_k + \alpha d_k^x \right) - b_i \geq (1 - \tau_i)(A_i x_k - b_i) \right\} \tag{B.13}$$

$$\alpha_k^z = \max \left\{ \alpha \in (0, 1] : z_k + \alpha d_k^z \geq (1 - \tau_i)(z_k) \right\} \tag{B.14}$$

The fraction-to-boundary parameter is defined by

$$\tau_i = \max\{\tau_{\min}, 1-\mu_i\}, \tag{B.15}$$

with $\tau_{\min} \in (0,1)$. Note that the fraction-to-boundary parameter changes each iteration in the outer loop, but defines the maximum step sizes in the iterations of the inner loop. For the first barrier problems, when μ_i is still large, the fraction-to-boundary parameter is $\tau_{\min}$. For later barrier problems, when the barrier parameter μ_i becomes smaller, τ_i approaches 1. This means that for smaller barrier parameters the inner loop iterations are more limited in the steps towards the boundary.

Equation B.13 defines a maximum step size in direction d_k^x. The actual step size is determined using the backtracking line search. In the backtracking line search, a decreasing sequence of step sizes α_k is considered, starting from $\alpha_k^{\max}$. In order to determine if the step size is accepted or not, a filter method is used. The idea behind the filter method is that a step size is accepted if it either decreases the constraint violation or improves the objective function. Wächter and Biegler (2005a) describes the details of this filter line search procedure.

Appendix C

Derivative matrices stage 1

Gradient of the objective The gradient of the objective function is a vector of length $(4T_{\text{opt}})$ of partial derivatives of the objective function for each of the variables. This means

$$\text{grad} = g = \nabla f = \begin{bmatrix} \frac{\partial f}{\partial S_{\text{res}}^1} \\ \frac{\partial f}{\partial Q_{\text{s}}^1} \\ \frac{\partial f}{\partial Q_{\text{c}}^1} \\ \frac{\partial f}{\partial Q_{\text{ir}}^1} \\ \vdots \\ \frac{\partial f}{\partial S_{\text{res}}^{T_{\text{opt}}}} \\ \frac{\partial f}{\partial Q_{\text{s}}^{T_{\text{opt}}}} \\ \frac{\partial f}{\partial Q_{\text{c}}^{T_{\text{opt}}}} \\ \frac{\partial f}{\partial Q_{\text{ir}}^{T_{\text{opt}}}} \end{bmatrix}, \tag{C.1}$$

with

$$\frac{\partial f}{\partial S_{\text{res}}^k} = \beta_1 \frac{1}{T_{\text{opt}} \overline{S_{\text{res}} Q_{\text{c}}}} Q_{\text{c}}^k, \tag{C.2}$$

$$\frac{\partial f}{\partial Q_{\text{s}}^k} = 0, \tag{C.3}$$

$$\frac{\partial f}{\partial Q_{\text{c}}^k} = \beta_1 \frac{1}{T_{\text{opt}} \overline{S_{\text{res}} Q_{\text{c}}}} S_{\text{res}}^k, \tag{C.4}$$

$$\frac{\partial f}{\partial Q_{\text{ir}}^k} = \beta_2 \frac{1}{T_{\text{opt}} \overline{Q_{\text{ir}}}}. \tag{C.5}$$

Jacobian of the constraints The Jacobian of the constraints is the matrix of first-order partial derivatives of the constraints. The size of the Jacobian of the constraints is $(3T_{\text{opt}})$ $(4T_{\text{opt}})$. For stage 1 this is defined as

$$\text{jac} = J = \begin{bmatrix} \frac{\partial c^1_{\text{eq1}}}{\partial S^1_{\text{res}}} & \frac{\partial c^1_{\text{eq1}}}{\partial Q^1_{\text{s}}} & \frac{\partial c^1_{\text{eq1}}}{\partial Q^1_{\text{c}}} & \frac{\partial c^1_{\text{eq1}}}{\partial Q^1_{\text{ir}}} & \cdots & \frac{\partial c^1_{\text{eq1}}}{\partial S^{T\text{opt}}_{\text{res}}} & \frac{\partial c^1_{\text{eq1}}}{\partial Q^{T\text{opt}}_{\text{s}}} & \frac{\partial c^1_{\text{eq1}}}{\partial Q^{T\text{opt}}_{\text{c}}} & \frac{\partial c^1_{\text{eq1}}}{\partial Q^{T\text{opt}}_{\text{ir}}} \\ \frac{\partial c^2_{\text{eq1}}}{\partial S^1_{\text{res}}} & \frac{\partial c^2_{\text{eq1}}}{\partial Q^1_{\text{s}}} & \frac{\partial c^2_{\text{eq1}}}{\partial Q^1_{\text{c}}} & \frac{\partial c^2_{\text{eq1}}}{\partial Q^1_{\text{ir}}} & \cdots & \frac{\partial c^2_{\text{eq1}}}{\partial S^{T\text{opt}}_{\text{res}}} & \frac{\partial c^2_{\text{eq1}}}{\partial Q^{T\text{opt}}_{\text{s}}} & \frac{\partial c^2_{\text{eq1}}}{\partial Q^{T\text{opt}}_{\text{c}}} & \frac{\partial c^2_{\text{eq1}}}{\partial Q^{T\text{opt}}_{\text{ir}}} \\ \vdots & \vdots & \vdots & \vdots & \ddots & \vdots & \vdots & \vdots & \vdots \\ \frac{\partial c^m_{\text{eq1}}}{\partial S^1_{\text{res}}} & \frac{\partial c^m_{\text{eq1}}}{\partial Q^1_{\text{s}}} & \frac{\partial c^m_{\text{eq1}}}{\partial Q^1_{\text{c}}} & \frac{\partial c^m_{\text{eq1}}}{\partial Q^1_{\text{ir}}} & \cdots & \frac{\partial c^m_{\text{eq1}}}{\partial S^{T\text{opt}}_{\text{res}}} & \frac{\partial c^m_{\text{eq1}}}{\partial Q^{T\text{opt}}_{\text{s}}} & \frac{\partial c^m_{\text{eq1}}}{\partial Q^{T\text{opt}}_{\text{c}}} & \frac{\partial c^m_{\text{eq1}}}{\partial Q^{T\text{opt}}_{\text{ir}}} \\ \frac{\partial c^1_{\text{ineq1}}}{\partial S^1_{\text{res}}} & \frac{\partial c^1_{\text{ineq1}}}{\partial Q^1_{\text{s}}} & \frac{\partial c^1_{\text{ineq1}}}{\partial Q^1_{\text{c}}} & \frac{\partial c^1_{\text{ineq1}}}{\partial Q^1_{\text{ir}}} & \cdots & \frac{\partial c^1_{\text{ineq1}}}{\partial S^{T\text{opt}}_{\text{res}}} & \frac{\partial c^1_{\text{ineq1}}}{\partial Q^{T\text{opt}}_{\text{s}}} & \frac{\partial c^1_{\text{ineq1}}}{\partial Q^{T\text{opt}}_{\text{c}}} & \frac{\partial c^1_{\text{ineq1}}}{\partial Q^{T\text{opt}}_{\text{ir}}} \\ \frac{\partial c^2_{\text{ineq1}}}{\partial S^1_{\text{res}}} & \frac{\partial c^2_{\text{ineq1}}}{\partial Q^1_{\text{s}}} & \frac{\partial c^2_{\text{ineq1}}}{\partial Q^1_{\text{c}}} & \frac{\partial c^2_{\text{ineq1}}}{\partial Q^1_{\text{ir}}} & \cdots & \frac{\partial c^2_{\text{ineq1}}}{\partial S^{T\text{opt}}_{\text{res}}} & \frac{\partial c^2_{\text{ineq1}}}{\partial Q^{T\text{opt}}_{\text{s}}} & \frac{\partial c^2_{\text{ineq1}}}{\partial Q^{T\text{opt}}_{\text{c}}} & \frac{\partial c^2_{\text{ineq1}}}{\partial Q^{T\text{opt}}_{\text{ir}}} \\ \vdots & \vdots & \vdots & \vdots & \ddots & \vdots & \vdots & \vdots & \vdots \\ \frac{\partial c^m_{\text{ineq1}}}{\partial S^1_{\text{res}}} & \frac{\partial c^m_{\text{ineq1}}}{\partial Q^1_{\text{s}}} & \frac{\partial c^m_{\text{ineq1}}}{\partial Q^1_{\text{c}}} & \frac{\partial c^m_{\text{ineq1}}}{\partial Q^1_{\text{ir}}} & \cdots & \frac{\partial c^m_{\text{ineq1}}}{\partial S^{T\text{opt}}_{\text{res}}} & \frac{\partial c^m_{\text{ineq1}}}{\partial Q^{T\text{opt}}_{\text{s}}} & \frac{\partial c^m_{\text{ineq1}}}{\partial Q^{T\text{opt}}_{\text{c}}} & \frac{\partial c^m_{\text{ineq1}}}{\partial Q^{T\text{opt}}_{\text{ir}}} \\ \frac{\partial c^1_{\text{ineq2}}}{\partial S^1_{\text{res}}} & \frac{\partial c^1_{\text{ineq2}}}{\partial Q^1_{\text{s}}} & \frac{\partial c^1_{\text{ineq2}}}{\partial Q^1_{\text{c}}} & \frac{\partial c^1_{\text{ineq2}}}{\partial Q^1_{\text{ir}}} & \cdots & \frac{\partial c^1_{\text{ineq2}}}{\partial S^{T\text{opt}}_{\text{res}}} & \frac{\partial c^1_{\text{ineq2}}}{\partial Q^{T\text{opt}}_{\text{s}}} & \frac{\partial c^1_{\text{ineq2}}}{\partial Q^{T\text{opt}}_{\text{c}}} & \frac{\partial c^1_{\text{ineq2}}}{\partial Q^{T\text{opt}}_{\text{ir}}} \\ \frac{\partial c^2_{\text{ineq2}}}{\partial S^1_{\text{res}}} & \frac{\partial c^2_{\text{ineq2}}}{\partial Q^1_{\text{s}}} & \frac{\partial c^2_{\text{ineq2}}}{\partial Q^1_{\text{c}}} & \frac{\partial c^2_{\text{ineq2}}}{\partial Q^1_{\text{ir}}} & \cdots & \frac{\partial c^2_{\text{ineq2}}}{\partial S^{T\text{opt}}_{\text{res}}} & \frac{\partial c^2_{\text{ineq2}}}{\partial Q^{T\text{opt}}_{\text{s}}} & \frac{\partial c^2_{\text{ineq2}}}{\partial Q^{T\text{opt}}_{\text{c}}} & \frac{\partial c^2_{\text{ineq2}}}{\partial Q^{T\text{opt}}_{\text{ir}}} \\ \vdots & \vdots & \vdots & \vdots & \ddots & \vdots & \vdots & \vdots & \vdots \\ \frac{\partial c^m_{\text{ineq2}}}{\partial S^1_{\text{res}}} & \frac{\partial c^m_{\text{ineq2}}}{\partial Q^1_{\text{s}}} & \frac{\partial c^m_{\text{ineq2}}}{\partial Q^1_{\text{c}}} & \frac{\partial c^m_{\text{ineq2}}}{\partial Q^1_{\text{ir}}} & \cdots & \frac{\partial c^m_{\text{ineq2}}}{\partial S^{T\text{opt}}_{\text{res}}} & \frac{\partial c^m_{\text{ineq2}}}{\partial Q^{T\text{opt}}_{\text{s}}} & \frac{\partial c^m_{\text{ineq2}}}{\partial Q^{T\text{opt}}_{\text{c}}} & \frac{\partial c^m_{\text{ineq2}}}{\partial Q^{T\text{opt}}_{\text{ir}}} \end{bmatrix}, \tag{C.6}$$

with

$$\frac{\partial c^k_{\text{eq1}}}{\partial S^{k-1}_{\text{res}}} = 1, \tag{C.7}$$

$$\frac{\partial c^k_{\text{eq1}}}{\partial Q^{k-1}_{\text{s}}} = -\Delta k, \tag{C.8}$$

$$\frac{\partial c^k_{\text{eq1}}}{\partial Q^{k-1}_{\text{c}}} = -\Delta k, \tag{C.9}$$

$$\frac{\partial c^k_{\text{eq1}}}{\partial S^{k}_{\text{res}}} = -1, \tag{C.10}$$

and

$$\frac{\partial c^k_{\text{ineq1}}}{\partial S^{k}_{\text{res}}} = -1, \tag{C.11}$$

$$\frac{\partial c^k_{\text{ineq1}}}{\partial Q^{k}_{\text{c}}} = 1, \tag{C.12}$$

and

$$\frac{\partial c^k_{\text{ineq2}}}{\partial Q^{k}_{\text{c}}} = -1, \tag{C.13}$$

$$\frac{\partial c^k_{\text{ineq2}}}{\partial Q^{k}_{\text{ir}}} = 1. \tag{C.14}$$

and all other elements zero.

Hessian of the Lagrangian The Lagrange function for this problem is defined as

$$L(x,u,v_1,v_2) = f(x) + \sum_{k=1}^{T_{\text{opt}}} u^k c^k_{\text{eq1}}(x) + \sum_{k=1}^{T_{\text{opt}}} v_1^k c^k_{\text{ineq1}}(x) + \sum_{k=1}^{T_{\text{opt}}} v_2^k c^k_{\text{ineq2}}(x). \tag{C.15}$$

The Hessian of the Lagrange is defined as

$$H(L) = \begin{bmatrix} 0 & \frac{\partial g}{\partial \mathbf{x}} \\ \left(\frac{\partial g}{\partial \mathbf{x}}\right)^T & \frac{\partial^2 L}{\partial \mathbf{x}^2}. \end{bmatrix} \tag{C.16}$$

This means that in stage 1 the Hessian is a $\left(1+4T_{\text{opt}}\right)$ by $\left(1+4T_{\text{opt}}\right)$ matrix, with the block $\frac{\partial^2 L}{\partial \mathbf{x}^2}$ of size $\left(4T_{\text{opt}}\right)$ by $\left(4T_{\text{opt}}\right)$. Since all constraints are linear, the derivative of the gradient is zero, $\frac{\partial g}{\partial \mathbf{x}} = 0$.

$$\frac{\partial^2 L}{\partial \mathbf{x}^2} = \begin{bmatrix} \frac{\partial^2 f}{(\partial S^1_{\text{res}})^2} & \frac{\partial^2 f}{\partial S^1_{\text{res}} \partial Q^1_{\text{s}}} & \frac{\partial^2 f}{\partial S^1_{\text{res}} \partial Q^1_{\text{c}}} & \frac{\partial^2 f}{\partial S^1_{\text{res}} \partial Q^1_{\text{ir}}} & \cdots & \cdots & \cdots & \cdots & \cdots \\ \frac{\partial^2 f}{\partial Q^1_{\text{s}} \partial S^1_{\text{res}}} & \frac{\partial^2 f}{(\partial Q^1_{\text{s}})^2} & \frac{\partial^2 f}{\partial Q^1_{\text{s}} \partial Q^1_{\text{c}}} & \frac{\partial^2 f}{\partial Q^1_{\text{s}} \partial Q^1_{\text{ir}}} & \cdots & \cdots & \cdots & \cdots & \cdots \\ \frac{\partial^2 f}{\partial Q^1_{\text{c}} \partial S^1_{\text{res}}} & \frac{\partial^2 f}{\partial Q^1_{\text{c}} \partial Q^1_{\text{s}}} & \frac{\partial^2 f}{(\partial Q^1_{\text{c}})^2} & \frac{\partial^2 f}{\partial Q^1_{\text{c}} \partial Q^1_{\text{ir}}} & \cdots & \cdots & \cdots & \cdots & \cdots \\ \frac{\partial^2 f}{\partial Q^1_{\text{ir}} \partial S^1_{\text{res}}} & \frac{\partial^2 f}{\partial Q^1_{\text{ir}} \partial Q^1_{\text{s}}} & \frac{\partial^2 f}{\partial Q^1_{\text{ir}} \partial Q^1_{\text{c}}} & \frac{\partial^2 f}{(\partial Q^1_{\text{ir}})^2} & \cdots & \cdots & \cdots & \cdots & \cdots \\ \vdots & \vdots & \vdots & \vdots & \ddots & \vdots & \vdots & \vdots & \vdots \\ \cdots & \cdots & \cdots & \cdots & \cdots & \frac{\partial^2 f}{(\partial S^{T_{\text{opt}}}_{\text{res}})^2} & \frac{\partial^2 f}{\partial S^{T_{\text{opt}}}_{\text{res}} \partial Q^{T_{\text{opt}}}_{\text{s}}} & \frac{\partial^2 f}{\partial S^{T_{\text{opt}}}_{\text{res}} \partial Q^{T_{\text{opt}}}_{\text{c}}} & \frac{\partial^2 f}{\partial S^{T_{\text{opt}}}_{\text{res}} \partial Q^{T_{\text{opt}}}_{\text{ir}}} \\ \cdots & \cdots & \cdots & \cdots & \cdots & \frac{\partial^2 f}{\partial Q^{T_{\text{opt}}}_{\text{s}} \partial S^{T_{\text{opt}}}_{\text{res}}} & \frac{\partial^2 f}{(\partial Q^{T_{\text{opt}}}_{\text{s}})^2} & \frac{\partial^2 f}{\partial Q^{T_{\text{opt}}}_{\text{s}} \partial Q^{T_{\text{opt}}}_{\text{c}}} & \frac{\partial^2 f}{\partial Q^{T_{\text{opt}}}_{\text{s}} \partial Q^{T_{\text{opt}}}_{\text{ir}}} \\ \cdots & \cdots & \cdots & \cdots & \cdots & \frac{\partial^2 f}{\partial Q^{T_{\text{opt}}}_{\text{c}} \partial S^{T_{\text{opt}}}_{\text{res}}} & \frac{\partial^2 f}{\partial Q^{T_{\text{opt}}}_{\text{c}} \partial Q^{T_{\text{opt}}}_{\text{s}}} & \frac{\partial^2 f}{(\partial Q^{T_{\text{opt}}}_{\text{c}})^2} & \frac{\partial^2 f}{\partial Q^{T_{\text{opt}}}_{\text{c}} \partial Q^{T_{\text{opt}}}_{\text{ir}}} \\ \cdots & \cdots & \cdots & \cdots & \cdots & \frac{\partial^2 f}{\partial Q^{T_{\text{opt}}}_{\text{ir}} \partial S^{T_{\text{opt}}}_{\text{res}}} & \frac{\partial^2 f}{\partial Q^{T_{\text{opt}}}_{\text{ir}} \partial Q^{T_{\text{opt}}}_{\text{s}}} & \frac{\partial^2 f}{\partial Q^{T_{\text{opt}}}_{\text{ir}} \partial Q^{T_{\text{opt}}}_{\text{c}}} & \frac{\partial^2 f}{(\partial Q^{T_{\text{opt}}}_{\text{ir}})^2} \end{bmatrix}, \tag{C.17}$$

with

$$\frac{\partial^2 f}{\partial S^k_{\text{res}} \partial Q^k_{\text{c}}} = \frac{\partial^2 f}{\partial Q^k_{\text{c}} \partial S^k_{\text{res}}} = \frac{\beta_1}{T_{\text{opt}} \overline{S_{\text{res}} Q_{\text{c}}}}, \tag{C.18}$$

and all other elements zero.

Appendix D

Derivative matrices stage 2

Gradient of the objective In stage 2, the gradient of the objective is a vector of length $\left(56T_{\text{opt}}\right)$.

$$\text{grad} = g = \nabla f = \begin{bmatrix} \frac{\partial f}{\partial \mathbf{x}_{\text{res}}^1} \\ \frac{\partial f}{\partial \mathbf{x}_{\text{riv}}^1} \\ \vdots \\ \frac{\partial f}{\partial \mathbf{x}_{\text{res}}^{T_{\text{opt}}}} \\ \frac{\partial f}{\partial \mathbf{x}_{\text{riv}}^{T_{\text{opt}}}} \end{bmatrix}. \tag{D.1}$$

For stage 2, the term

$$\frac{\partial f}{\partial \mathbf{x}_{\text{res}}^k} = \begin{bmatrix} \frac{\partial f}{\partial S_{\text{res}}^k} & \frac{\partial f}{\partial Q_{\text{s}}^k} & \frac{\partial f}{\partial Q_{\text{c}}^k} & \frac{\partial f}{\partial Q_{\text{ir}}^k} \end{bmatrix}^T, \tag{D.2}$$

is similar to the gradient of the objective for stage 1, with the partial derivatives of the spillway constraint added:

$$\frac{\partial f}{\partial S_{\text{res}}^k} = \beta_1 \frac{1}{T_{\text{opt}} \overline{S_{\text{res}} Q_{\text{c}}}} Q_{\text{c}}^k + \rho_2 Q_{\text{s}}^k \tag{D.3}$$

$$\frac{\partial f}{\partial Q_{\text{s}}^k} = -\rho_2 \left(2 Q_{\text{s}}^k \Delta k - \alpha^k\right) \tag{D.4}$$

$$\frac{\partial f}{\partial Q_{\text{c}}^k} = \beta_1 \frac{1}{T_{\text{opt}} \overline{S_{\text{res}} Q_{\text{c}}}} S_{\text{res}}^k - \rho_2 Q_{\text{s}}^k \tag{D.5}$$

$$\frac{\partial f}{\partial Q_{\text{ir}}^k} = \beta_2 \frac{1}{T_{\text{opt}} \overline{Q_{\text{ir}}}}. \tag{D.6}$$

Note that $\frac{\partial f}{\partial \mathbf{x}_{\text{riv}}^1} = 0$. Finally,

$$\frac{\partial f}{\partial d^k} = -\rho_1 \frac{1}{\sum_{k=1}^{T_{\text{opt}}} \overline{d^k}}. \tag{D.7}$$

Hence, the gradient of the objective is a linear function of the state vector.

Jacobian of the constraints The size of the Jacobian matrix for stage 2 is $\left(55T_{\text{opt}}\right)$ by $\left(56T_{\text{opt}}\right)$. Let's define

$$\frac{\partial \mathbf{c}_{\text{eq1}}}{\partial \mathbf{x}} = \begin{bmatrix} \frac{\partial c^1_{\text{eq1}}}{\partial \mathbf{x}^1_{\text{res}}} & \frac{\partial c^1_{\text{eq1}}}{\partial \mathbf{x}^1_{\text{riv}}} & \frac{\partial c^1_{\text{eq1}}}{\partial d^1} & \cdots & \frac{\partial c^1_{\text{eq1}}}{\partial \mathbf{x}^{T_{\text{opt}}}_{\text{res}}} & \frac{\partial c^1_{\text{eq1}}}{\partial \mathbf{x}^{T_{\text{opt}}}_{\text{riv}}} & \frac{\partial c^1_{\text{eq1}}}{\partial d^{T_{\text{opt}}}} \\ \vdots & \vdots & \vdots & \ddots & \vdots & \vdots & \vdots \\ \frac{\partial c^{T_{\text{opt}}}_{\text{eq1}}}{\partial \mathbf{x}^1_{\text{res}}} & \frac{\partial c^{T_{\text{opt}}}_{\text{eq1}}}{\partial \mathbf{x}^1_{\text{riv}}} & \frac{\partial c^{T_{\text{opt}}}_{\text{eq1}}}{\partial d^1} & \cdots & \frac{\partial c^{T_{\text{opt}}}_{\text{eq1}}}{\partial \mathbf{x}^{T_{\text{opt}}}_{\text{res}}} & \frac{\partial c^{T_{\text{opt}}}_{\text{eq1}}}{\partial \mathbf{x}^{T_{\text{opt}}}_{\text{riv}}} & \frac{\partial c^{T_{\text{opt}}}_{\text{eq1}}}{\partial d^{T_{\text{opt}}}} \end{bmatrix}, \tag{D.8}$$

and $\frac{\partial (\mathbf{c}_{\text{eq2}})_i}{\partial \mathbf{x}}$, $\frac{\partial (\mathbf{c}_{\text{eq3}})_i}{\partial \mathbf{x}}$, $\frac{\partial (\mathbf{c}_{\text{eq4}})_i}{\partial \mathbf{x}}$ for $i = 1, \ldots, 17$ and $\frac{\partial \mathbf{c}_{\text{ineq1}}}{\partial \mathbf{x}}$, $\frac{\partial \mathbf{c}_{\text{ineq2}}}{\partial \mathbf{x}}$ and $\frac{\partial \mathbf{c}_{\text{ineq3}}}{\partial \mathbf{x}}$ in the same way. The Jacobian matrix is then defined as

$$\text{jac} = J = \begin{bmatrix} \frac{\partial \mathbf{c}_{\text{eq1}}}{\partial \mathbf{x}} \\ \frac{\partial (\mathbf{c}_{\text{eq2}})_1}{\partial \mathbf{x}} \\ \vdots \\ \frac{\partial (\mathbf{c}_{\text{eq2}})_{17}}{\partial \mathbf{x}} \\ \frac{\partial (\mathbf{c}_{\text{eq3}})_1}{\partial \mathbf{x}} \\ \vdots \\ \frac{\partial (\mathbf{c}_{\text{eq3}})_{17}}{\partial \mathbf{x}} \\ \frac{\partial (\mathbf{c}_{\text{eq4}})_1}{\partial \mathbf{x}} \\ \vdots \\ \frac{\partial (\mathbf{c}_{\text{eq4}})_{17}}{\partial \mathbf{x}} \\ \frac{\partial \mathbf{c}_{\text{ineq1}}}{\partial \mathbf{x}} \\ \frac{\partial \mathbf{c}_{\text{ineq2}}}{\partial \mathbf{x}} \\ \frac{\partial \mathbf{c}_{\text{ineq3}}}{\partial \mathbf{x}} \end{bmatrix} \tag{D.9}$$

Equation C.7 to C.9 show that

$$\frac{\partial c^k_{\text{eq1}}}{\partial \mathbf{x}^{k-1}_{\text{res}}} = \begin{bmatrix} 1 & -\Delta k & -\Delta k & 0 \end{bmatrix}. \tag{D.10}$$

Equation C.10 show that

$$\frac{\partial c^k_{\text{eq1}}}{\partial \mathbf{x}^{k}_{\text{res}}} = \begin{bmatrix} -1 & 0 & 0 & 0 \end{bmatrix}. \tag{D.11}$$

Equation C.11 and C.12 result in

$$\frac{\partial c^k_{\text{ineq1}}}{\partial \mathbf{x}^{k}_{\text{res}}} = \begin{bmatrix} -1 & 0 & 1 & 0 \end{bmatrix}. \tag{D.12}$$

And Equation C.13 and C.14 show that

$$\frac{\partial c^k_{\text{ineq2}}}{\partial \mathbf{x}^{k}_{\text{res}}} = \begin{bmatrix} 0 & 0 & -1 & 1 \end{bmatrix}. \tag{D.13}$$

For $\left(c_{\text{eq2}}\right)_i$ it holds

$$\frac{\partial\left(c^k_{\text{eq2}}\right)_i}{\partial \mathbf{x}^k_{\text{riv}}} = \begin{bmatrix} \dots & \frac{\partial\left(c^k_{\text{eq2}}\right)_i}{\partial\left(S^k_{\text{riv}}\right)_i} & \frac{\partial\left(c^k_{\text{eq2}}\right)_i}{\partial\left(Q^k_{\text{riv,in}}\right)_i} & \frac{\partial\left(c^k_{\text{eq2}}\right)_i}{\partial\left(Q^k_{\text{riv,out}}\right)_i} & \dots \end{bmatrix} = \begin{bmatrix} \dots & 1 & \frac{\Delta k}{2} & -\frac{\Delta k}{2} & \dots \end{bmatrix} \tag{D.14}$$

$$\frac{\partial\left(c^k_{\text{eq2}}\right)_i}{\partial \mathbf{x}^{k+1}_{\text{riv}}} = \begin{bmatrix} \dots & \frac{\partial\left(c^k_{\text{eq2}}\right)_i}{\partial\left(S^{k+1}_{\text{riv}}\right)_i} & \frac{\partial\left(c^k_{\text{eq2}}\right)_i}{\partial\left(Q^{k+1}_{\text{riv,in}}\right)_i} & \frac{\partial\left(c^k_{\text{eq2}}\right)_i}{\partial\left(Q^{k+1}_{\text{riv,out}}\right)_i} & \dots \end{bmatrix} = \begin{bmatrix} \dots & -1 & \frac{\Delta k}{2} & -\frac{\Delta k}{2} & \dots \end{bmatrix}, \tag{D.15}$$

and all other elements zero. For $\left(c_{\text{eq3}}\right)_i$ it holds

$$\frac{\partial\left(c^k_{\text{eq3}}\right)_i}{\partial \mathbf{x}^k_{\text{riv}}} = \begin{bmatrix} \dots & \frac{\partial\left(c^k_{\text{eq3}}\right)_i}{\partial\left(S^{k+1}_{\text{riv}}\right)_i} & \frac{\partial\left(c^k_{\text{eq3}}\right)_i}{\partial\left(Q^{k+1}_{\text{riv,in}}\right)_i} & \frac{\partial\left(c^k_{\text{eq3}}\right)_i}{\partial\left(Q^{k+1}_{\text{riv,out}}\right)_i} & \dots \end{bmatrix} = \begin{bmatrix} \dots & \frac{\partial\left(c^k_{\text{eq3}}\right)_i}{\partial\left(S^k_{\text{riv}}\right)_i} & \frac{\partial\left(c^k_{\text{eq3}}\right)_i}{\partial\left(Q^k_{\text{riv,in}}\right)_i} & \frac{\partial\left(c^k_{\text{eq3}}\right)_i}{\partial\left(Q^k_{\text{riv,out}}\right)_i} & \dots \end{bmatrix} = \begin{bmatrix} \dots & 0 & c_2 & c_3 & \dots \end{bmatrix} \tag{D.16}$$

$$\frac{\partial\left(c^k_{\text{eq3}}\right)_i}{\partial \mathbf{x}^{k+1}_{\text{riv}}} = \begin{bmatrix} \dots & \frac{\partial\left(c^k_{\text{eq3}}\right)_i}{\partial\left(S^{k+1}_{\text{riv}}\right)_i} & \frac{\partial\left(c^k_{\text{eq3}}\right)_i}{\partial\left(Q^{k+1}_{\text{riv,in}}\right)_i} & \frac{\partial\left(c^k_{\text{eq3}}\right)_i}{\partial\left(Q^{k+1}_{\text{riv,out}}\right)_i} & \dots \end{bmatrix} = \begin{bmatrix} \dots & 0 & c_1 & -1 & \dots \end{bmatrix}, \tag{D.17}$$

and all other elements zero. For $\left(c_{\text{eq4}}\right)_i$ it holds

$$\frac{\partial\left(c^k_{\text{eq4}}\right)_i}{\partial \mathbf{x}^k_{\text{res}}} = \begin{cases} \begin{bmatrix} 0 & 1 & 1 & -1 \end{bmatrix}, & \text{if } \widehat{j} \in \mathbb{S}_i \\ 0, & \text{if otherwise} \end{cases} \tag{D.18}$$

$$\frac{\partial\left(c^k_{\text{eq4}}\right)_i}{\partial \mathbf{x}^k_{\text{riv}}} = \begin{bmatrix} \dots & \frac{\partial\left(c^k_{\text{eq4}}\right)_i}{\partial\left(Q^k_{\text{riv,out}}\right)_{i-1}} & \frac{\partial\left(c^k_{\text{eq4}}\right)_i}{\partial\left(S^k_{\text{riv}}\right)_i} & \frac{\partial\left(c^k_{\text{eq4}}\right)_i}{\partial\left(Q^k_{\text{riv,in}}\right)_i} & \dots \end{bmatrix} = \begin{bmatrix} \dots & 1 & 0 & -1 & \dots \end{bmatrix}, \tag{D.19}$$

and all other elements zero. For c_{ineq3} it holds

$$\frac{\partial c^k_{\text{ineq3}}}{\partial \mathbf{x}^k_{\text{riv}}} = \begin{bmatrix} \dots & \frac{\partial c^k_{\text{ineq3}}}{\partial\left(S^k_{\text{riv}}\right)_i} & \frac{\partial c^k_{\text{ineq3}}}{\partial\left(Q^k_{\text{riv,in}}\right)_i} & \frac{\partial c^k_{\text{ineq3}}}{\partial\left(Q^k_{\text{riv,out}}\right)_i} & \dots \end{bmatrix} = \begin{bmatrix} \dots & 1 & 0 & 0 & \dots \end{bmatrix} \tag{D.20}$$

$$\frac{\partial c^k_{\text{ineq3}}}{\partial d^k} = -1, \tag{D.21}$$

and all other elements zero.

Hessian of the Lagrangian For stage 2 the Hessian of the Lagrangian is $\left(1+56T_{\text{opt}}\right)$ by $\left(1+56T_{\text{opt}}\right)$ with the block $\frac{\partial^2 L}{\partial \mathbf{x}^2}$ of size $\left(56T_{\text{opt}}\right)$ by $\left(56T_{\text{opt}}\right)$.

Similar to stage 1, the gradient of the constraints is constant, hence $\frac{\partial g}{\partial \mathbf{x}} = 0$. The term given in equation C.18 remains the same,

$$\frac{\partial^2 f}{\partial S^k_{\text{res}} \partial Q^k_{\text{c}}} = \frac{\partial^2 f}{\partial Q^k_{\text{c}} \partial S^k_{\text{res}}} = \frac{\beta_1}{T_{\text{opt}} \overline{S_{\text{res}} Q_{\text{c}}}}. \tag{D.22}$$

The three additional terms to the Hessian of the Lagrangian are

$$\frac{\partial^2 f}{\partial S_{\text{res}}^k \partial Q_{\text{s}}^k} = \frac{\partial^2 f}{\partial Q_{\text{s}}^k \partial S_{\text{res}}^k} = \rho_2, \tag{D.23}$$

$$\frac{\partial^2 f}{\partial Q_{\text{s}}^k \partial Q_{\text{c}}^k} = \frac{\partial^2 f}{\partial Q_{\text{c}}^k \partial Q_{\text{s}}^k} = -\rho_2, \tag{D.24}$$

$$\frac{\partial^2 f}{\left(\partial Q_{\text{s}}^k\right)^2} = -2\Delta k \rho_2. \tag{D.25}$$

All other terms in the Hessian of the Lagrangian are zero.

Appendix E

Data quality analysis

First remark: This chapter was written as part of a report about the development of a hydrological model for the Sittaung basin. The purpose of that model was to serve as a prediction model for the external disturbances. Investigation of the data lead to the conclusion that available data were not sufficient to develop a hydrological model for this purpose. The chapter is included in this thesis as an appendix. because its findings are considered valuable for researchers of the Sittaung river basin.

Methods for data quality assessment

Ground station data for the Sittaung basin were measured and digitalized manually. Not much research has been done to verify the reliability fo TRMM data in Myanmar. Therefore, a detailed analysis of the data quality was performed. The methods for this analysis are presented in section E and the results in section E.

Discharge data The inflow data to the reservoirs were considered to be discharges at the outflow of the subcatchment to the reservoir. Inflows to the reservoirs are derived from outflow measurements and storage in the reservoir. The storage in the reservoir was derived from the water level measurements through a reservoir curve, expressing the relation between water level and storage. This reservoir curve was not provided with the data. We derived the reservoir curve from the water level measurements and the storages in the dataset and removed the outliers from the timeseries by visual inspection in two steps. First, the points for which the water levels are outside the range of the other points have been removed. In the second step this was repeated for points with deviating storages.

Precipitation data Precipitation measurements at ground stations are only available at nine locations in the Sittaung river basin for this research. Spatial variability of precipitation in the basin is high. For the remaining subcatchments, no ground measurements are available at all. TRMM precipitation data have better spatial coverage and are available for the whole Sittaung basin. The reliability of TRMM precipitation measurements in Myanmar have only been investigated to a limited extend in other studies (Rathore, 2014). In order to verify the reliability of TRMM data is the Sittaung basin, timeseries of the ground stations and TRMM were compared to the discharge observations by visual inspection. Also, correlations between TRMM measurements and ground stations were calculated. It is likely that "no measurement" were replaced by zero precipitation in the ground station datasets, as none of the timeseries for precipitation contained gaps whereas the discharge measurements did. Therefore, correlations were only determined for days on which the two datasets measured more than 0.2 mm of precipitation. The correlations of interests were those of the precipitation amounts and the detection of wet days and dry days.

Coherence between potential evaporation, precipitation and discharge data The coherence between potential evaporation, precipitation and discharge was studied using their cumulative sums over time. Finally, each of the subcatchments were plotted in a Budyko framework using the TRMM data and the ground station data.

Results for data quality assessment

Discharge measurements

Removal of outliers with respect to the reservoir curve from the timeseries of the discharge measurement was performed by visual inspection as described in **??**. Figure E.1 shows the process for each of the reser-

voirs. The left figure shows all datapoints in blue, with the points removed in step 1 in red. The middle figure shows the remaining datapoints after step 1, with the points removed in step 2 in red. The right figure shows the remaining datapoints after this process. Above each figure the number of points removed in that step is mentioned. In total between 0.0 % (Paunglaung dam) and 5.3 % (Yenwe dam) of the datapoints was removed. Table E.1 shows the length of the timeseries available, the percentage of missing discharge data, the percentage of discharge data removed by visual inspection of the reservoir curve and the total percentage of remaining discharge data per catchment.

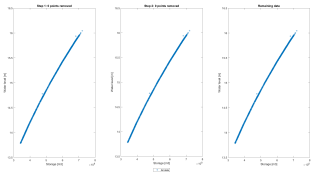

(a) Paunglaung dam, 0.0 % removed.

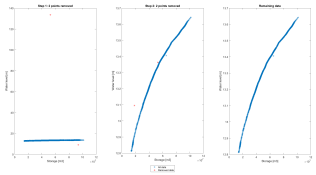

(b) Ngalaik dam, 0.7 % removed.

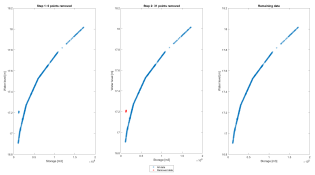

(c) Sinthe dam, 1.4 % removed.

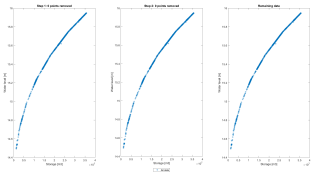

(d) Madan dam, 0.1 % removed.

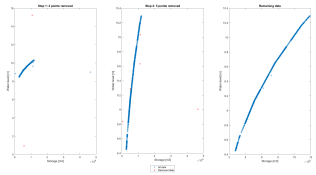

(e) Kabaung dam, 2.8 % removed.

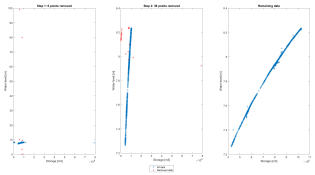

(f) Yenwe dam, 5.3 % removed.

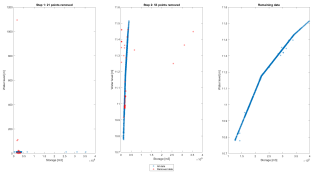

(g) Bainda dam, 4.1 % removed.

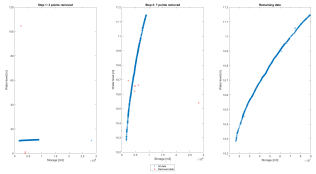

(h) Yezin dam, 0.4 % removed

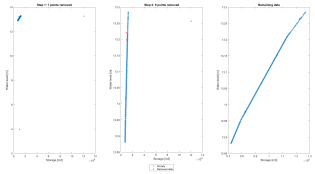

(i) Chaungmange dam, 0.4 % removed.

Figure E.1: Two-step process of removing Q measurements by visual inspection of water level and storage outliers. The figures show the datapoints (blue) and removed datapoints (red) for each time step. The number of removed datapoints in each step are mentioned above the figures. The percentage of removed datapoints is mentioned in subcaption.

Table E.1: Overview of the data for the gauged catchments, start and end date of the data, missing discharge datapoints as percentage of the length of timeseries, removed discharge datapoints by data cleaning as a percentage of available discharge datapoints, the total remainig datapoints as a percentage of length of the timeseries and as absolute number.

No.	**Reservoir**	**Start data**	**End data**	**Missing discharge data**	**Removed discharge data**	**Total remaining data**	**Total number datapoints**
1	Chaung Mange Dam	1/1/'09	28/2/'15	15 %	0.4 %	84.8 %	1907
2	Madan Dam	1/6/'09	28/2/'15	76 %	0.1 %	24.2 %	507
3	Ngalaik Dam	1/1/'09	31/3/'15	51 %	0.7 %	49.3 %	1123
4	Yezin Dam	1/1/'09	19/3/'15	41 %	0.4 %	59.0 %	1339
5	Sinthe Dam	1/1/'09	19/3/'15	27 %	1.4 %	71.8 %	1623
6	Paunglaung Dam	1/1/'10	28/2/'15	0 %	0.0 %	100.0 %	1885
7	Yenwe Dam	1/1/'11	28/2/'15	0 %	5.3 %	94.7 %	1441
8	Bainda Dam	1/1/'10	28/2/'15	19 %	4.1 %	76.8 %	1423
9	Kabaung Dam	1/1/'08	28/2/'15	15 %	2.8 %	93.1 %	1223

Evaporation

The potential evaporation considered here is a basin wide average over 6 stations within the region with latitudes 17.5-20.75°and longitudes 95.5-97°. The names of these stations are Yamethin, Tharrawaddy, Bago, Toungoo, Pyinmana, Loikaw.

Precipitation measurements - Ground stations versus TRMM data

When considering correlations between the ground stations and TRMM measurements, the temporal and spatial scale of both measurements should be taken into account. The TRMM satellite reports daily precipitation from 22:30:00 UTC the day before until 22:29:59 UTC on the data day. Ground stations measure the total precipitation from 6AM local time on the data day to 6AM the following day, which means 23:30 UTC on the day before to 23:30 UTC on the data day. The time windows of both measurements are overlapping 23 hours a day, hence this is not expected to affect correlation to a large extend. Spatial variation of precipitation may affect correlations, as TRMM data averages the total precipitation over a gridcell of size 0.25°and ground stations provide point measurements with tipping buckets.

Correlations of amounts of precipitation are low. It was verified whether the correlation is higher for days with high rainfall amounts by studying the correlation between the two timeseries on days they both measure a precipitation amount above a certain threshold. Figure E.2 shows the results for the Pearson linear correlation coefficient for the thresholds of 0.2, 1, 2, 5, 10, 15 and 20 mm. Above the bars in the barplot the number of data points with precipitation higher than this threshold is given. The correlations are very low for almost all cases. The p-values in figure E.3 for the hypothesis that Pearson's linear correlation between ground stations and TRMM data is zero against the alternative hypothesis that the correlation is nonzero are high, meaning the correlations are not significantly different from zero. Spearman's rank correlations, comparing the rank of precipitation amounts rather than the amounts themselves, are also very low with high p-values. No significant correlations have been found between measured precipitation amounts by ground stations and TRMM data.

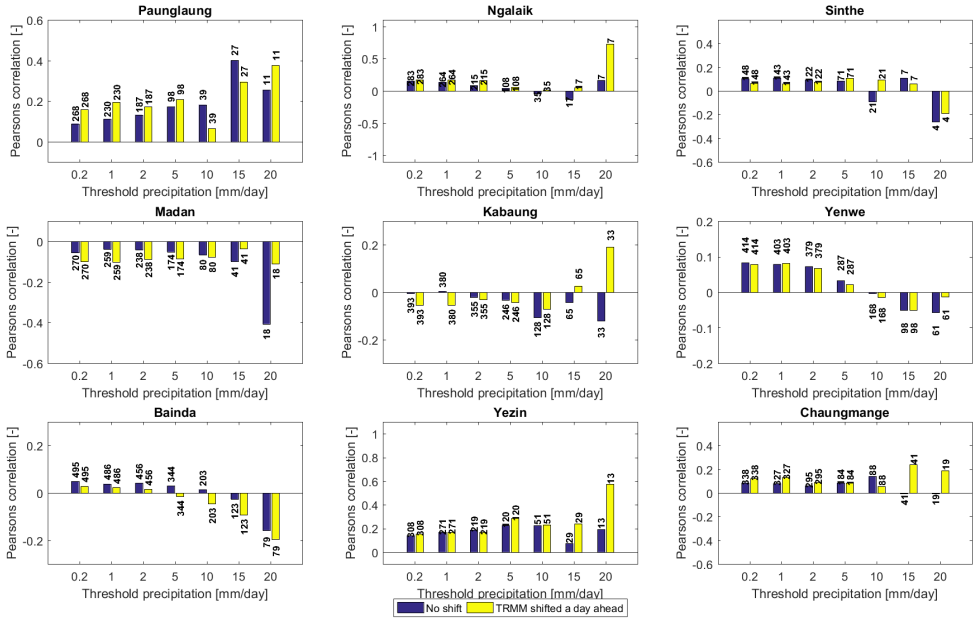

Figure E.2: Pearson's linear correlation coefficients between ground stations and TRMM data for all days on which both TRMM and ground stations measured rainfall amounts above a threshold. Results are shown for thresholds 0.2, 1, 2, 5, 10, 15 and 20 mm.

In order to verify whether the two timeseries do accurately measure the occurrence of rainfall events, rather than amounts of precipitation, the timeseries are compared by their measurement of wet and dry days. Wet and dry days are defined based on a threshold amount of rainfall. Table **??** shows the number of cases in which the two timeseries measure a wet day, a dry day or when one measures a wet day and the other does not, for

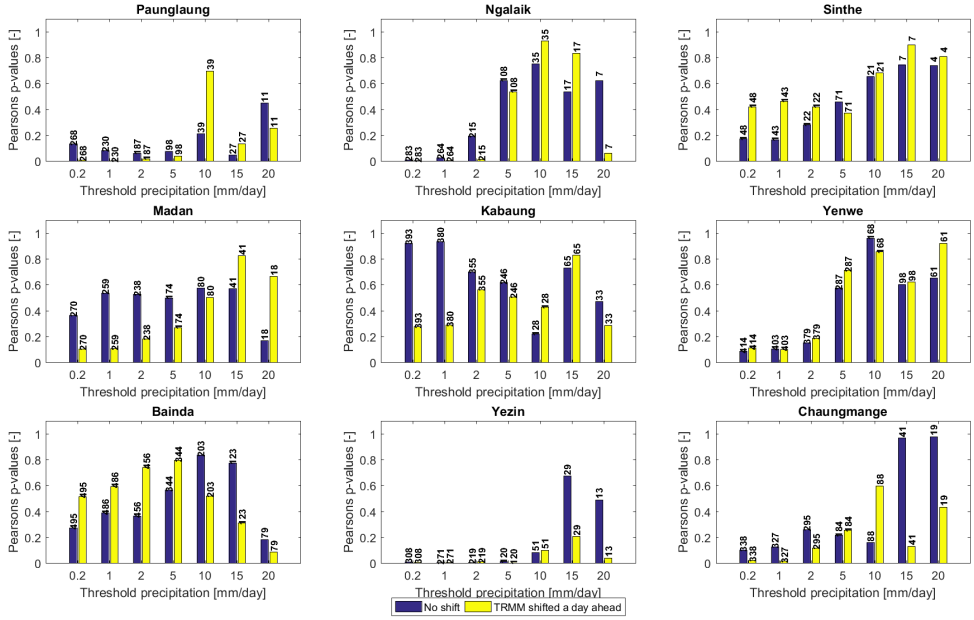

Figure E.3: P-values for the hypothesis that Pearson's linear correlation between ground stations and TRMM data is zero against the alternative hypothesis that the correlation is nonzero. P-values are calculated for all days on which both TRMM and ground stations measured rainfall amounts above a threshold. Results are shown for thresholds 0.2, 1, 2, 5, 10, 15 and 20 mm.

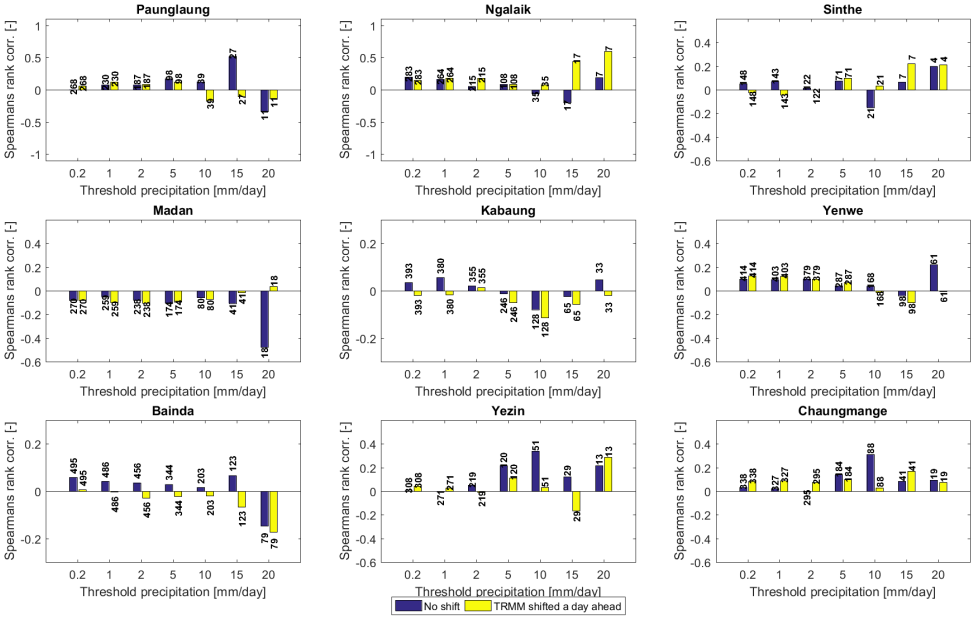

Figure E.4: Spearman's rank correlation coefficient between ground stations and TRMM data for all days on which both TRMM and ground stations measured rainfall amounts above a threshold. Results are shown for thresholds 0.2, 1, 2, 5, 10, 15 and 20 mm.

different thresholds defining a wet/dry day from 0.2 mm to 20 mm. TRMM and the ground stations overlap, i.e. both measure a wet or a dry day, in 73 - 81 % of the days for the threshold of 0.2 milimeter. This overlap increases with increasing threshold with 81 - 95 % for a 20 mm threshold. Overlapping days seem reasonably high, but majority of the overlapping days are dry days.For larger threshold, the number of overlapping wet days is very low, between 1-11 % for a threshold of 10 mm and between 0-4 % for a threshold of 20 mm. For these thresholds, the number of times either the ground stations or TRMM measure a wet day is larger than

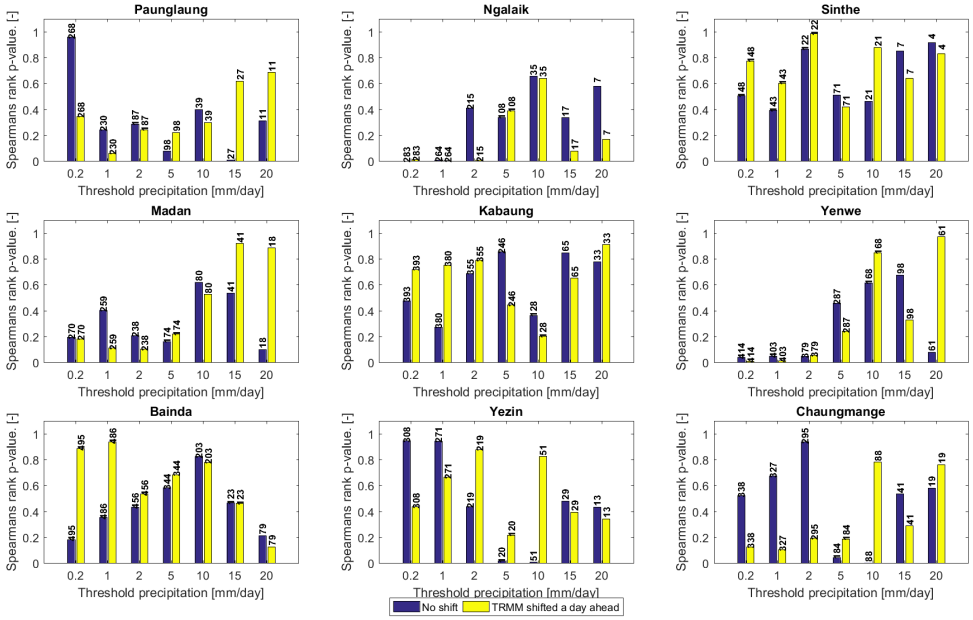

Figure E.5: P-values for the hypothesis that Spearman's rank correlation between ground stations and TRMM data is zero against the alternative hypothesis that the correlation is nonzero. P-values are calculated for all days on which both TRMM and ground stations measured rainfall amounts above a threshold. Results are shown for thresholds 0.2, 1, 2, 5, 10, 15 and 20 mm.

the number of times they overlap. It can be concluded from the table that TRMM measures wet days more often than the ground stations in most cases, which would also support the assumption that "no data" has been replaced by zero precipitation measurements for the ground stations. However, the number of times ground stations measure a wet day when TRMM detects a dry day is not neglectable.

Comparing the precipitation measurements of TRMM and the ground stations with the discharge measurements for that day visually, comparing timing of high peaks for example, suggests better performance of TRMM for some catchments (Paunglaung, Sinthe) and better performance of the ground station for others (Yezin, Chaungmange). It should be noted that the quality of discharge data has not fully been verified either, so this test can only be used as an indication.

Figure **??** shows cumulative plots of the measured discharge, measured precipitation by TRMM, measured precipitation by the ground stations and the aggregation of discharge and potential evaporation. The sum of potential evaporation and discharge should be larger then the sum of the measured precipitation. This is not the case for the catchments Madan, Kabaung, Yenwe and to a smaller extend Bainda. In case of Madan this could be explained by an underestimation of the discharge, considering that the timeseries contain only in 24.2 % of the days discharge measurements, see table E.1. The catchments Kabaung, Yenwe and Bainda have discharge measurements for 93.1%, 94.7 % and 76.8 % of the datapoints, so for those catchment these plots might indicate an overestimation of precipitation by both measurement methods. Another explanation could be that the potential evaporation of the dataseries is too low. Figure **??** shows the location of these reservoirs are further away from the Climwat stations included in the calculation of the average potential evaporation.The catchment Yezin shows that the total discharge is larger than precipitation measurement of both TRMM and the ground station, indicating that both precipitation measurements are off or the discharge data are irreliable for the Yezin catchment.

Another way of looking at the aggregation of all data for the catchments is the Budyko framework, figure E.7.For each catchment the ratio of total actual evaporation over total precipitation, $\frac{E_a}{P}$, with respect to the ratio of total potential evaporation over total precipitation, $\frac{E_p}{P}$, for each catchment are displayed in the plot, both for TRMM precipitation (figure E.7b) and ground station measurements (figure E.7a) . Actual evaporation is calculated as the difference between total measured precipitation and total measured discharge. For three catchments the ratio $\frac{E_a}{P}$ is larger than the $\frac{E_p}{P}$ when using TRMM rainfall data, Madan and Yenwe, of for

Table E.2: Water Balance, fluxes and parameters for the simple lumped model

TRMM - GS	Dry - Dry	Threshold Wet - Wet	0.2 mm Wet - Dry	Dry - Wet	Dry - Dry	Threshold Wet - Wet	1 mm Wet - Dry	Dry - Wet	Dry - Dry	Threshold Wet - Wet	2 mm Wet - Dry	Dry - Wet
Paunglaung	58 % (1089)	15 % (289)	19 % (360)	8 % (144)	60 % (1132)	13 % (245)	19 % (360)	8 % (145)	63 % (1192)	11 % (201)	18 % (333)	8 % (156)
Ngalaik	61 % (1383)	13 % (289)	19 % (437)	7 % (169)	63 % (1435)	12 % (270)	17 % (394)	8 % (179)	66 % (1514)	10 % (222)	15 % (345)	9 % (197)
Sinthe	66 % (1503)	7 % (167)	22 % (499)	4 % (86)	68 % (1546)	7 % (158)	20 % (458)	4 % (93)	71 % (1617)	6 % (136)	17 % (388)	5 % (114)
Madan	60 % (1251)	13 % (280)	22 % (468)	5 % (97)	61 % (1283)	13 % (271)	21 % (436)	5 % (106)	63 % (1331)	11 % (241)	19 % (393)	6 % (131)
Kabaung	48 % (625)	31 % (402)	15 % (191)	7 % (93)	49 % (636)	29 % (384)	14 % (180)	8 % (111)	50 % (656)	27 % (350)	13 % (165)	11 % (140)
Yenwe	53 % (801)	28 % (427)	13 % (199)	6 % (90)	55 % (830)	28 % (418)	11 % (170)	7 % (99)	56 % (855)	25 % (387)	11 % (163)	7 % (112)
Bainda	52 % (987)	27 % (507)	14 % (263)	5 % (94)	54 % (1020)	26 % (497)	12 % (230)	6 % (104)	56 % (1050)	25 % (465)	11 % (215)	6 % (121)
Yezin	59 % (1328)	15 % (336)	19 % (429)	7 % (170)	61 % (1380)	13 % (296)	18 % (407)	8 % (180)	64 % (1451)	10 % (228)	17 % (392)	8 % (192)
Chaungmange	59 % (1328)	16 % (363)	18 % (414)	6 % (143)	61 % (1366)	16 % (352)	17 % (377)	7 % (153)	63 % (1419)	14 % (322)	15 % (327)	8 % (180)

TRMM - GS	Dry - Dry	Threshold Wet - Wet	5 mm Wet - Dry	Dry - Wet	Dry - Dry	Threshold Wet - Wet	10 mm Wet - Dry	Dry - Wet	Dry - Dry	Threshold Wet - Wet	15 mm Wet - Dry	Dry - Wet
Paunglaung	72 % (1351)	6 % (107)	14 % (262)	9 % (162)	82 % (1541)	3 % (49)	10 % (185)	6 % (107)	88 % (1648)	1 % (25)	7 % (129)	4 % (80)
Ngalaik	75 % (1714)	6 % (129)	12 % (272)	7 % (163)	84 % (1915)	2 % (50)	9 % (201)	5 % (112)	89 % (2031)	1 % (26)	6 % (137)	4 % (84)
Sinthe	78 % (1775)	4 % (80)	12 % (279)	5 % (121)	87 % (1966)	1 % (26)	8 % (187)	3 % (76)	92 % (2080)	0 % (11)	5 % (120)	2 % (44)
Madan	70 % (1462)	8 % (177)	13 % (279)	8 % (178)	78 % (1633)	4 % (74)	11 % (228)	8 % (161)	83 % (1739)	2 % (36)	8 % (177)	7 % (144)
Kabaung	56 % (731)	18 % (241)	12 % (154)	14 % (185)	65 % (852)	10 % (133)	11 % (145)	14 % (181)	73 % (956)	5 % (67)	10 % (134)	12 % (154)
Yenwe	61 % (929)	19 % (296)	10 % (145)	10 % (147)	67 % (1019)	11 % (167)	11 % (165)	11 % (166)	74 % (1120)	7 % (109)	9 % (137)	10 % (151)
Bainda	60 % (1129)	19 % (354)	11 % (198)	9 % (170)	67 % (1256)	10 % (191)	12 % (220)	10 % (184)	73 % (1374)	6 % (121)	10 % (185)	9 % (171)
Yezin	73 % (1645)	5 % (121)	13 % (301)	9 % (196)	82 % (1848)	3 % (60)	9 % (208)	6 % (147)	87 % (1969)	2 % (35)	7 % (148)	5 % (111)
Chaungmange	69 % (1552)	9 % (208)	12 % (259)	10 % (229)	78 % (1752)	4 % (100)	9 % (209)	8 % (187)	84 % (1886)	3 % (58)	7 % (158)	6 % (146)

TRMM - GS	Dry - Dry	Threshold Wet - Wet	20 mm Wet - Dry	Dry - Wet
Paunglaung	92 % (1724)	1 % (11)	5 % (87)	3 % (60)
Ngalaik	92 % (2098)	0 % (11)	4 % (100)	3 % (69)
Sinthe	95 % (2144)	0 % (4)	3 % (78)	1 % (29)
Madan	88 % (1837)	1 % (13)	7 % (139)	5 % (107)
Kabaung	79 % (1041)	3 % (38)	8 % (106)	10 % (126)
Yenwe	79 % (1192)	4 % (64)	8 % (126)	9 % (135)
Bainda	77 % (1457)	4 % (73)	9 % (163)	8 % (158)
Yezin	91 % (2056)	1 % (15)	4 % (100)	4 % (92)
Chaungmange	89 % (1992)	2 % (36)	5 % (118)	5 % (102)

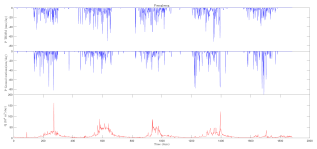

(a) Paunglaung dam

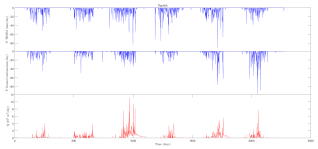

(b) Ngalaik dam

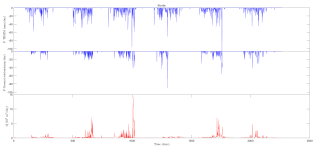

(c) Sinthe dam

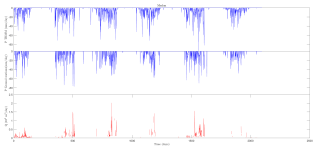

(d) Madan dam

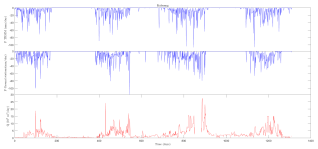

(e) Kabaung dam

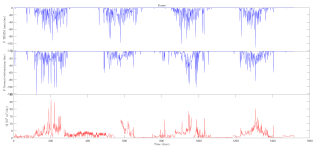

(f) Yenwe dam

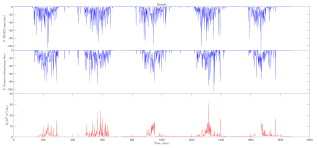

(g) Bainda dam

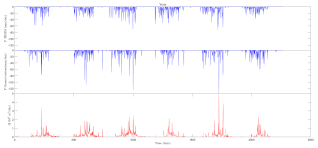

(h) Yezin dam

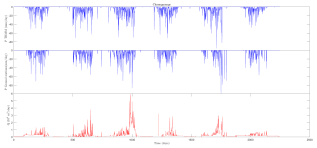

(i) Chaungmange dam

both rainfall data sources, Kabaung. As the actual evaporation is derived from precipitation and discharge measurements, this could either mean that the total discharge is underestimated, the precipitation is overestimated or the potential evaporation is underestimated by the data. For Madan it was already concluded that the total discharge is an underestimation. For Kabaung and Yenwe, this analysis leads to the same conclusion

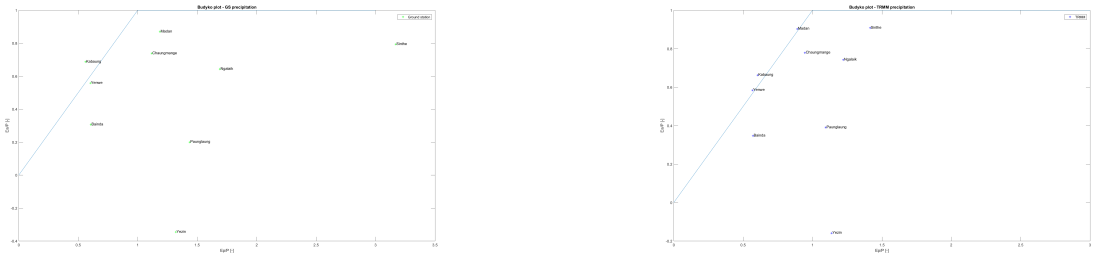

(a) Ground station precipitation measurements.

(b) TRMM precipitation measurements

Figure E.7: Budyko framework showing the ratio of total actual evaporation over total precipitation with respect to the ratio of total potential evaporation over total precipitation for each catchment, both for TRMM precipitation and groudn station measurements. Actual evaporation is calculated as the difference between total measured precipitation and total measured discharge.

as resulted from figure **??**, i.e. the precipitation is overestimated or the potential evaporation underestimated. The Yezin catchment has a negative $\frac{E_a}{P}$ ratio, which is a result of the discharge being larger than the precipitation. This could imply the catchment receives groundwater from another catchment, or the observations are wrong.

This analysis does not prove TRMM data to be accurate nor inaccurate as the quality of the ground measurements is not verified either. Advantages of TRMM data over station measurements are a better coverage in space and time and its availability for the ungauged subcatchments. For this reason it was decided to use TRMM data instead of ground measurements as model input for the calibration.

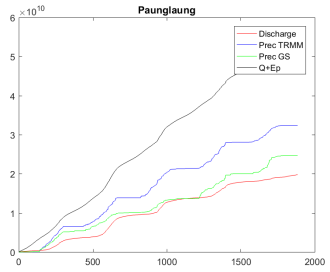

(a) Paunglaung dam

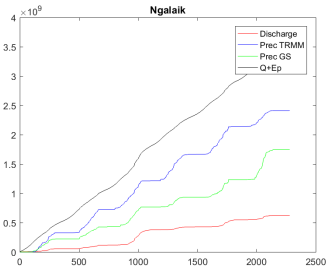

(b) Ngalaik dam

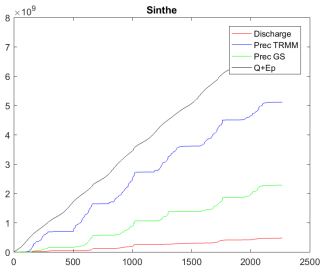

(c) Sinthe dam

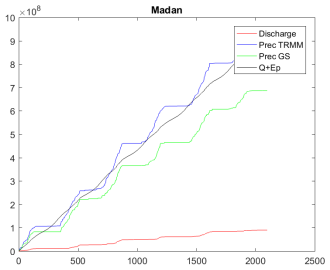

(d) Madan dam

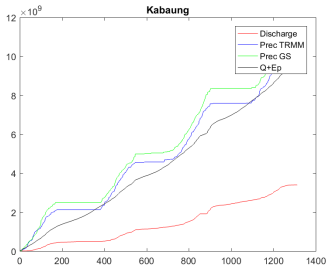

(e) Kabaung dam

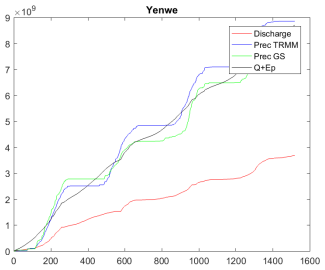

(f) Yenwe dam

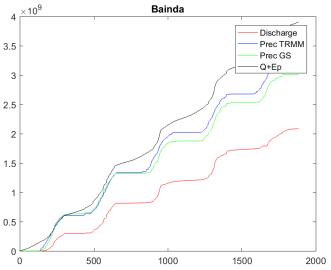

(g) Bainda dam

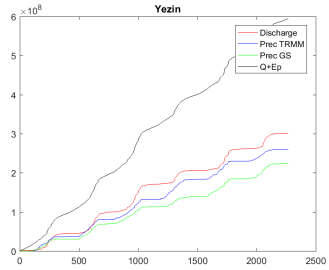

(h) Yezin dam

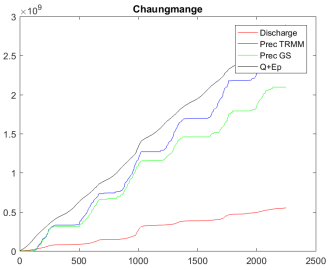

(i) Chaungmange dam

Figure E.8: Cumulative sum of measured discharge, measured precipitation by TRMM, measured precipitation by the ground stations and the aggregation of discharge and potential evaporation over time.

Appendix F

Reservoir characteristics

For most reservoirs the storage capacity, conduit capacity, waterspread area, irrigable area and reservoir catchment area are available. For some reservoirs one or more of these characteristics were not available. Assumptions were made for these reservoirs. Table F.1 gives these characteristics for each reservoir. The values indicated with † are assumed values. The assumptions of these values is discussed here. The reservoirs indicated with * before their number are reservoirs upstream of Taungoo city, the locations for which floods are considered. Subcatchments of the Sittaung river basin were defined for the development of the model. The table indicated for each reservoir in which subcatchment it is located, the size of that subcatchment and the ratio of the reservoir catchment area and the subcatchment area. In Appendix **??** the irrigation demands are estimated per month in mm d^{-1}. The irrigation demand in 10^6 $m^3 d^{-1}$ for each reservoir for each month is estimated by multiplying the estimated demand in mm d^{-1} with the irrigable area in 10^3 km^2. The last column in table F.1 gives the mean irrigation demand per reservoir throughout the year.

Assumption of storage capacity For the reservoirs Kawliya (7), Bawni (8) and Yanaungmyin (10) no storage capacity was available. An estimation for the storage capacity was made by looking at the ratio of conduit and storage capacity and the ratio of storage capacity and reservoir area for other reservoirs in the basin. The typical ratios for the reservoirs in the basin were based on the ratio for all other reservoirs except for the Paunglaung (3) and Thaukyegat (19) reservoirs and the Yanaungmyin (10), Ngalaik (12), Yezin (14), Chaungmagyi Pyi (17) and Minye (20). The Paunglaung (3) and Thaukyegat (19) reservoirs are much larger than the other reservoirs and their ratios deviated from the others. Their dimensions are not considered 'typical' for the basin. For the reservoirs the Yanaungmyin (10), Ngalaik (12), Yezin (14), Chaungmagyi Pyi (17) and Minye (20) no conduit capacities were available as will be discussed in section F. Since the Kawliya (7), Bawni (8) and Yanaungmyin (10) reservoirs were not of a similar size Paunnglaung and Thaukyegat, they were not considered 'typical' in their dimensions. The average conduit - storage ratio for the remaining reservoirs is 9.3. The average ratio for the storage capacity and the catchment area is 69.4. The standard deviations of these values are high, 4.2 and 53.1 respectively, indicating that the 'typical' dimensions of a reservoir in the basin do not exist. Better methods may be available to estimate the storage capacity of reservoirs when they are unknown, but this is beyond the scope of this research. The effect of assumptions for dimensions of the reservoirs on the results will be discussed in chapter 6.

Using both ratios to estimate the storage capacity for the Kawliya (7) and Bawni (8) reservoir, leads to two different estimations. For the Kawliya (7) reservoir these were 81 $\cdot 10^6$ m^3 for the storage capacity - catchment area ratio and 268 $\cdot 10^6$ m^3 for the conduit - storage capacity ratio. For the Bawni (8) reservoir these were 31 $\cdot 10^6$ m^3 for the storage capacity - catchment area ratio and 46 $\cdot 10^6$ m^3 for the conduit - storage capacity ratio. The average value was used as estimation of the storage capacity, which is 174 $\cdot 10^6$ m^3 for Kawliya and 38 for Bawni. For the Yanaungmyin reservoir no conduit capacity was available either, so the estimation of the storage capacity was only based in the typical ratio of storage capacity and reservoir area in the basin. This estimation is 19 $\cdot 10^6$ m^3.

Assumption of conduit capacity For the reservoirs Yanaungmyin (10), Ngalaik (12), Yezin (14), Chaungmagyi Pyi (17) and Minye (20) no conduit capacity was available. The estimation of the conduit capacity is based on the 'typical' conduit - storage capacity ratio of reservoirs in the basin as determined in section F at a value 9.3. The estimated conduit capacities for the reservoirs Yanaungmyin (10), Ngalaik (12), Yezin (14), Chaungmagyi Pyi (17) and Minye (20) are respectively 1.81 $m^3 s^{-1}$, 8.67 $m^3 s^{-1}$, 8.39 $m^3 s^{-1}$, 1.12 $m^3 s^{-1}$ and 0.19 $m^3 s^{-1}$. In section F it was mentioned that the 'typical' dimensions for reservoirs in the basin are difficult to define, meaning that these are very rough assumptions. The reservoirs Ngaliak(12) and Yezin (14) have approximately average reservoir areas and storage capacities, so for these reservoirs using 'average' dimensions might lead to a reasonable estimation. The reserovirs Chaungmagyi Pyi (17) and Miny (20) are relatively

small, so a erroneous assumption of their conduit is not expected to effect the results of the optimization to a large extend. For Yanaungmyin both the conduit and the reservoir capacity were estimated, its characteristics are now comparable to the Yathoe (16) reservoir.

Assumption of irrigable area For the reservoirs Kawliya (7), Bawni (8), Yanaungmyin (10), Swegyin (18), Thaukyegat (19) and Kunchaung (21) no irrigable areas were available. For all other reservoirs the ratio of irrigable area over total reservoir catchment area was calculated resulting in an average of 0.29. The standard deviation is 0.22, showing that also in this case the assumption of a 'typical' relation between the catchment area and the irrigable area is probably not valid. Better estimation of irrigable area was beyond the scope of this research, so the irrigable areas were estimated based on this ratio. For the Kawliya (7), Bawni (8), Yanaungmyin (10), Swegyin (18), Thaukyegat (19) and Kunchaung (21) reservoirs, this resulted in the values presented in table F.1.

Assumption of waterspread area For the reservoirs Kawliya (7), Bawni (8), Yanaungmyin (10), Swegyin (18), Thaukyegat (19) and Kunchaung (21) no waterspread area $ResA$ [m^2] was available. The waterspread areas are only used when calculating the hydropower generation in the reservoir. They were estimated by deriving a relation between the waterspread area and the reservoir capacity $\overline{S_{res}}$ [m^3] with linear regression for the other reservoirs in the basin, resulting in the relation $ResA = 6 \cdot \overline{S_{res}} + 545$. The estimated waterspread areas for the reservoirs are presented in table F.1. For this estimation also holds that there are better ways to estimate the waterspread area of these reservoirs, such as by satellite images, but this was beyond the scope of this research.

Table E1: Summary of reservoir characteristics. † indicated the value is an assumed value. * indicates the reservoir is located upstream of Taungoo city, the location considered for floods.

Reservoir	Name	Storage capacity (10^6 m^3)	Conduit capacity (10^6 m^3d^{-1})	Water-spread area (km^2)	Reservoir catchment area (km^2)	Irrigable area (km^2)	Sub-catchment	Sub-catchment area (km^2)	Ratio reservoir / sub-catchment area (%)	Mean irr. demand (10^6 m^3d^{-1})
1	Yenwe	988	4.32	74.3	804	480	16	1433	56	1.14†
2	Phyu	726	4.32	59.0	1051	405	9	3421	31	0.97†
*3	Paunglaung	360	26.44	16.6	4791	142	1	7934	60	0.34†
4	Kabaung	890	3.37	59.3	1178	216	9	3421	34	0.51†
5	Baingda	461	2.94	6.2	246	189	17	2450	10	0.45†
*6	Sinthe	176	1.47	27.0	809	131	1	7934	10	0.31†
7	Kawliya	174†	2.16	16.2	116	34†	17	2450	5	0.08†
8	Bawni	38†	0.37	7.8	45	13†	17	2450	2	0.03†
*9	Swa	267	1.84	27.9	1077	142	3	1517	71	0.34†
*10	Yanaungmyin	19†	0.16†	6.7	28	8†	2	3509	1	0.02†
*11	Chaungmange	113	0.61	12.7	265	32	2	3509	8	0.08†
*12	Ngalaik	93	0.75†	15.6	328	85	2	3509	9	0.20†
*13	Madan	45	0.69	4.5	100	32	2	3509	3	0.08†
*14	Yezin	90	0.72†	11.3	33	65	1	7934	0	0.15†
*15	Pathi	38	0.31	3.8	66	12	6	344	19	0.03†
16	Yathoe	19	0.24	5.7	33	8	9	3421	1	0.02†
*17	Chaungmagyi Pyi	12	0.10†	16.7	119	12	2	3509	3	0.03†
18	Swegyin	1450	18.40	95.0	875	254†	15	1732	51	0.61†
*19	Thaukyegat	295	18.14	23.7	2161	627†	7	2473	87	1.50†
20	Minye	2	0.02†	0.8	23	4	9	3421	1	0.01†
21	Kunchaung	843	5.70	57.5	875	254†	12	1903	46	0.61†

Appendix G

River characteristics

Table G.1: Summary of river characteristics. Numbers of the river sections indicate the subbasin connected to that reach with the subbasins numbered as in figure 3.3a. The parameters c_1, c_2, c_3 and K are the parameters for the Muskingum routing.

River section	Stream length (km)	c_1	c_2	c_3	K (s)
1	28	0.85	0.62	-0.46	22618.4
2	41	0.80	0.50	-0.31	32799.2
3	8	0.94	0.86	-0.80	6792.8
4	43	0.80	0.49	-0.28	34454.4
5	11	0.93	0.83	-0.76	8479.2
6	42	0.80	0.50	-0.30	33586.4
7	9	0.94	0.86	-0.80	6904.8
8	11	0.93	0.82	-0.74	9028.8
9	33	0.83	0.57	-0.40	26668.8
10	10	0.94	0.84	-0.78	7756.0
11	24	0.87	0.67	-0.53	18826.4
12	26	0.86	0.64	-0.50	20808.0
13	29	0.85	0.61	-0.46	22938.4
14	27	0.85	0.63	-0.48	21740.8
15	27	0.85	0.63	-0.48	21836.0
16	34	0.82	0.56	-0.38	27587.2
17	10	0.93	0.84	-0.77	7999.2

Appendix H

Estimation of irrigation demands

There are two growing cycles for rice in Myanmar. In cycle 1 the ricee is planted between June and August and harvested between November and January, in cycle 2 the rice is planted November and December and harvested in April and May (Maclean et al.). The water demand is estimated by multiplying the water demand for a hypothetical reference crop with the crop factor. The reference crop is defined as a hypothetical extensive surface of green grass of uniform height, actively growing, completely shading the ground and with adequate water. The crop factor is determined per crop, per climate and per growth stage and extracted from the Food and Agricultural Organization database on May 13th, 2017 (FAO). Table H.1 gives the growth stages of paddy rice with duration and corresponding crop factors.

Table H.1: The growth stages of paddy rice with duration and corresponding crop factors extracted from the Food and Agricultural Organization database (FAO) on May 13th, 2017.

Growth stage	Duration (months)	Crop factor
Initial	1	1.05
Crop development	1	1.225
Mid season	2	1.2
Late season	1	0.75
Harvesting	-	

The potential evaporation for the reference crop is given by FAO for each month of the year in mm day^{-1}. The rice planted in the two cycles of growth are assumed to be planted throughout the entire planting season. This means that for cycle 1, one third of the rice is planted in June, one third in July and one third in August. For cycle 2, half of the plants is planted in November and half is planted in December. This results in 5 actual cycles of rice plants. The demands crop factor per month is averaged over the 5 cycles of rice production, as presented in table H.2. The potential transpiration of the reference crop ET_0 [mm d^{-1}] and the irrigation demand [mm d^{-1}] calculated by multiplying the average crop factor with the potenial transpiration of the reference crop are given in table H.2 as well. To determine the irrigation demand per reservoir, the irrigation demand in mm d^{-1} is multiplied by the irrigable area of the reservoir. Table F.1 in Appendix F gives the irrigable area as well as the average daily irrigation demand per year.

For three reservoirs in the basin, Yezin (14), Sinthe (6) and Ngalaik (12), actual irrigation offtakes are were available for the period between September 1st, 2009 to March 19th, 2015. The average daily offtake for irrigation for these reservoirs are $99 \cdot 10^3$, $48 \cdot 10^3$ and $80 \cdot 10^3$ m^3 d^{-1}. The average estimated daily demand for these reservoirs was $150 \cdot 10^3$ m^{3}d^{-1}, $310 \cdot 10^3$ m^{3}d^{-1} and $200 \cdot 10^3$ m^{3}d^{-1}, as presented in table F.1. No data are available for irrigation offtakes in other reservoirs. It is likely that the estimations for other reservoirs are overestimations as well for reasons mentioned above. Also, the reservoirs Yezin (14), Sinthe (6) and Ngalaik (12) are located in the north of the basin (see figure 2.3), which is drier than the south of the basin.

Table H.2: The crop factors per month for the 5 cycles in rice production and the average crop factor per month. The transpiration of the reference crop per month and the daily water demand for the crop based on the crop factor and reference crop.

	Crop factor							
Month	Cycle 1-1	Cycle 1-2	Cycle 1-3	Cycle 2-1	Cycle 2-2	Average	ET_0 (mm d^{-1})	Irrigation demand (mm day^{-1})
January	-	-	-	1.2	1.125	1.16	2.70	3.14
February	-	-	-	1.2	1.2	1.2	2.57	3.08
March	-	-	-	0.75	1.2	0.98	2.50	2.44
April	-	-	-	-	0.75	0.75	2.74	2.06
May	-	-	-	-	-	-	2.84	0
June	1.05	-	-	-	-	1.05	3.00	3.15
July	1.125	1.05	-	-		1.09	3.18	3.46
August	1.2	1.125	1.05	-	-	1.13	1.12	1.26
September	1.2	1.2	1.125	-	-	1.18	1.40	1.65
October	0.75	1.2	1.2	-	-	1.05	1.48	1.56
November	-	0.75	1.2	1.05	-	1	1.83	1.83
December	-	-	0.75	1.125	1.05	0.98	5.00	4.88

Appendix I

The spillway behaviour for increasing penalty

Table I.1: Spillway behaviour for increasing penalty per reservoir for the period between April 1st, 2010 until March 31st, 2011. The total spilled volume in that period, the number of days spilling occured, the numbr of days spilling occured when the reservoir was less than 95% full, the hydropower generation (MWh), the volume above flood level, the average number of iterations used to solve the optimization problem for one timestep and the total CPU time for all timesteps.

Res.	ρ_2	Spilled volume (10^6 m^3)	Spilling days	Spilling when res. not full	Hydro-power (MWh)	Flood volume (10^6 m^3)	Average number of iter-ations	CPU time (min)
3	0	834	44	44	5.48E+04	56	141	15
	10^{-15}	58	15	2	7.38E+04	40	307	33
	10^{-14}	367	51	1	7.41E+04	42	566	62
6	0	204	45	25	2.71E+03	46	73	8
	10^{-15}	197	93	1	3.15E+03	42	119	13
	10^{-14}	208	96	0	3.11E+03	43	168	18
9	0	266	55	29	5.03E+03	52	64	7
	10^{-15}	263	100	0	5.80E+03	43	114	12
	10^{-14}	266	100	0	5.78E+03	43	177	19
10	0	0	0	0	4.77E+01	43	305	32
	10^{-15}	0	0	0	4.77E+01	43	253	26
	10^{-14}	0	0	0	4.77E+01	43	211	22
11	0	15	7	3	1.64E+03	45	69	7
	10^{-15}	15	31	0	1.65E+03	45	134	14
	10^{-14}	15	45	0	1.65E+03	43	164	17
12	0	42	14	6	1.32E+03	45	85	9
	10^{-15}	44	59	8	1.37E+03	43	134	14
	10^{-14}	44	68	0	1.38E+03	43	172	18
13	0	0	0	0	6.00E+02	42	243	25
	10^{-15}	0	0	0	6.03E+02	42	199	21
	10^{-14}	0	0	0	6.00E+02	42	192	20
14	0	1	3	3	3.20E+01	42	244	26
	10^{-15}	0	0	0	3.50E+01	42	198	21
	10^{-14}	0	0	0	3.26E+01	40	203	21
15	0	0	0	0	4.04E+02	42	228	24
	10^{-15}	0	0	0	4.01E+02	42	174	18
	10^{-14}	0	0	0	4.01E+02	42	154	16
17	0	60	203	8	2.58E+01	43	179	18
	10^{-15}	60	197	10	2.56E+01	42	219	23
	10^{-14}	60	217	0	2.59E+01	42	307	32
19	0	246	22	22	1.60E+04	50	156	16
	10^{-15}	0	0	0	1.55E+04	48	237	25
	10^{-14}	56	9	0	1.42E+04	40	407	43

Appendix J

Matlab Code

Matlab code developed for this research is available at
`https://github.com/dorienlugt/OperatingSittaungsReservoirs.git`.

Bibliography

Food and Agriculture Organization. URL http://www.fao.org/docrep/X0490E/x0490e0b.htm{%}0A.

Abhay Anand, S. Galelli, Samavedham, Lakshminarayanan, and Sithanandam Sundaramoorthy. Coordinating multiple model predictive controllers for the management of large-scale water systems. *Jounal of Hydroinformatics*, 15(2):293–305, 2013. ISSN 1464-7141. doi: 10.1109/ICNSC.2011.5874948.

John T. Betts. *Practical Methods for Optimal Control and Estimation Using Nonlinear Programming*. Society for Industrial and Applied Mathematics, Philadelphia, 2010.

Maarten Breckpot, Toni Barjas Blanco, and Bart De Moor. Flood control of rivers with nonlinear model predictive control and moving horizon estimation. *49th IEEE Conference on Decision and Control (CDC)*, pages 6107–6112, 2010. doi: 10.1109/CDC.2010.5717620.

Richard H Byrd, Mary E Hribar, and Jorge Nocedal. An interior point algorithm for large-scale nonlinear programming. *SIAM Journal on Optimization*, 9(4):877–900, 1999.

Eduardo F. Camacho, Carlos Bordons Alba, and C Bordons. *Model Predictive control*. 2007. ISBN 9781852336943. doi: 10.1007/978-0-85729-398-5.

Alcigeimes B. Celeste and Max Billib. The role of spill and evaporation in reservoir optimization models. *Water Resources Management*, 24(4):617–628, 2010. ISSN 09204741. doi: 10.1007/s11269-009-9468-4.

Panagiotis D. Christofides, Riccardo Scattolini, David Muñoz de la Peña, and Jinfeng Liu. Distributed model predictive control: A tutorial review and future research directions. *Computers and Chemical Engineering*, 51:21–41, 2013. ISSN 00981354. doi: 10.1016/j.compchemeng.2012.05.011.

A R Conn, N I M Gould, D Orban, and P L Toint. A primal-dual trust-region algorithm for minimizing a nonconvex function subject to general inequality and linear equality constraints.pdf. Technical report, Council for the Central Laboratory of Research Councils 1999, Oxfordshire, 1999.

Minh Dang Doan, Pontus Giselsson, Tamás Keviczky, Bart De Schutter, and Anders Rantzer. A distributed accelerated gradient algorithm for distributed model predictive control of a hydro power valley. *Control Engineering Practice*, 21(11):1594–1605, 2013. ISSN 09670661. doi: 10.1016/j.conengprac.2013.06.012.

Tim Dobermann. Energy in Myanmar, 2016. URL www.theigc.org.

Rodrigo G Eustaquio, Elizabeth W Karas, and Ademir A Ribeiro. Constraint Qualifications for Nonlinear Programming. Technical report, 2008.

Andrea Ficchi, Luciano Raso, Maxime Jay-allemand, David Dorchies, and Pierre-olivier Malaterre. A centralized real-time controller for the reservoir ' s management on the Seine River using ensemble weather forecasting. 15(April):10420, 2013.

Carlos E. García, David M. Prett, and Manfred Morari. Model predictive control: Theory and practice-A survey. *Automatica*, 25(3):335–348, 1989. ISSN 00051098. doi: 10.1016/0005-1098(89)90002-2.

Mohammad Akram Gill. Flood routing by the Muskingum method. *Journal of Hydrology*, 36(3-4):353–363, 1978. ISSN 00221694. doi: 10.1016/0022-1694(78)90153-1.

Nicholas I M Gould, Dominique Orban, Annick Sartenaer, and Philippe L Toint. Superlinear convergence of primal-dual interior point algorithms for nonlinear programming. *SIAM Journal on Optimization*, 11(4): 974–1002, 2001.

Nick Gould, Dominique Orban, and Philippe Toint. Numerical methods for large-scale nonlinear optimization. *Acta Numerica*, 14:299–361, 2005. ISSN 09624929. doi: 10.1017/S0962492904000248.

Morgan A. Hanson. On sufficiency of the Kuhn-Tucker conditions in nondifferentiable programming. *Journal of mathematical analysis and applicaitons*, 80(2):545–550, 1981. ISSN 17551633. doi: 10.1017/S0004972700012041.

Rens Hasman. *Water allocation assessment to support IWRM in the major river basins of Myanmar - now and in the future*. PhD thesis, 2014.

J.D. Hogg and J.A. Scott. On the effects of scaling on the performance of Ipopt. 2013. ISSN 03769429. doi: 10.1007/BF00032330.

Masakazu Kojima, Nimrod Megiddo, and Shinji Mizuno. A primal-dual infeasible-interior-point algorithm for linear programming. *Mathematical Programming*, 61(1-3):263–280, 1993. ISSN 00255610. doi: 10.1007/BF01582151.

Antonis D. Koussis. Assessment and review of the hydraulics of storage flood routing 70 years after the presentation of the Muskingum method. *Hydrological Sciences Journal*, 54(1):43–61, 2009. ISSN 02626667. doi: 10.1623/hysj.54.1.43.

Wan Kyi. Hydropower Developments in Sittaung Basin. *Unpublished*, 2015. URL `uwankyi@gmail.com`.

Wan Kyi. Myanmar Engineering Society Annual General Meeting 2016 - Hyropower Developments in Sittaung Valley, 2016.

John W. Labadie. Optimal Operation of Multireservoir Systems : State-of-the-Art Review. *Journal of water resources planning and management*, 130(April):93–111, 2004.

Nay Myo Lin and Martine Rutten. Optimal Operation of a Network of Multi-purpose Reservoir: A Review. *Procedia Engineering*, 154:1376–1384, 2016. ISSN 18777058. doi: 10.1016/j.proeng.2016.07.504.

Jay Maclean, Bill Hardy, and Gene Hettel. *Rice Almanac*. International Rice Research Institute. URL `http://ricepedia.org/myanmar`.

J M Maestre, D. Munoz de la Pena, and Camacho. Distributed model predictive control based on a cooperative game. *Optimal Control Applications and Methods*, 32(3):153–176, 2011. ISSN 01432087. doi: 10.1002/oca.

Numan R Mizyed, Jim C. Loftis, Darrell G Fontane, and ASCE. Operation of large multireservoir systems using optimal-control theory. *Journal of water resources planning and management*, 118(4):371–387, 1992.

Nay Myo Lin. Flood mitigation by using model predictive control for a network of reservoirs, 2016.

R R Negenborn, P J Van Overloop, T Keviczky, and B De Schutter. Distributed model predictive control of irrigation canals. *Network and Heterogeneous Media*, 4(2):359–380, 2009. ISSN 1556-1801. doi: 10.3934/nhm.2009.4.359.

Ewa Niewiadomska-Szynkiewicz, Krzysztof Malinowski, and Andrzej Karbowski. Predictive methods for real-time control of flood operation of a multireservoir system: Methodology and comparative study. *Water Resources Research*, 32(9):2885–2895, 1996. ISSN 00431397. doi: 10.1029/96WR01443.

Oluwatosin Olofintoye, Fred Otieno, and Josiah Adeyemo. Real-time optimal water allocation for daily hydropower generation from the Vanderkloof dam, South Africa. *Applied Soft Computing Journal*, 47:119–129, 2016. ISSN 15684946. doi: 10.1016/j.asoc.2016.05.018.

Filippo Pecci, Edo Abraham, and Ivan Stoianov. Penalty and relaxation methods for the optimal placement and operation of control valves in water supply networks. *Computational Optimization and Applications*, 67(1):201–223, 2017. ISSN 15732894. doi: 10.1007/s10589-016-9888-z.

Florian A Potra and Stephen J Wright. Interior-point methods. *Journal of Computational and Applied Mathematics*, 124(1-2):281–302, 2000. ISSN 03770427. doi: 10.1016/S0377-0427(00)00433-7.

Luciano Raso. *Optimal Control of Water Systems Under Forecast Uncertainty*. Phd, Delft University of Technology, 2013.

Luciano Raso and Pierre Olivier Malaterre. Combining Short-Term and Long-Term Reservoir Operation Using Infinite Horizon Model Predictive Control. *Journal of Irrigation and Drainage*, pages 1–7, 2016. ISSN 0733-9437. doi: 10.1061/(ASCE)IR.1943-4774.0001063.

P Rathore. *Error Analysis of TRMM , WFD and APHRODITE datasets using Triple Collocation Error Analysis of TRMM , WFD and APHRODITE datasets using Triple Collocation*. PhD thesis, Delft University of Technology, 2014.

James B. Rawlings and Brett T. Stewart. Coordinating multiple optimization-based controllers: New opportunities and challenges. *IFAC Proceedings Volumes (IFAC-PapersOnline)*, 40(5):19–28, 2007. ISSN 14746670. doi: 10.3182/20070606-3-MX-2915.00003.

Max Van Rest. *Monitoring of the Sittaung River*. Msc, Delft University of Technology, 2015.

Riccardo Scattolini. Architectures for distributed and hierarchical Model Predictive Control – A review. *Journal of Process Control*, 19(5):723–731, 2009. ISSN 0959-1524. doi: 10.1016/j.jprocont.2009.02.003.

Dirk Schwanenberg, Fernando Mainardi Fan, Steffi Naumann, Julio Issao Kuwajima, Rodolfo Alvarado Montero, and Alberto Assis dos Reis. Short-Term Reservoir Optimization for Flood Mitigation under Meteorological and Hydrological Forecast Uncertainty: Application to the Três Marias Reservoir in Brazil. *Water Resources Management*, 29(5):1635–1651, 2015. ISSN 09204741. doi: 10.1007/s11269-014-0899-1.

Cornelia Setz, Adrienne Heinrich, Philipp Rostalski, Georgios Papafotiou, and Manfred Morari. *Application of model predictive control to a cascade of river power plants*, volume 17. IFAC, 2008. ISBN 9783902661005. doi: 10.3182/20080706-5-KR-1001.3011.

Xiao-meng Song, Fan-zhe Kong, and Zhao-xia Zhu. Application of Muskingum routing method with variable parameters in ungauged basin. *Water Science and Engineering*, 4(1):1–12, 2011. ISSN 16742370. doi: 10.3882/j.issn.1674-2370.2011.01.001.

Xin Tian, Peter Jules van Overloop, Rudy R. Negenborn, and Nick van de Giesen. Operational flood control of a low-lying delta system using large time step Model Predictive Control. *Advances in Water Resources*, 75:1–13, 2015. ISSN 03091708. doi: 10.1016/j.advwatres.2014.10.010.

United Nations - Sittaung river valley survey mission. Report on Sittang Valley Water Resources Development. Technical report, UN - Sittang River Valley Survey Mission, Rangoon, Burma, 1964.

Ton J J Van den Boom and Tcpm Backx. Model predictive control. Technical report, 2005.

P.-J. Van Overloop. *Model Predictive Control on Open Water Systems*. Phd thesis, Delft University of Technology, 2006.

Andreas Wächter and Lorenz T Biegler. Line Search Filter Methods for Nonlinear Programming: Motivation and Global Convergence. *SIAM Journal on Optimization*, 16(1):1–31, 2005a. ISSN 1052-6234. doi: 10.1137/S1052623403426556.

Andreas Wächter and Lorenz T Biegler. On the implementation of an interior-point filter line-search algorithm for large-scale nonlinear programming. *Mathematical Programming*, 106(1):25–57, 2005b. ISSN 00255610. doi: 10.1007/s10107-004-0559-y.